

**Versatile silicone rubber samplers for trace
organic analysis in a Chromatography-Mass
Spectrometry laboratory**

by

Yvette Cronjé Naudé

Submitted in partial fulfilment of the requirements for the degree

PHILOSOPHIAE DOCTOR

Chemistry

In the Faculty of Natural and Agricultural Sciences

Department of Chemistry

University of Pretoria

April 2013



I declare that the thesis, which I hereby submit for the degree *Philosophiae Doctor* (Chemistry) at the University of Pretoria, is my own work and has not previously been submitted by me for a degree at this or any other tertiary institution.

Yvette Cronjé Naudé

Date

I dedicate this to

My mother, Lynette Craul Robertson Cronjé, and my father, Christopher Jackson Cronjé. Their can-do manner and modesty have always been an inspiration. My husband Bennie, and our beloved son Christiaan, for believing in me, for encouragement and joy.

Summary

Extraction is required to separate and concentrate trace level analytes from the sample matrix prior to gas chromatography (GC). Classical extraction procedures utilise large amounts of hazardous solvents, generate waste, and sensitivity limitations are associated with the injection of microlitre amounts of the final solvent extract.

In response to real world challenges, and to overcome the problems associated with solvent extraction, novel silicone rubber (polydimethylsiloxane (PDMS)) samplers were developed for solvent free enrichment of trace level analytes from indoor air, contaminated soil, desert soil, ultra high temperature (UHT) milk and Pinotage wine. Versatile PDMS samplers as a loop, a multichannel trap, or a denuder for trace environmental forensics, geochemical and aroma investigations are presented. A unique off-line multidimensional GC approach involving heart-cut gas chromatographic fraction collection is described, as is off-line olfactory assessment of recombined heart-cuts for synergistic odour effects.

PDMS loop samplers were used for the extraction of DDT (1,1,1-trichloro-2,2-bis(*p*-chlorophenyl)ethane) and its associated environmental pollutants from soil samples. Miniature denuder samplers accomplished separate concentration of vapour phase and of particulate phase fractions of DDT and its associated environmental pollutants from indoor air, in a single step. Ratios of airborne *p,p'*-DDD/*p,p'*-DDT and of *o,p'*-DDT/*p,p'*-DDT are

unusual and do not match the ideal certified ingredient composition required of commercial DDT. Results suggest that commercial DDT used for indoor residual spraying may have been compromised with regards to insecticidal efficacy, demonstrating the power of this new environmental forensics tool. Multichannel PDMS trap samplers were used in a unique heart-cut multidimensional GC approach for off-line enantiomeric separation of *o,p'*-DDT and *o,p'*-DDD in air and soil. This alternative multidimensional method is compared to the complementary technique of comprehensive two-dimensional gas chromatography with time-of-flight mass spectrometry detection (GCxGC-TOFMS).

PDMS loop samplers were also employed for the solvent free extraction of hydrocarbons from desert soil to investigate, for the first time, a possible geochemical origin of the enigmatic fairy circles of Namibia. It is proposed that microseepages of natural gas and low volatility hydrocarbons are expressed at the surface as a geobotanical anomaly of barren circles and circles of altered vegetation.

Multichannel PDMS trap samplers were utilised for sampling of the headspace of UHT milk and of Pinotage wine, and to study off-line, using a portable olfactometer, synergistic effects between recombined heart-cut aroma compounds. Olfactory results show that a synergistic combination of 2-heptanone and 2-nonanone was responsible for a pungent cheese-like odour in UHT milk, while a synergistic combination of furfural and 2-furanmethanol was responsible for a roast coffee bean-like odour in coffee style Pinotage wine.

The small, low cost samplers are quick and easy to assemble and they fit commercial thermal desorber systems. The PDMS samplers are reusable. Solvent extraction of the sampling materials, extract clean-up and pre-concentration are not required. Thus, potential loss of analyte, introduction of contaminants and waste disposal are minimised. Solvent free thermal desorption permits transfer of the entire sample mass to the cooled injection system (CIS) inlet of a GC resulting in greater sensitivity when compared to injection of microlitre amounts of a solvent extract. This allowed for sampling of smaller sized soil samples, shorter air sampling times and lower air sampling flow rates when compared to solvent based methods.

Acknowledgements

“The most exciting phrase to hear in science, the one that heralds new discoveries, is not “Eureka!” but “That’s funny...” - Isaac Asimov

First and foremost, my immense gratitude to my study supervisor, Professor Egmont Rohwer, for granting me the opportunity, the freedom and the adventure to explore the versatility of novel solvent free samplers and multidimensional chromatographic approaches, for his expert mentorship, for generously sharing his “what if?” vision and vast knowledge. It is a great privilege.

The work described in this thesis is the direct result of valuable transdepartmental collaboration. Special thanks are given to:

Professor Gretel van Rooyen from the Department of Plant Science, University of Pretoria, for the exciting opportunity to collaborate and to investigate the enigmatic fairy circles of Namibia, southern Africa. This truly is a once in a lifetime, awe inspiring experience.

Professor Riëtte de Kock from the Department of Food Science, University of Pretoria, for the chance to discover the challenging and fascinating field of flavour compounds in milk.

Professor Riana Bornman from the Department of Urology, University of Pretoria, for an opportunity to collaborate on the crucial DDT project, and for arranging sample collection of indoor air and outdoor soil in a malaria area of South Africa.

I would also like to thank Gerhard Overbeek for assisting with the extraction of wine samples and olfactometric evaluation; Dr Marleen van Aardt for assisting with the olfactometric evaluation of milk; Philip Langenhoven from LECO Africa (Pty) Ltd. for kind sponsorship of wine and laboratory assistance; Dr Peter Gorst-Allman from LECO Africa (Pty) Ltd. for the use of a LECO Pegasus 4 D GC×GC–TOFMS, for technical advice, encouragement, fun and friendship; Jack Cochran from Restek, United States of America, for generous donation of GC columns and consumables; my colleagues, Dr Patricia Forbes; Dr Siegie Bauermeister; David Masemula; Niel Malan; Elize Smit and Marc Bouwer.

My employer, the University of Pretoria, is gratefully acknowledged for the opportunity to enrol for a PhD, as are Sasol Fuels and the National Research Foundation (NRF) for providing research funding.

Publications, presentations and provisional patents

This thesis is based on the following manuscripts:

Published papers

Naudé, Y. and Rohwer, E.R., 2013. Investigating the coffee flavour in South African Pinotage wine using novel off-line olfactometry and comprehensive gas chromatography with time of flight mass spectrometry. *Journal of Chromatography A* 1271, 176-180. DOI:10.1016/j.chroma.2012.11.019

Naudé, Y. and Rohwer, E.R., 2012. Novel method for determining DDT in vapour and particulate phases within contaminated indoor air in a malaria area of South Africa. *Analytica Chimica Acta* 730, 112–119. DOI:10.1016/j.aca.2012.02.054

Naudé, Y. and Rohwer, E.R., 2012. Two multidimensional chromatographic methods for enantiomeric analysis of *o,p'*-DDT and *o,p'*-DDD in contaminated soil and air in a malaria area of South Africa. *Analytica Chimica Acta* 730, 120–126. DOI:10.1016/j.aca.2012.03.028

Naudé, Y., Van Rooyen, M.W., Rohwer, E.R., 2011. Evidence for a geochemical origin of the mysterious circles in the Pro-Namib desert. *Journal of Arid Environments* 75, 446-456. DOI:10.1016/j.jaridenv.2010.12.018

Naudé, Y., Van Aardt, M., Rohwer, E.R., 2009. Multi-channel open tubular traps for headspace sampling, gas chromatographic fraction collection and olfactory assessment of milk volatiles. *Journal of Chromatography A*, 2798–2804. DOI:10.1016/j.chroma.2008.09.065

Book chapter

Naudé, Y. and Rohwer, E.R., 2012. The olfactometric analysis of milk volatiles with a novel gas chromatography based method – a case study in synergistic perception of aroma compounds. In: Marsili, R. (Ed.), *Flavor, Fragrance, and Odor Analysis*, Second Edition. Taylor & Francis Group LLC, Boca Raton, Florida, pp. 93-110 (Chapter 5).

Additional outputs based on thesis work

Oral presentation

Y. Naudé, P. Gorst-Allman and E.R. Rohwer, “Investigating the coffee flavour in South African Pinotage wine using novel off-line olfactometry and TDS-GCxGC-TOFMS”, *The 36th International Symposium on Capillary Chromatography 2012*, 28 May-01 June 2012, Riva del Garda, Italy.

Poster presentations

Y. Naudé, M. van Rooyen and E.R. Rohwer, “Investigating the origin of the enigmatic fairy circles of Namibia by using a simple silicone rubber sampling device and GCxGC-TOFMS”, *ChromSAAMS 2012*, 7-10 October 2012, Dikhololo, South Africa.

Y. Naudé and E.R. Rohwer, “Investigating the coffee-chocolate flavour in South African Pinotage wine using novel off-line olfactometry and TDS-GCxGC-TOFMS”, *ChromSAAMS 2012*, 7-10 October 2012, Dikhololo, South Africa.

Y. Naudé and E.R. Rohwer, “New multidimensional chromatographic methods for enantiomeric analysis of *o,p'*-DDT/D in soil”, *The 34th International Symposium on Capillary Chromatography 2010*, 30 May-04 June, Riva del Garda, Italy. Also presented at *Analitika 2010*, 05-09 December 2010, Stellenbosch, South Africa.

Y. Naudé, R. Bornman and E.R. Rohwer, “A new method for quantitative determination of free molecular and particle bound DDT in contaminated indoor air by GC-MS”, *The 18th International Mass Spectrometry Conference 2009*, 30 August-04 September 2009, Bremen, Germany.

Y. Naudé, R. Bornman and E.R. Rohwer, “A new sampling method for the detection of DDT in contaminated indoor air”, *ChromSAAMS 2008*, 12-15 October 2008, Bela Bela, South Africa.

Y. Naudé, M. van Aardt, E.M. Buys, R. de Kock and E.R. Rohwer, “The olfactory assessment of milk volatiles by a new method of capturing and releasing gas chromatographic fractions”, *The 32nd International Symposium on Capillary Chromatography 2008*, 25-30 May 2008, Riva del Garda, Italy. Also presented at *ChromSAAMS 2008*, 12-15 October 2008, Bela Bela, South Africa.

Provisional patents

Fraction Collector, SA provisional patent application ZA 2006/07538; E.R. Rohwer, M.J. Lim Ah Tock, Y. Naudé; filed on 5 September 2006.

A method of analysing a gas sample, SA provisional patent application ZA 2006/07760; E.R. Rohwer, B. Dryden-Schofield, P.B.C. Forbes and Y. Naudé; filed on 15 September 2006.

Table of contents

Summary	iv	
Acknowledgements	vii	
Publications, presentations and provisional patents	ix	
Abbreviations	xvi	
List of Tables	xvii	
List of Figures	xviii	
CHAPTER 1	INTRODUCTION	1
1.1	DDT in indoor air	1
1.2	Enantiomeric analysis of DDT in soil and air	5
1.3	Mysterious fairy circles of Namibia – a geochemical investigation	9
1.4	Aroma investigations	10
	1.4.1 Ultra high temperature (UHT) milk	10
	1.4.2 Pinotage wine	13
1.5	Aim of this study	15
1.6	Structure of the thesis	16
1.7	References	17
CHAPTER 2	NOVEL METHOD FOR DETERMINING DDT IN VAPOUR AND PARTICULATE PHASES WITHIN CONTAMINATED INDOOR AIR IN A MALARIA AREA OF SOUTH AFRICA	21
2.1	Introduction	24
2.2	Materials and methods	27
	2.2.1 Chemical standards	27
	2.2.2 Denuder sampling device	28
	2.2.2.1 Battery operated field pump	30
	2.2.3 Indoor air sampling	30
	2.2.4 Indoor air analyses by GC-MS	31
	2.2.4.1 Quantification	32
2.3	Results and discussion	35
	2.3.1 Evaluation of <i>p,p'</i> -DDT degradation during thermal desorption and CIS injection	35
	2.3.2 Vapour phase and particulate phase DDT in indoor air	37
	2.3.2.1 Ratios of <i>o,p'</i> -DDT relative to <i>p,p'</i> -DDT	43
	2.3.2.2 Ratios of DDD and DDE relative to DDT	44
	2.3.2.3 Indoor air chemical profile	46
	2.3.3 Comparison of PUF and denuder (multi-channel PDMS trap + filter + multi-channel PDMS trap) samplers	47
2.4	Conclusions	49
2.5	Acknowledgements	50
2.6	References	51

CHAPTER 3	TWO MULTIDIMENSIONAL CHROMATOGRAPHIC METHODS FOR ENANTIOMERIC ANALYSIS OF <i>o,p'</i>-DDT AND <i>o,p'</i>-DDD IN CONTAMINATED SOIL AND AIR IN A MALARIA AREA OF SOUTH AFRICA	53
3.1	Introduction	56
3.2	Materials and methods	58
	3.2.1 Sampling site	58
	3.2.2 Chemicals and equipment	59
	3.2.3 Solventless concentration methods for <i>p,p'</i> -DDT, <i>o,p'</i> -DDT, <i>p,p'</i> -DDD, <i>o,p'</i> -DDD, <i>p,p'</i> -DDE and <i>o,p'</i> -DDE	60
	3.2.3.1 Soil sampling with PDMS loops	60
	3.2.3.2 Denuder indoor air sampling	61
	3.2.4 Multichannel open tubular PDMS traps (MCTs) for heart-cut collection of GC separated isomer peaks	62
	3.2.5 Multidimensional GC techniques	62
	3.2.5.1 Apolar separation	62
	3.2.5.2 Chiral separation	65
	3.2.6 Data analysis	67
3.3	Results and discussion	68
	3.3.1 Solventless extraction and desorption-injection	68
	3.3.2 Novel isomer selective off-line heart-cutting by GC fraction collection onto PDMS MCTs	69
	3.3.3 Comparison of chiral separation by one dimensional and multidimensional gas chromatography	70
	3.3.4 Multidimensional chromatographic performance	72
	3.3.5 Enantiomeric signatures of outdoor soil and indoor air samples by off-line heart-cut GCFC and GCxGC	75
3.4	Conclusions	79
3.5	Acknowledgements	80
3.6	References	80
CHAPTER 4	EVIDENCE FOR A GEOCHEMICAL ORIGIN OF THE MYSTERIOUS CIRCLES IN THE PRO-NAMIB DESERT	82
4.1	Introduction	85
4.2	Materials and methods	90
	4.2.1 Study area	91
	4.2.2 Measurement of CO and O ₂	91
	4.2.3 Extraction of compounds from soil	92
	4.2.4 Identification of compounds by GC-MS	94
4.3	Results and discussion	95
	4.3.1 Gas detection	95
	4.3.1.1 Plant stress response to natural gas seeps	95
	4.3.1.2 Bare soil circles	98
	4.3.1.3 Newly formed circles	101
	4.3.2 TDS-CIS-GC-MS of extracted soil samples	104
	4.3.2.1 Saturated alkanes	104
	4.3.2.2 Alkenes	106

4.3.3	Seepage-induced stimulation of vegetation growing on the edge of fairy circles	109
4.3.4	Hydrocarbon-induced magnetic anomalies	111
4.3.5	Relationships between mima mounds (“heuweltjies”) and fairy circles	113
4.4	Conclusions	118
4.5	Acknowledgements	119
4.6	References	120
4.7	Appendix A	124
CHAPTER 5	MULTI-CHANNEL OPEN TUBULAR TRAPS FOR HEADSPACE SAMPLING, GAS CHROMATOGRAPHIC FRACTION COLLECTION AND OLFACTORY ASSESSMENT OF MILK VOLATILES	127
5.1	Introduction	130
5.2	Experimental	133
5.2.1	Chemical standards	133
5.2.2	Milk samples	133
5.2.3	Extraction of Aroma Compounds	134
5.2.3.1	Multi-channel open tubular PDMS trap	134
5.2.3.2	Sample preparation	134
5.2.4	GC-FID with thermal desorption and cryo inlet system	135
5.2.5	Quantification	136
5.2.6	Capturing of single compounds and fractions by gas chromatography fraction collection (GCFC)	137
5.2.7	Olfactory evaluation of captured fractions and single compounds on secondary MCTs	138
5.2.8	Identification of volatile compounds by GC-MS	139
5.3	Results and discussion	140
5.3.1	Extraction of aroma compounds and GC-FID with thermal desorption and CIS	140
5.3.2	Quantification of the aroma compounds	142
5.3.3	Capturing of single compounds and fractions by GCFC	143
5.3.4	GC-MS of a compound recaptured by GCFC	146
5.3.5	Release of recaptured aroma compounds and the aroma of the overall milk profile from the MCTs for off-line olfactory assessment	146
5.3.6	Evaluation of combinations of compounds to assess synergistic effects	150
5.4	Conclusions	151
5.5	Acknowledgements	152
5.6	References	152
CHAPTER 6	THE OLFACTOMETRIC ANALYSIS OF MILK VOLATILES WITH A NOVEL GAS CHROMATOGRAPHY BASED METHOD – A CASE STUDY IN SYNERGISTIC PERCEPTION OF AROMA COMPOUNDS	154
6.1	Introduction	155

6.2	Sorptive extraction	158
	6.2.1 Commercial sample enrichment techniques	158
	6.2.2 Novel multi-channel sample enrichment devices	159
	6.2.2.1 Multi-channel silicone (PDMS) rubber traps	160
6.3	High capacity headspace sorptive extraction of aroma compounds from milk followed by TDS-CIS-GC-FID	162
6.4	Novel heart-cutting fraction collection GC based methods	164
	6.4.1 Capturing of single compounds and their combinations by off-line heart-cut gas chromatography fraction collection (GCFC)	165
6.5	Off-line olfactory evaluation of single compounds and their combinations	168
	6.5.1 Slow release of the aroma of single compounds captured by GCFC on individual secondary MCTs	169
	6.5.2 Slow release of the total milk aroma profile captured by purge-and-trap on primary MCTs	169
	6.5.3 Slow release of heart-cuts of combinations of single compounds captured by GCFC on individual secondary MCTs	172
6.6	Summary	174
6.7	Acknowledgements	175
6.8	References	175
 CHAPTER 7 INVESTIGATING THE COFFEE FLAVOUR IN SOUTH AFRICAN PINOTAGE WINE USING NOVEL OFF-LINE OLFACTOMETRY AND COMPREHENSIVE GAS CHROMATOGRAPHY WITH TIME OF FLIGHT MASS SPECTROMETRY		 180
7.1	Introduction	183
7.2	Materials and methods	186
	7.2.1 Wine samples	186
	7.2.2 Chemical standards	186
	7.2.3 Sorptive extraction with multichannel open tubular PDMS traps	186
	7.2.4 Heart-cutting with GC-FID: Capturing of single compounds, combinations of compounds, or fractions by GC-FC	188
	7.2.5 Off-line olfactometry	189
	7.2.6 GCxGC-TOFMS	189
7.3	Results and discussion	
	7.3.1 Multichannel PDMS traps	191
	7.3.2 Heart-cutting by GC-FC and off-line olfactometry	191
	7.3.3 Identification of the compounds in the roast coffee bean-like fraction M2 by GCxGC-TOFMS	195
7.4	Conclusions	198
7.5	Acknowledgements	199
7.6	References	199
 CHAPTER 8 CONCLUSION		 202

Abbreviations

Amu	Atomic mass unit
AOMT	American oak medium toast
AOMT+	American oak medium toast plus
CIS	Cooled injection system
CO	Carbon monoxide
DDD	1,1-Dichloro-2,2-bis(<i>p</i> -chlorophenyl)ethane
DDE	1,1-Dichloro-2,2-bis(<i>p</i> -chlorophenyl)ethene
DDT	1,1,1-Trichloro-2,2-bis(<i>p</i> -chlorophenyl)ethane
EF	Enantiomeric fraction
FID	Flame ionisation detector
FOMT	French oak medium toast
FOMT+	French oak medium toast plus
GC	Gas chromatography
GCFC	Gas chromatographic fraction collection
GC-FID	Gas chromatography flame ionisation detection
GCxGC-TOFMS	Comprehensive two-dimensional gas chromatography time of flight mass spectrometry
GC-MS	Gas chromatography mass spectrometry
GC-O	Gas chromatography olfactometry
GC-TOFMS	Gas chromatography time of flight mass spectrometry
HS-SPDE	Headspace solid phase dynamic extraction
HS-SPME	Head space solid phase microextraction
IRS	Indoor residual spraying
LLE	Liquid-liquid extraction
MCT	Multichannel open tubular silicone rubber trap
MDGC	Multidimensional gas chromatography
MSD	Mass selective detector
O ₂	Oxygen
PAH	Polycyclic aromatic hydrocarbon
PDMS	Polydimethylsiloxane
POP	Persistent organic pollutant
POPs	Persistent organic pollutants
PTFE	Polytetrafluoroethylene
PTV	Programmable temperature vaporisation
PUF	Polyurethane foam
RI	Retention index
SAFE	Solvent extraction with solvent-assisted flavour evaporation
SBSE	Stir bar sorptive extraction
SIM	Selected ion monitoring
SPE	Solid phase extraction
SPE-tD	Solid phase extraction-thermal desorption
SPME	Solid phase microextraction
TDS	Thermal desorber system
UCM	Unresolved complex mixture
UHT	Ultra high temperature

List of tables

Table 2.1	Linear regression analysis for <i>p,p'</i> -DDT, <i>o,p'</i> -DDT, <i>p,p'</i> -DDD, <i>o,p'</i> -DDD, <i>p,p'</i> -DDE and <i>o,p'</i> -DDE	34
Table 2.2	Comparison of the effect of TDS and CIS heating rates and of conventional injection on % degradation of DDT	36
Table 2.3	Advantages and disadvantages of thermal desorption-injection	39
Table 2.4	DDT, DDD, DDE ($\mu\text{g m}^{-3}$) in indoor air and fraction of the concentration in vapour phase (%) of five huts sampled at intervals prior to IRS, directly after IRS, 4 h and 24 h after IRS	42
Table 2.5	Comparison of mean indoor airborne Σ DDT ($\mu\text{g m}^{-3}$) values obtained with PUF and a denuder PDMS trap+filter+PDMS trap sampler directly after indoor DDT-spraying (0 h), 4 h and 24 h after IRS	49
Table 3.1	Comparison of enantiomeric fractions (EF) of <i>o,p'</i> -DDD and <i>o,p'</i> -DDT in outdoor soil and indoor air from a DDT exposed village determined by off-line GCFC–GC-TOFMS and GCxGC-TOFMS	74
Table 3.2	Enantiomeric fractions (EF) of <i>o,p'</i> -DDD and <i>o,p'</i> -DDT in indoor air vapour phase and indoor airborne particulate phase from a DDT exposed village directly after indoor residual spraying (0 h)	77
Table 4.1	GCxGC-TOFMS method parameters	125
Table 5.1	GCFC event times - peak capturing time table	138
Table 5.2	Regression equations for UHT milk aroma compounds spiked into long life packaged UHT milk (2% milk fat)	143
Table 5.3	Concentrations of the aroma compounds in UHT milk (2% milk fat) used for GCFC and olfactory assessment	143
Table 5.4	Olfactory assessment of recaptured single compounds on individual secondary MCTs ¹ , the overall milk aroma on primary MCTs ² and combinations of compounds recaptured onto secondary MCTs ³	149
Table 6.1	Olfactory assessment of single compounds captured by GCFC on individual secondary MCTs ¹ , the overall milk aroma collected on a primary MCT ² and binary combinations of compounds captured by GCFC onto secondary MCTs ³	171

List of figures

Figure 1.1	Miniature denuder sampler.	5
Figure 1.2	A) Degradation of DDT to form DDD by reductive dechlorination. (B) Degradation of DDT to form DDE by elimination of HCl.	6
Figure 1.3	Silicone elastomer (PDMS) loop sampler fits a commercial glass desorption tube.	8
Figure 1.4	Multichannel PDMS trap sampler.	11
Figure 2.1	(A) Cross-section of a multichannel silicone rubber trap. (B) A novel low pressure-drop miniature denuder. (C) Silicone elastomer (PDMS) tubes are arranged in parallel inside of a commercial glass desorption tube to give a PDMS sorptive volume of 600 μL .	29
Figure 2.2	(A) SIM chromatogram of the lowest calibration standard 0.5 $\text{pg } \mu\text{L}^{-1}$ – 2.4 $\text{pg } \mu\text{L}^{-1}$. (B) Overlay of SIM chromatograms of 4 L of indoor air: prior to DDT IRS and after DDT IRS.	37
Figure 2.3	Concentrations of <i>p,p'</i> -DDT, <i>o,p'</i> -DDT, <i>p,p'</i> -DDD, <i>o,p'</i> -DDD, <i>p,p'</i> -DDE and <i>o,p'</i> -DDE ($\mu\text{g m}^{-3}$) in vapour (VP) and particulate phases (PP) in indoor air averaged for five huts.	41
Figure 3.1	PDMS loop prior to (A) and after extraction (B) of soil. A loop arrangement prevents soil from entering the silicone rubber tubing.	61
Figure 3.2	Collection of heart-cuts of <i>o,p'</i> -DDD and <i>o,p'</i> -DDT from the GC effluent onto a multichannel trap.	64
Figure 3.3	Enantiomeric profiling by off-line GCFC–GC-TOFMS.	69
Figure 3.4	Comparison of conventional and multidimensional GC techniques.	71
Figure 4.1a	Pock marked landscape of the Pro-Namib desert.	89
Figure 4.1b	Circular patch of barren soil in the NamibRand Nature Reserve in Namibia, southern Africa.	89
Figure 4.2	Map of Namibia indicating the approximate location where gases were monitored and soil samples were collected in NamibRand Nature Reserve and of some major faults and fault thrusts in the vicinity of the sampling site.	90
Figure 4.3	PDMS loop (tube ends joined with a piece of capillary column) used for the extraction of soil (bottom), PDMS loop after extraction and inserted inside a TDS tube for desorption into a GC-MS (top).	94
Figure 4.4	Field measurement of O_2 and CO in the soil of barren circles and controls (matrix).	100
Figure 4.5	Field measurement of O_2 and CO in the soil of a patch of dead vegetation, control (matrix) and a patch of dead and yellowed vegetation.	103
Figure 4.6	Reconstructed ion chromatogram (112 amu) of alkenes (microbiological degradation product of alkanes) relative to alkanes measured in soils collected from barren soil circles (Circles 2.1 and 1.3), between barren soil circles (Matrix 2,1, 1.3) and two newly formed circles (dead and stressed vegetation; dead vegetation).	106

Figure 4.7a	Magnetic stir bar with magnetic soil particles accumulated from 40 g soil collected from a circular patch of dead and yellowed vegetation. See section 3.4 for details.	113
Figure 4.7b	Magnetic stir bar with magnetic soil particles accumulated from 40 g soil collected between the circles (Matrix 1.3). See section 3.4 for details.	113
Figure 4.8	Fossil fuel biomarkers, pristane and phytane, are present in soil from a newly developed fairy circle (patch of dead vegetation). Pristane and phytane confirm a geochemical origin of the fairy circles.	126
Figure 5.1	(A) Cross section of a MCT. (B) MCT fits a commercial glass desorption tube.	135
Figure 5.2	Removed detector top assembly and collector. MCT placed on GC-FID flame tip to recapture single peaks or various fractions. Helium was used as the make-up gas.	138
Figure 5.3	Trapping and re-injection efficiency: comparison of the desorption of the secondary MCTs containing the recaptured compounds (single compounds were recaptured from the GC effluent all on the same secondary MCT) of spiked (195 - 245 µg/l) and unspiked (1 - 44 µg/l) UHT milk (2% milk fat) to the primary chromatogram of UHT milk (2% milk fat) spiked at 195 - 245 µg/l.	145
Figure 5.4	Secondary chromatograms of packaged long life UHT milk spiked at 195 - 245 µg/l. The single compounds (2-nonanone and nonanal) were separately collected on two different MCTs. The peaks captured were 23 s apart.	145
Figure 6.1	Multichannel silicone (PDMS) rubber trap (MCT).	162
Figure 6.2	Fraction collection and off-line evaluation of synergistic perceptions of aroma compounds.	167
Figure 7.1	Solvent free concentration with silicone rubber PDMS tubing.	188
Figure 7.2	Heart-cutting and off-line olfactometry: identifying the fraction of a chromatogram responsible for a coffee odour.	193
Figure 7.3	Contour plot of a reconstructed ion chromatogram (96 + 98 amu) shows the presence of furfural (440 s, 3.070 s) and 2-furanmethanol (465 s, 2.430 s) in heart-cut M2.	196
Figure 7.4	Reconstructed first dimension ion chromatograms of furfural (96 amu) and 2-furanmethanol (98 amu) in a coffee style Pinotage wine (oak staves in tanks, maturation for three months) (orange chromatogram A) compared to a traditional style Pinotage wine (used French oak barrel maturation for ten months) (green chromatogram B).	198

Chapter 1

Introduction

Extraction is needed to separate and concentrate trace level analytes from the sample matrix prior to gas chromatographic (GC) analyses. Classical extraction procedures utilise large amounts of expensive solvents, generate hazardous waste, and sensitivity limitations are associated with the injection of microlitre amounts of the final solvent extract volume [1,2]. To overcome the problems associated with solvent extraction, solvent free sorptive techniques for the isolation of analytes from matrices are required.

1.1 DDT in indoor air

DDT (1,1,1-trichloro-2,2-bis(*p*-chlorophenyl)ethane), an organochlorine insecticide, is still used for malaria vector control in risk regions in South Africa. The strict Stockholm Convention on Persistent Organic Pollutants (POPs) permits Indoor Residual Spraying (IRS) of traditional dwellings with DDT. In South Africa, IRS with DDT resulted in a 65% decrease in the number of deaths caused by malaria and an 83% decrease in the number of confirmed malaria cases [3]. At present there are no effective insecticides that could replace DDT

[4]. To evaluate the potential health risk of exposure of populations to endocrine disrupting chemicals reliable analytical data is essential. This study was initiated after a request from Professor Riana Bornman, Department of Urology, University of Pretoria, to collaborate and to measure the levels of DDT in contaminated indoor air and soil in a malaria area of South Africa.

Semivolatile organic compounds are present in air, either adsorbed onto dust particles or as free gas phase molecules [5,6]. Exposure may be *via* inhalation of gas and particulate phase compounds, or by ingestion. Once larger sized contaminated particles are inhaled it deposits in the upper respiratory tract and is swallowed [7]. In rural villages contaminated dust presents a pathway for exposure to DDT, especially when the dust is disturbed during domestic activities in and around traditional dwellings. Conventional high volume collection systems for POPs are polyurethane foam (PUF) [7,8] or polymeric resin (XAD-2 or XAD-4) [8,9]. PUF samples total air, *i.e.*, vapour and particulate phases, and does not distinguish between contributions from each phase. In order to sample both phases, glass fibre or quartz filters are placed upstream of the solid sorbents to first collect particulate phase pesticides while vapour phase is trapped onto the sorbent [8,10-16]. After sampling the materials are separately extracted by Soxhlet extraction (16-36 h) with large amounts of solvents, or by sonication [9,11,17], concentrated by Kuderna Danish or rotary evaporation, followed by nitrogen gas blow-down [8,10-16]. Microlitre amounts are injected for analysis. This approach is quite successful but involves many preparation steps, large amounts of solvents, loss of analyte, introduction of interferences and potential errors [2]. Moreover, sensitivity

limitations are associated with injection of only a fraction of the final solvent concentrate [2].

By placing the filter upstream of a solid sorbent particulate phase organic compounds may be underestimated due to a loss of the reversibly adsorbed molecules on the filter – the so called blow-off effect [10,12,18]. Adsorption of the gas phase fraction onto particles already collected, or by the filter itself, may also occur [10,13]. Diffusion denuder samplers were developed to overcome the problems associated with filter+PUF samplers [13]. By placing a filter after the low-flow denuder sampler to collect the particles, the collection of gas and particulate phases is reversed from the conventional high-volume sampler [18]. Due to a difference in vapour and particle diffusivities, diffusion denuders first separate the vapour phase from the particulate phase [13]. Denuder fabrication procedures are cumbersome. Denuder materials are solvent extracted or thermally desorbed [13]. The use of adsorptive sorbents in combination with thermal desorption to analyse high molecular-weight compounds is problematic due to incomplete desorption [2]. Sample trapping using polydimethylsiloxane (PDMS) performs well in combination with thermal desorption [2]. In contrast with adsorptive concentration, PDMS functions as a hydrophobic solvent for the analytes [2,19]. Ortner and Rohwer [20] constructed thick film silicone rubber (PDMS) traps in a multichannel configuration to concentrate semivolatile organic air pollutants. Advantages of the multichannel PDMS trap over commercial packed or coated sorptive devices are its open tubular structure and low pressure drop associated with laminar multichannel flow [20-22]. Forbes et al. [22] showed that multichannel PDMS traps in combination with

quartz fibre filters could be used as denuders for the sampling of airborne vapour phase and particulate phase polycyclic aromatic hydrocarbons (PAHs).

Considerations for transporting of equipment and sampling in rural areas of South Africa are that electricity is not freely available, travel distances from rural areas to city laboratories are considerable, road conditions are rough both on and off- road, and cargo space is often limited. Simple, small, battery operated field monitoring equipment is therefore preferable to bulky, expensive, conventional high flow PUF based equipment. To address these challenges a miniature denuder sampler for the solvent free determination of DDT in indoor air was employed in this study: vapour and particulate phases are collected separately in a single step with a multichannel open tubular PDMS trap combined with a micro quartz fibre filter (Fig. 1.1). The multichannel PDMS trap consists of multiple silicone elastomer tubes arranged in parallel inside of a commercial glass desorption tube (Fig. 1.1). Air is drawn through the denuder sampler with a small and simple, battery-operated field pump at a low air flow sampling rate and short collection time. The denuder sampler materials are analysed by desorption-injection gas chromatography mass spectrometry (GC-MS).

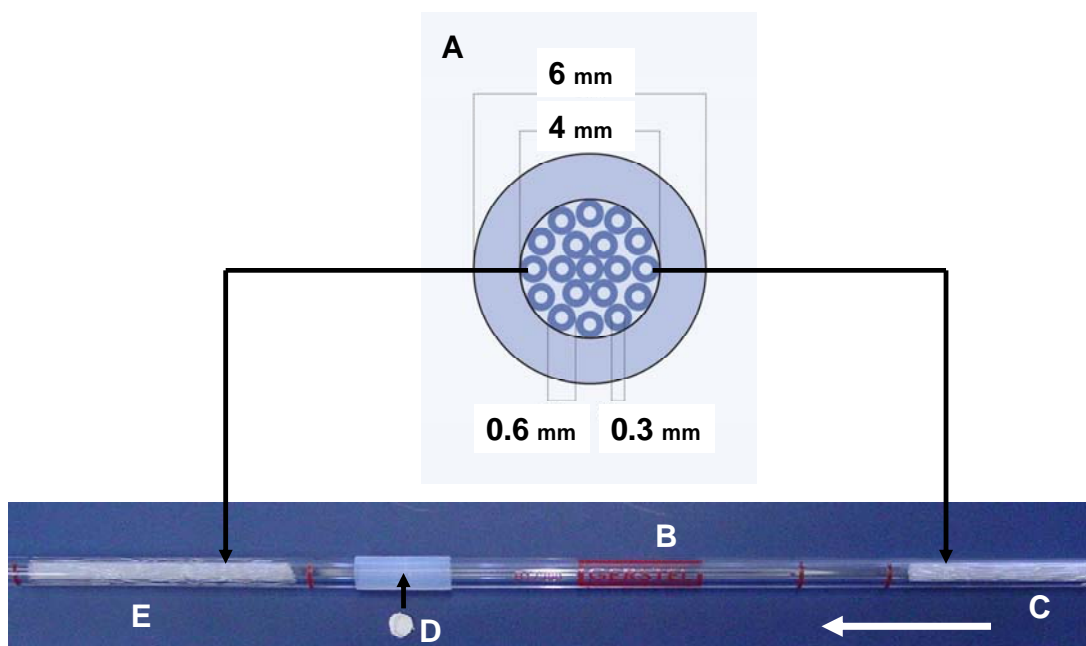


Figure 1.1. Miniature denuder sampler. (A,B) A bundle of silicone elastomer (PDMS) tubes are arranged in parallel inside of a commercial glass desorption tube. (C) Airborne vapour phase is collected on the first multichannel PDMS trap. (D) Airborne particulate phase is collected on the micro quartz fibre filter. (E) Back-up multichannel PDMS trap to collect blow-off and potential breakthrough. Arrow indicates the direction of the flow of air during sampling. During desorption the flow of carrier gas is in the opposite direction.

1.2 Enantiomeric analysis of DDT in soil and air

Technical grade DDT (75% wettable powder) used for IRS in South Africa contains 72-75% of *p,p'*-DDT, the active ingredient, and ~22% of *o,p'*-DDT [23,24]. In the environment DDT degrades to form DDD (1,1-Dichloro-2,2-bis(*p*-chlorophenyl)ethane) under anaerobic conditions, and DDE (1,1-Dichloro-2,2-bis(*p*-chlorophenyl)ethene) under aerobic conditions [25] [Fig. 1.2].

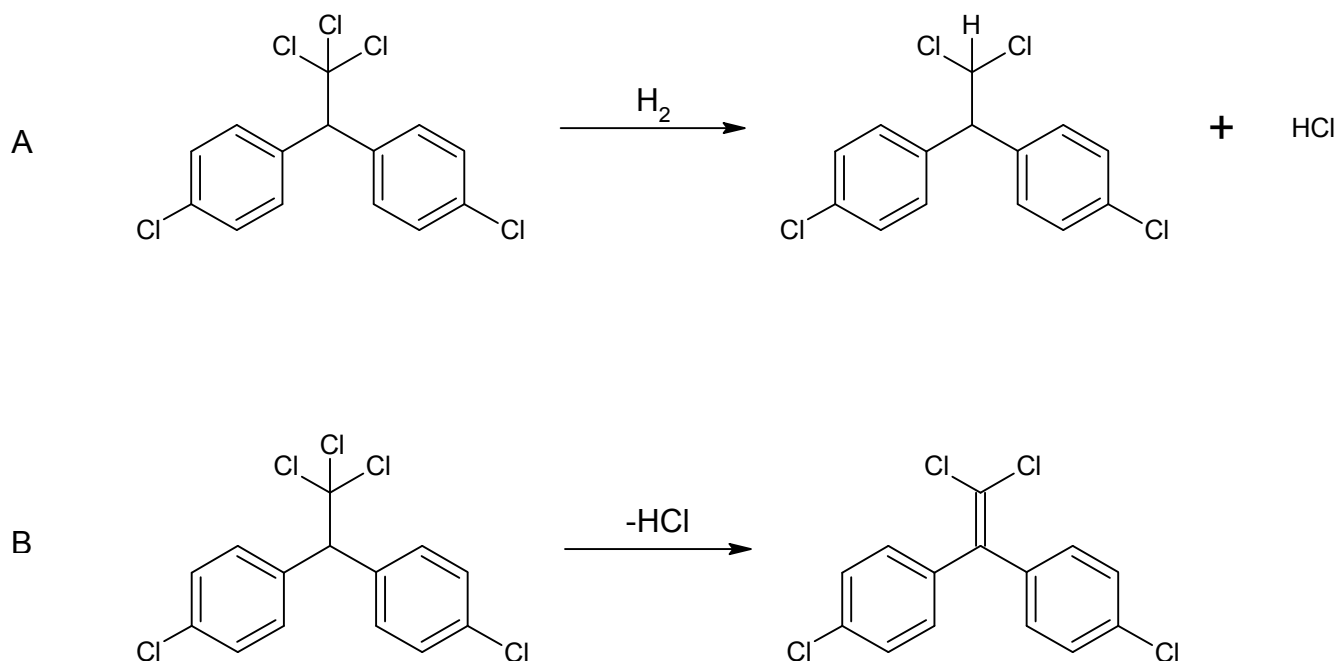


Figure 1.2. (A) Degradation of DDT to form DDD by reductive dechlorination. (B) Degradation of DDT to form DDE by elimination of HCl.

Technical DDT has oestrogen-like properties, mainly due to *o,p'*-DDT [26,27]. *o,p'*-DDT and its degradation product *o,p'*-DDD are chiral molecules (*o,p'*-DDE is achiral). Both *o,p'*-DDT and *o,p'*-DDD exist as enantiomeric pairs (-)-*o,p'*-DDT and (+)-*o,p'*-DDT, and (-)-*o,p'*-DDD and (+)-*o,p'*-DDD [28,29]. New treatment with technical DDT will have a chiral signature where enantiomers of *o,p'*-DDT and of *o,p'*-DDD are present as a 1:1 racemic mixture corresponding to an enantiomeric fraction (EF) = 0.5 [30]. Due to microbial degradation processes in the environment selective breakdown of one enantiomer of a pair can result in non-racemic residues [30]. Therefore, a deviation of an EF from 0.5 in samples may be used to differentiate between recent and past inputs of POPs [29,31,32]. *o,p'*-DDT is reported to show enantioselective oestrogenicity since (-)-*o,p'*-DDT is a weak oestrogen mimic

while (+)-*o,p'*-DDT is inactive [27,33,34]. These chiral compounds are separated by using GC columns with a β -cyclodextrin stationary phase specifically developed for this purpose [29,30,34-39]. However, coelution of compounds in complex environmental mixtures can make forensic determinations difficult. To overcome the problem of coelution, chiral analysis of POPs is generally performed by heart-cut multidimensional gas chromatography (MDGC) [29,32,36-38,40-44] and comprehensive two-dimensional gas chromatography (GCxGC) [32,36,38,40,44]. In the heart-cut MDGC technique two independent GC systems are coupled so that one or more unresolved fractions are transferred directly (on-line), by means of a Deans switch, from a first non-enantioselective column (first dimension) to a second enantioselective column (second dimension) where separation of the compounds will occur. In GCxGC the entire sample is separated on two different columns, the first column provides a regular GC elution and the second, shorter, column is fast eluting [37].

Organochlorine pesticides are typically solvent extracted from soil by Soxhlet extraction [7,30,39,41,42,45] and by sonication [29]. In general, final solvent extract volumes range from 20 μ l to 1 ml. As was previously stated, sensitivity limitations are associated with injection of only a fraction of the final solvent extract volume. In contrast to extraction procedures using solvents, the procedure applied in this study is a novel solvent free sorptive extraction technique where DDT is concentrated from soil using PDMS loops (Fig. 1.3). After extraction the loop is inserted into a commercial thermal desorption tube for solventless introduction into a GC. Chiral columns are sensitive to moisture

and matrix components, and therefore desorption-injection rather than liquid extract injection is preferable in order to protect the expensive column.

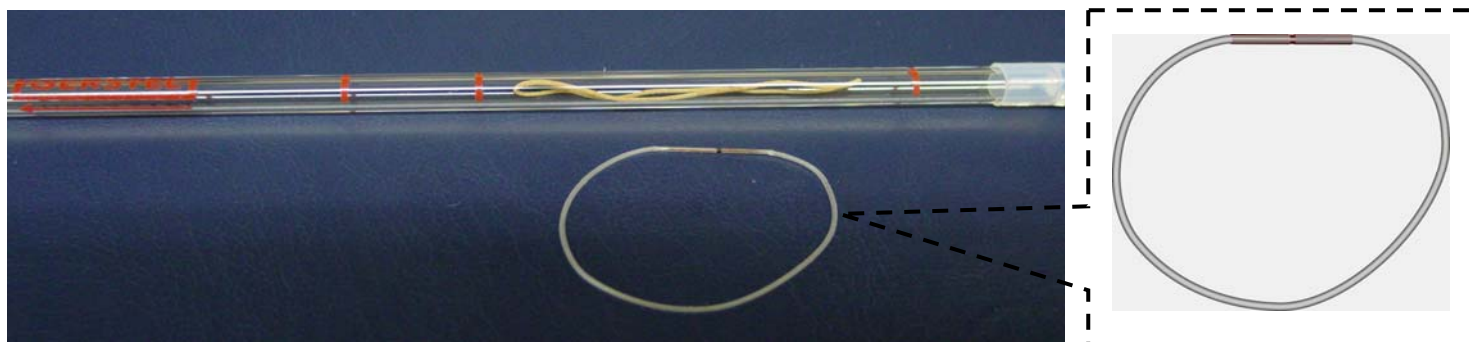


Figure 1.3. Silicone elastomer (PDMS) loop sampler fits a commercial glass desorption tube.

Taking into consideration that DDT residues in soil are emitted into air (soil-air exchange) [30] and that contaminated airborne dust presents a pathway for exposure to DDT, enantiomeric signatures are also determined for indoor air samples in this study. Here, DDT in indoor air is concentrated with a denuder configuration of a multichannel open tubular silicone rubber PDMS trap combined with a micro quartz fibre filter for single-step collection of vapour phase and particulate phase DDT [46].

Novel solvent free sorptive extraction using PDMS loop and multichannel PDMS trap samplers, and an alternative multidimensional approach for heart-cut gas chromatographic fraction collection from a non-enantioselective column followed by second dimension off-line re-injection for isomer selective enantiomeric separation of *o,p'*-DDT and *o,p'*-DDD by GC-TOFMS are reported. Although the conventional on-line heart-cut process of using a Deans switch device is simple an off-line approach offers versatility in that the second

dimension is independent of a specific instrument or even location. This alternative multidimensional procedure is compared to the complementary technique of GCxGC-TOFMS using the same enantioselective column, this time as the first dimension of separation.

1.3 Mysterious fairy circles of Namibia – a geochemical investigation

The origin of the enigmatic pock mark (“fairy circle”) patterned landscape of the Namib Desert, Namibia, southern Africa, has fascinated scientists and the general public for many decades. Causal agents that were proposed are termites, ants, radioactivity, or toxins released by *Euphorbia damarana* plants, all of which lacked conclusive evidence [47,48]. Currently there is no scientifically sound explanation as to the cause of these circular depressions which are usually devoid of vegetation and are often surrounded by a fringe of tall grasses [47]. Van Rooyen et al.’s [47] research confirmed that there is a factor present in the soil that inhibits plant growth inside fairy circles. This study was initiated after an invitation from Professor Gretel van Rooyen, Department of Plant Science, University of Pretoria, to collaborate on the investigation of the origin of the fairy circles of Namibia.

Typically the method for extracting solid samples is Soxhlet extraction of a sizeable soil sample with large volumes of hazardous solvents which potentially can introduce contaminants, followed by the analyses of microlitre amounts of the diluted final extract [1]. A simple, cheap, nonhazardous, solvent free extraction PDMS sampler for the introduction of the total amount of sorbed

analytes into a GC-MS was constructed in-house to specifically manage the easily magnetised desert soil (Fig. 1.3). For the first time, a possible geochemical origin of the fairy circles of Namibia is investigated.

1.4 Aroma investigations

1.4.1 Ultra high temperature (UHT) milk

Professor Riëtte de Kock and co-workers, Department of Food Science, University of Pretoria, are researching innovative active packaging for UHT milk [49]. To evaluate the effectiveness of these packaging materials to reduce off odours they required chromatographic analyses and olfactometry. This study was initiated to meet their requirements.

UHT treatment of milk imparts an undesirable cooked (cabbage, sulphurous, stale, heated, sterile milk) flavour to packaged long life milk [50-53]. In certain cases solvent free aroma extracts may be more representative of food aroma when compared to those obtained by solvent extraction [54]. Solvent free approaches to the isolation of volatile components from food matrices include head space solid phase microextraction (HS-SPME), stir bar sorptive extraction (SBSE), headspace solid phase dynamic extraction (HS-SPDE), headspace trap technology and solid phase extraction-thermal desorption (SPE-tD) [52-68]. SPME (pioneered by Pawliszyn and co-workers), is a fibre coated with a small sorbent volume of 0.6 – 0.9 μl [56,57,68,69]; SBSE (developed by Baltussen and Sandra), is a glass encapsulated magnetic stir bar

coated with volumes of 25 – 200 μl PDMS [57,70]; SPDE is a sorptive coating with a sorbent volume of 6 μl on the inside wall of a stainless steel needle of a gas tight syringe [57,66-68]; while headspace trap technology makes use of a headspace sampler and a built-in trap [68]. The built-in trap is a tube filled with a solid sorbent with a volume of 160 μl [68]. A SPE-tD cartridge is a titanium tube coated with PDMS on both the inside and the outside of the tube. Two lengths are available with a total exposed PDMS volume of 29.5 μl for the 6 mm length and 147 μl for the 30 mm length respectively [61,62]. In contrast to fibres, coated stir bars or tubes filled with a solid sorbent, the high capacity headspace samplers employed in this study for the isolation of aroma volatile compounds from UHT milk are multichannel open tubular silicone rubber (PDMS) traps prepared in-house based on a method by Ortner and Rohwer [20] (Fig. 1.4). The multichannel PDMS trap has a considerably larger volume of 0.6 ml PDMS thereby providing for a greater sample enrichment capacity [71].

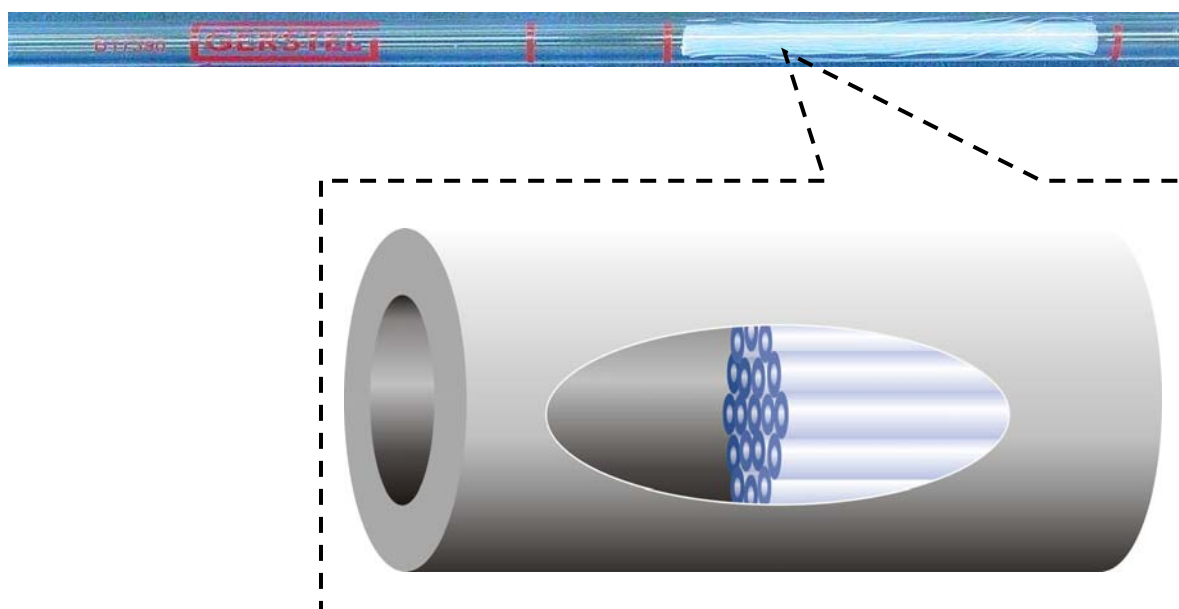


Figure 1.4. Multichannel PDMS trap sampler. Silicone elastomer tubes are arranged in parallel inside of a commercial glass desorption tube.

Analytical methods that have been used to study the aroma of dairy products are GC-MS and gas chromatography olfactometry (GC-O) [55,72-74]. GC-O is traditionally used to investigate individual odour active substances. Aroma perception of the GC effluent is recorded by the human nose, in real time, at the olfactometer outlet. By comparing olfactometric data with chromatographic data, an individual compound can be matched with an odour [75]. However, the rapid elution of compounds may be problematic in terms of recalling appropriate odour descriptors. Furthermore, potential synergistic effects cannot be observed when single compounds are evaluated over time. The result of combining single compounds in a complex matrix may be the emergence of a strikingly different sensory perception, completely unrelated to that of the individual compounds alone [71,76]. Addressing the limitations of evaluating rapidly eluting single compounds as opposed to selective combinatorial mixtures, a heart-cut gas chromatographic fraction collection approach to study, off-line, synergistic perceptions of odourants, was developed [71]. Combinations of compounds are selectively collected from the GC effluent onto multichannel PDMS traps. The odour heart-cuts are gradually released from the multichannel PDMS traps at a selected temperature with a flow of nitrogen gas in a portable off-line olfactometer. Panellists then take turns to sniff the odour (not humidified) thus released. After publication of Naudé et al.'s first report of a combinatorial approach in 2009 [71] gas chromatography recomposition-olfactometry was later independently reported by Johnson et al. (2012) [77]. Although similar in approach Johnson et al.'s (2012) publication does not refer to Naudé et al.'s (2009) [71] first report of selectively combining compounds to study the aroma of mixtures. In Johnson et al.'s (2012) approach

compounds are also recombined as they elute off the GC column. Compounds are collected onto a cold trap. After compound collection the cold trap is rapidly heated and the released mixture is smelled at an olfactory port. An advantage of the technique is the use of a GC-MS equipped with a pneumatic Deans switch and a flow splitter to allow for simultaneous GC-MS/O.

The open tubular structure and low pressure drop of multichannel PDMS traps are features particularly suited to the selective recapturing of aroma fractions, combinations, or single aroma compounds, from the GC effluent during a run and also to the controlled release of the recaptured aroma compounds from the multichannel PDMS traps for off-line olfactometric evaluation. The advantage of a low pressure drop is not offered by conventional packed traps. Multichannel PDMS traps containing recaptured compounds of unknown identity are desorbed into a GC-MS for tentative compound identification. Confirmation of compound identity is performed by comparing retention times and mass spectra to that of authentic reference standards.

1.4.2 Pinotage wine

Pinotage is a unique South African red wine cultivar cross-bred from Pinot Noir and Cinsaut (Hermitage). Isoamyl acetate is a key impact odourant responsible for the distinctive character of Pinotage wines [78]. Recently, Pinotage wine from several South African wine cellars has been produced with a novel coffee flavour. This contemporary aroma profile is deliberately derived

from a particular combination of Pinotage, alternative toasted wood products and malolactic fermentation.

Traditionally, high-quality red wines are matured in oak barrels [79,80]. Compounds present in the wood are extracted into the wine during the aging process. Volatiles transferred into the wine produce distinctive flavours depending on the type of oak, level of toasting and seasoning [80,81]. Barrels are expensive, have a short lifetime (3-5 years) and maturation is a slow process. Recently, as an alternative to traditional wine aging, the maturation process is accelerated by adding toasted oak chips or staves to wine kept in stainless steel tanks or used barrels [79-81]. By exploiting the larger surface area of these alternative oak products wood derived compounds are transferred rapidly into the wine in relative short periods compared to traditional barrel maturation. A desired flavour profile can be selected depending on the toast level and type of oak product used.

Sample preparation techniques for isolating compounds from wine for analysis are SBSE [82-85], SPME [80,85-88], solid phase extraction (SPE) [89,90], or liquid-liquid extraction (LLE) [81,89]. In the case of SPE or LLE, once again sensitivity limitations are associated with analysis of microlitre amounts of the final solvent extract volume. Milder than solvent extraction solvent free sample enrichment may provide aroma extracts that are a closer representation of food aroma when compared to those obtained by solvent extraction [54]. SPME and SBSE are efficient commercial solvent free sorptive extraction alternatives to procedures using solvents. However, as was

discussed earlier multichannel open tubular silicone rubber (PDMS) samplers, assembled in-house and employed in this study, have a considerably larger volume of 0.6 ml PDMS, thus offering a higher sample enrichment capacity when compared to SPME or SBSE [71]. The analytes are concentrated by a purge-and-trap method onto a multichannel PDMS trap, followed by thermal desorption of the PDMS trap into a gas chromatograph with flame ionisation detection (GC-FID) or GCxGC-TOFMS.

The same heart-cut technique and off-line olfactometry approach used to evaluate the aroma of UHT milk is also applied to the investigation of the coffee flavour in coffee style Pinotage wine. Selective recapturing of odor active compounds from the GC effluent onto multichannel PDMS traps allows for off-line second dimension analysis by GCxGC-TOFMS.

Solvent free sampling using PDMS for high capacity analyte enrichment from Pinotage wines, GC fraction collection (heart-cutting) onto multichannel PDMS traps for 1) off-line olfactory evaluation of synergistic effects and for 2) off-line second dimension analysis by GCxGC-TOFMS for compound separation and identification (using authentic reference standards) to correlate odour with specific compounds are reported.

1.5 Aim of this study

In view of the challenges facing laboratories in developing countries in terms of equipment availability and cost, the purpose of this study is to construct

versatile PDMS samplers in-house for solvent free sample enrichment; for a versatile multidimensional chromatographic approach involving heart-cut gas chromatographic fraction collection; and for environmental, geochemical and aroma investigations.

1.6 Structure of the thesis

The research chapters do not follow a chronological order, but are presented accordingly to theme. The format of the research chapters, including the style of referencing, follows that required by the particular journals to which the chapters were submitted to, and published in. For this reason the style is not consistent and some repetition of technical detail is unavoidable. Chapter 2 describes multichannel PDMS traps combined with micro quartz fibre filters as denuder samplers for measuring trace airborne vapour and particulate phase DDT and its associated environmental pollutants in indoor air by GC-MS. Chapter 3 describes PDMS loop samplers for the extraction of DDT and DDD from soil, and an off-line multidimensional GC approach for enantiomeric separation and its comparison to the complementary technique of GCxGC-TOFMS; while in Chapter 4 the extraction of geochemical hydrocarbons from desert soil with a PDMS loop sampler is presented. Multichannel PDMS traps for headspace sampling, for heart-cutting by gas chromatographic fraction collection, for off-line olfactory evaluation of synergistic aroma effects and for an off-line multidimensional chromatographic approach for the investigation of the aroma of UHT milk are described in Chapters 5 and 6; and are also reported in

Chapter 7 for the investigation of the aroma of Pinotage wine. Lastly, overall conclusions are drawn in Chapter 8.

1.7 References

- [1] J. Pawliszyn, *Anal. Chem.* 75 (2003) 2543-2558.
- [2] E. Baltussen, C.A. Cramers, P.J.F. Sandra, *Anal. Bioanal. Chem.* 373 (2002) 3-22.
- [3] World Malaria Report, World Health Organisation (2010) [online]. Available: http://www.who.int/malaria/publications/country-profiles/profile_zaf_en.pdf (Accessed 28.06.2011).
- [4] World Malaria Report, World Health Organisation (2011) [online]. Available: http://who.int/malaria/world_malaria_report_2011/en/index.html (Accessed 31.01.2012).
- [5] J. Volckens, D. Leith, *Ann. Occup. Hyg.* 47(2) (2003) 157-164.
- [6] P. Larsson, O. Berglund, C. Backe, G. Bremle, A. Eklöv, C. Järnmark, A. Persson, *Naturwissenschaften* 82 (1995) 559-561.
- [7] J.C. Van Dyk, H. Bouwman, I.E.J. Barnhoorn, M.S. Bornman, *Sci. Total Environ.* 408 (2010) 2745-2752.
- [8] M. Millet, in: J.L. Tadeo (Ed.), *Sampling and Analysis of Pesticides in the Atmosphere*, CRC Press, Boca Raton, Florida, 2008, pp. 257-286.
- [9] E. Borrás, P. Sánchez, A. Muñoz, L.A. Tortajada-Genaro, *Anal. Chim. Acta* 699(1) (2011) 57-65.
- [10] M. Possanzini, V. Di Palo, P. Gigliucci, M.C.T. Scianò, A. Cecinato, *Atmos. Environ.* 38 (2004) 1727-1734.
- [11] M. Possanzini, V. Di Palo, G. Tagliacozzo, A. Cecinato, *Polycycl. Aromat. Comp.* 26(3) (2006) 185-195.
- [12] A.J. Peters, D.A. Lane, L.A. Gundel, G.L. Northcott, K.C. Jones, *Environ. Sci. Technol.* 34 (2000) 5001-5006.
- [13] D.E. Tobias, J.A. Perlinger, P.S. Morrow, P.V. Doskey, D.L. Perram, *J. Chromatogr. A* 1140 (2007) 1-12.
- [14] S.A. Batterman, S.M. Chernyak, Y. Gounden, M. Matooane, R.N. Naidoo, *Sci. Total Environ.* 397 (2008) 119-130.
- [15] H. Alegria, T.F.R. Bidleman, M. Salvador Figueroa, *Environ. Pollut.* 140 (2006) 483-491.
- [16] R. Barro, J. Regueiro, M. Llompert, C. Garcia-Jares, *J. Chromatogr. A* 1216 (2009) 540-566.
- [17] M. Goriaux, B. Jourdain, B. Temime, J.-L. Besombes, N. Marchand, A. Albinet, E. Leoz-Garziandia, H. Wortham, *Environ. Sci. Technol.* 40 (2006) 6398-6404.
- [18] P. Bohlin, K.C. Jones, B. Strandberg, *J. Environ. Monit.* 9 (2007) 501-509.
- [19] P.B.C. Forbes, E.R. Rohwer, *Environ. Pollut.* 157 (2009) 2529-2535.
- [20] E.K. Ortner, E.R. Rohwer, *J. High Res. Chromatog.* 19 (1996) 339-344.
- [21] P.B.C. Forbes, E.R. Rohwer, *WIT Trans. Ecol. Envir.* 116 (2008) 345-

- 355.
- [22] P.B.C. Forbes, E.W. Karg, R. Zimmermann, E.R. Rohwer, *Anal. Chim. Acta* 730 (2012) 71-79.
- [23] H. Bouwman, R. Bornman, C. van Dyk, I. Barnhoorn, H. Kylin. Dynamics and risks of DDT applied indoors for malaria control. Poster presentation at the 12th EuCheMS International Conference on Chemistry and the Environment, Stockholm, Sweden, 14-17 June 2009.
- [24] H. Bouwman, B. Sereda, H.M. Meinhardt, *Environ. Pollut.* 144 (2006) 902 – 917.
- [25] Y. Naudé, W.H.J. de Beer, S. Jooste, L. van der Merwe, S.J. van Rensburg, *Water SA* 24(3) (1998) 205-214.
- [26] R. Bornman, C. de Jager, Z. Worku, P. Farias, S. Reif, *BJUI.* (2009) 1-7.
- [27] A.W. Garrison, V.A. Nzengung, J.K. Avants, J.J. Ellington, W.J. Jones, D. Rennels, N.L. Wolfe, *Environ. Sci. Technol.* 34 (2000) 1663-1670.
- [28] H.R. Buser, M.D. Muller, *Anal.Chem.* 67 (1995) 2691-2698.
- [29] J. Muñoz-Arnanz, C. Bosch, P. Fernandez, J.O. Grimalt, B. Jimenez, *J. Chromatogr. A.* 1216 (2009) 6141–6145.
- [30] K. Wiberg, T. Harner, J.L. Wideman, T.F. Bidleman, *Chemosphere* 45 (2001) 843-848.
- [31] S. Corsolini, A. Covaci, N. Ademollo, S. Focardi, P. Schepens, *Environ. Pollut.* 140 (2006) 371-382.
- [32] E. Eljarrat, P. Guerra, D.Barceló, *Trends Anal. Chem.* 27 (2008) 847-861.
- [33] P.F. Hoekstra, B. K. Burnison, T. Neheli, D.C.G. Muir, *Toxicol. Lett.* 125 (2001) 75-78.
- [34] X.-Z. Meng, Y. Guo, B.-I. Mai, E.Y. Zeng, *J. Agric. Food Chem.* 57 (2009) 4299-4304.
- [35] W. Vetter, V. Schurig, *J.Chromatogr.A.* 774 (1997) 143-175.
- [36] S.P.J. van Leeuwen, J. de Boer, *J. Chromatogr. A.* 1186 (2008) 161-182.
- [37] P. Marriott, R. Shellie, *Trends Anal. Chem.* 21 (2002) 573-583.
- [38] L.R. Bordajandi, L. Ramos, M.J. González, *J. Chromatogr. A.* 1125 (2006) 220-228.
- [39] F. Wong, M.Robson, M.L. Diamond, S. Harrad, J. Truong, *Chemosphere* 74(3) (2009) 404-411.
- [40] L.R. Bordajandi, P. Korytár, J. de Boer, M.J. González, *J. Sep. Sci.* 28 (2005) 163-171.
- [41] T.D. Bucheli, R.C. Brändli, *J. Chromatogr. A.* 1110 (2006) 156-164.
- [42] M. Koblíčková, L. Duček, J. Jarkovský, J. Hofman, T.D. Bucheli, J. Klánová, *Environ. Sci.Technol.* 42 (2008) 5978-5984.
- [43] H. Hühnerfuss, M.R. Shah, *J. Chromatogr. A.* 1216(3) (2009) 481-502.
- [44] T. Tuzimski, in: M. Stoytcheva (Ed.), *Multidimensional Chromatography in Pesticides Analysis, Pesticides - Strategies for Pesticides Analysis*, InTech, 2011, pp. 155-196. Available from: <http://www.intechopen.com/articles/show/title/multidimensional-chromatography-in-pesticides-analysis> (Accessed 23.11.2011).
- [45] Y. Naudé, W.H.J. de Beer, S. Jooste, L. van der Merwe, S.J. van Rensburg, *Water SA.* 24(3) (1998) 205-214.
- [46] Y. Naudé, E.R. Rohwer, *Anal. Chim. Acta* 730 (2012), 112-119.
- [47] M.W. Van Rooyen, G.K. Theron, N. Van Rooyen, W.J. Jankowitz, W.S. Matthews, *J. Arid Environ.* 57 (2004) 467-485.

- [48] M.D. Picker, V. Ross-Gillespie, K. Vlieghe, E. Moll, *Ecol. Entomol.* 37 (2012) 33-42.
- [49] A. Zabbia, Master's dissertation (2010) The effect of protein loaded paper-board on milk flavour compounds, University of Pretoria, Pretoria, South Africa [online]. Available: <http://upetd.up.ac.za/thesis/available/etd-10082010-134235/> (Access to this dissertation is restricted until 21 December 2014).
- [50] G. Contarini, M. Povolo, R. Leardi, P.M. Toppino, *J. Agric. Food Chem.* 45 (1997) 3171-3177.
- [51] H.E. Nursten, *Int. J. of Dairy Technol.* 50 (2) (1997) 48-56.
- [52] P.A. Vazquez-Landaverde, G. Velazquez, J.A. Torres, M.C. Qian, *J. Dairy Sci.* 88 (2005) 3764-3772.
- [53] P.A. Vazquez-Landaverde, J.A. Torres, M.C. Qian, *J. Agric. Food Chem.* 54 (2006) 9184-9192.
- [54] M. Qian, C. Nelson, S. Bloomer, *J. Am. Oil Chem. Soc.* 79 (2002) 663-667.
- [55] M. van Aardt, S.E. Duncan, J.E. Marcy, T.E. Long, S.F. O' Keefe, S.R. Nielsen-Sims, *J. Dairy Sci.* 88 (2005) 881-890.
- [56] C. Bicchi, C. Cordero, C. Iori, P. Rubiolo, P. Sandra, *J. High Res. Chromatog.* 23(9) (2000) 539-546.
- [57] C. Bicchi, C. Cordero, E. Liberto, P. Rubiolo, B. Sgorbini, *J. Chromatogr. A* 1024 (2004) 217-226.
- [58] A. Buettner, *Flavour Frag. J.* 22 (2007) 465-473.
- [59] G. Contarini, M. Povola, *J. Agric. Food Chem.* 50 (2002) 7350-7355.
- [60] M. Fabre, V. Aubry, E. Guichard, *J. Agric. Food Chem.* 50 (2002) 1497-1501.
- [61] Markes International Thermal Desorption Technical Support Note 88. 2010a. Enhancing olfactory profiling of fruit juices and wine using complementary analytical thermal desorption techniques.
- [62] Markes International Thermal Desorption Technical Support Note 94. 2010b. Using Markes' thermal desorption technology to automate high/low analysis of complex beer sample.
- [63] R.T. Marsili, *J. Agric. Food Chem.* 47 (1999) 648-654.
- [64] R.T. Marsili, *J. Agric. Food Chem.* 48 (2000) 3470-3475.
- [65] M.L. Perkins, B.R. D'Arcy, A.T. Lisle, H.C. Deeth, *J. Sci. Food Agric.* 85 (2005) 2421-2428.
- [66] K. Ridgway, S.P.D. Lalljie, R.M. Smith, *J. Chromatogr. A* 1124 (2006) 181-186.
- [67] K. Ridgway, S.P.D. Lalljie, R.M. Smith, *J. Chromatogr. A* 1174 (2007) 20-26.
- [68] K. Schulz, J. Dreßler, E. Sohnius, D.W. Lachenmeier, *J. Chromatogr. A* 1145 (2007) 204-226.
- [69] Z. Zhang, J. Pawliszyn, *J. Anal. Chem.* 65 (1993) 1843-1852.
- [70] E. Baltussen, P. Sandra, F. David, C. Cramers, *J. Microcol. Sep.* 11 (1999) 737-747.
- [71] Y. Naudé, M. van Aardt, E.R. Rohwer, *J. Chromatogr. A* 1216 (2009) 2798-2804.
- [72] J.E. Friedrich, T.E. Acree, *Int. Dairy J.* 8 (3) (1998) 235-241.
- [73] J.G. Bendall, *J. Agric. Food Chem.* 49 (2001) 4825-4832.
- [74] S.S. Mahajan, L. Goddik, M.C Qian, *J. Dairy Sci.* 87 (2004) 4057-4063.

- [75] M. Consuelo Díaz-Maroto, E. Guchu, L. Castro-Vázquez, C. de Torres, M. Soledad Pérez-Coello, *Flavour Fragr. J.* 23 (2008) 93-98.
- [76] Y. Naudé, E.R. Rohwer, in: R. Marsili (Ed.), *Flavor, Fragrance, and Odor Analysis*, Second Edition, Taylor & Francis Group LLC, Boca Raton, Florida, 2012, pp. 93-110.
- [77] A.J. Johnson, G.D. Hirson, S.E. Ebeler, *PLoS ONE* 7 (8) (2012) e42693.
- [78] C.J. van Wyk, O.P.H. Augustyn, P. de Wet, W.A. Joubert, *Am. J. Enol. Vitic.* 30(3) (1979) 167-173.
- [79] D. de Beer, E. Joubert, J. Marais, W. du Toit, B. Fourie, M. Manley, S. Afr. J. Enol. Vitic. 29(1) (2008) 39-49.
- [80] E. Koussissi, V.G. Dourtoglou, Ageloussis, Y. Paraskevopoulos, T. Dourtoglou, A. Paterson, A. Chatzilazarou, *Food Chem.* 114 (2009) 1503-1509.
- [81] A.B. Boutista-Ortín, A.G. Lencina, M. Cano-López, F. Pardo-Mínguez, J.M. López-Roca, E. Gómez-Plaza, *Aust. J. Grape Wine Res.* 14 (2008) 63-70.
- [82] B.T. Weldegergis, A.G.J. Tredoux, A.M. Crouch *J. Agric. Food Chem.* 55 (2007) 8696-8702.
- [83] B.T. Weldegergis, A.M. Crouch, *J. Agric. Food Chem.* 56 (2008) 10225-10236.
- [84] A. Tredoux, A. de Villiers, P. Majek, F. Lynen, A. Crouch, P. Sandra, *J. Agric. Food Chem.* 56 (2008) 4286-4296.
- [85] A. de Villiers, P. Alberts, A.G.J. Tredoux, H.H. Nieuwoudt, *Anal. Chim. Acta* 730 (2012) 2-23.
- [86] J. Vestner, S. Malherbe, M. du Toit, H.H. Nieuwoudt, A. Mostafa, T. Górecki, A.G.J. Tredoux, A. de Villiers, *J. Agric. Food Chem.* 59 (2011) 12732-12744.
- [87] B.T. Weldegergis, A. de Villiers, C. McNeish, S. Seethapathy, A. Mostafa, T. Górecki, A.M. Crouch, *Food Chem.* 129 (2011) 188-199.
- [88] J.E. Welke, V. Manfroi, M. Zanus, M. Lazarotto, C.A. Zini, *J. Chromatogr. A* 1226 (2012) 124-139.
- [89] B.T. Weldegergis, A.M. Crouch, T. Górecki, A. de Villiers, *Anal. Chim. Acta* 701 (2011) 98-111.
- [90] R. López, M. Aznar, J. Cacho, V. Ferreira, *J. Chromatogr. A* 966 (2002) 167-177.

Chapter 2

Novel method for determining DDT in vapour and particulate phases within contaminated indoor air in a malaria area of South Africa

This chapter was published in Analytica Chimica Acta. The format reflects the style set by the journal.

Naudé, Y. and Rohwer, E.R., 2012. Novel method for determining DDT in vapour and particulate phases within contaminated indoor air in a malaria area of South Africa. *Analytica Chimica Acta* 730, 112–119. DOI: 10.1016/j.aca.2012.02.054

Author contributions

Conceived and designed the experiments: Yvette Naudé and Egmont Rohwer. Performed experimental work and data analysis, wrote the chapter/article, submitted article to journal, response to reviewers: Yvette Naudé. Initiator of research and study supervisor: Egmont Rohwer.

The work in this chapter was presented at the 18th International Mass Spectrometry Conference 2009, Bremen, Germany and at ChromSAAMS 2008, Bela Bela, South Africa

Novel method for determining DDT in vapour and particulate phases within contaminated indoor air in a malaria area of South Africa

Yvette Naudé* and Egmont R. Rohwer

Department of Chemistry, University of Pretoria, Private Bag X20, Hatfield
0028, Pretoria, South Africa

ABSTRACT

The organochlorine insecticide DDT (1,1,1-trichloro-2,2-bis(*p*-chlorophenyl)ethane) is still used for malaria vector control in certain areas of South Africa. The strict Stockholm Convention on Persistent Organic Pollutants (POPs) allows spraying on the inside of traditional dwellings with DDT. In rural villages contaminated dust presents an additional pathway for exposure to DDT. A new method is presented for the determination of DDT in indoor air where separate vapour and particulate samples are collected in a single step with a denuder configuration of a multi-channel open tubular silicone rubber (polydimethylsiloxane (PDMS)) trap combined with a micro quartz fibre filter. The multi-channel PDMS trap section of the denuder concentrates vapour phase insecticide whereas particle associated insecticide is transferred downstream where it is collected on a micro-fibre filter followed by a second multi-channel PDMS trap to capture the blow-off from the filter. The multi-channel PDMS trap and filter combination are designed to fit a commercial thermal desorber for direct introduction of samples into a GC-MS. The technique is solvent-free. Analyte extraction and sample clean-up are not required. Two fractions, vapour phase and particulate phase *p,p'*-DDT, *o,p'*-

DDT; *p,p'*-DDD, *o,p'*-DDD; *p,p'*-DDE and *o,p'*-DDE in 4 L contaminated indoor air, were each quantitatively analysed by GC-MS using isotopically labeled ring substituted $^{13}\text{C}_{12}$ – *p,p'*-DDT as an internal standard. Limits of detection were 0.07-0.35 ng m⁻³ for *p,p'*-DDT, *o,p'*-DDT, *p,p'*-DDD, *o,p'*-DDD, *p,p'*-DDE and *o,p'*-DDE. Ratios of airborne *p,p'*-DDD/*p,p'*-DDT and of *o,p'*-DDT/*p,p'*-DDT are unusual and do not match the ideal certified ingredient composition required of commercial DDT. Results suggest that the DDT products used for indoor residual spraying (IRS) prior to, and during 2007, may have been compromised with regards to insecticidal efficacy, demonstrating the power of this new environmental forensics tool.

Keywords: Airborne contaminants; Multi-channel open tubular trap; Polydimethylsiloxane (PDMS) sorptive extraction; Denuder; Environmental forensics; Persistent organic pollutants (POPs)

*Corresponding author. Tel.: +27 12 420 2517; fax: +27 12 420 4687.

E-mail address: yvette.naude@up.ac.za

2.1 Introduction

DDT (1,1,1-trichloro-2,2-bis(*p*-chlorophenyl)ethane), an organochlorine insecticide, is still used for malaria vector control in risk regions in South Africa. The strict Stockholm Convention on Persistent Organic Pollutants (POPs) permits Indoor Residual Spray (IRS) of traditional dwellings with DDT. IRS with DDT decreased the number of deaths caused by malaria in South Africa by 65% and decreased the number of confirmed malaria cases by 83% [1]. At present there are no effective insecticides that could replace DDT [2].

Semivolatile organic compounds are present in air, either adsorbed onto dust particles or as free gas phase molecules [3,4]. Exposure may be *via* inhalation of gas and particulate phase compounds, or by ingestion. Once larger sized contaminated particles are inhaled it deposits in the upper respiratory tract and is swallowed [5]. In rural villages contaminated dust presents a pathway for exposure to DDT, especially when the dust is disturbed during domestic activities in and around traditional dwellings. Conventional high volume collection systems for POPs are polyurethane foam (PUF) [5,6] or polymeric resin (XAD-2 or XAD-4) [6,7]. PUF samples total air, *i.e.*, vapour and particulate phases, and does not distinguish between contributions from each phase. In order to sample both phases, glass fibre or quartz filters are placed upstream of the solid sorbents to first collect particulate phase pesticides while vapour phase is trapped onto the sorbent [6,8-14]. After sampling the materials are separately extracted by Soxhlet extraction (16-36 h) with large amounts of solvents, or by sonication [7,9,15], concentrated by Kuderna Danish or rotary

evaporation, followed by nitrogen gas blow-down [6,8-14]. Microlitre amounts are injected for analysis. This approach is quite successful but involves many preparation steps, large amounts of solvents, loss of analyte, introduction of interferences and potential errors. Moreover, sensitivity limitations are associated with injection of only a fraction of the final 100 μ L to 1 mL concentrate [16].

Particulate phase organic compounds may be underestimated by the above procedure due to loss of the reversibly adsorbed molecules on the filter – the so called blow-off effect [8,10,17]. Adsorption of the gas phase fraction onto particles already collected, or by the filter itself, may also occur [8,11]. Diffusion denuder samplers were developed to overcome the problems associated with filter+PUF samplers [11]. By placing a filter after the low-flow denuder sampler to collect the particles, the collection of gas and particulate phases is reversed from the conventional high-volume sampler [17]. Due to a difference in vapour and particle diffusivities, diffusion denuders first separate the vapour phase from the particulate phase [11]. Traditional diffusion denuders include annular, multi-capillary and honeycomb designs that are coated with various sorbents including silicone grease/gum, XAD, Tenax, Florisil [11]. Denuder fabrication procedures are cumbersome. Denuder materials are solvent extracted or thermally desorbed [11]. The use of adsorptive sorbents in combination with thermal desorption to analyse high molecular-weight compounds is problematic due to incomplete desorption [16]. Sample trapping using polydimethylsiloxane (PDMS) performs well in combination with thermal desorption [16]. In contrast

with adsorptive concentration, PDMS functions as a hydrophobic solvent for the analytes [16, 18].

Multi-channel configuration devices designed for air pollution studies have been reported by Lane et al. [19] who coated a collection of glass tubes on the inside and on the outside with stationary phase, and by Kriegler and Hites [20] who used a bundle of fused silica tubes cut from a single DB-1 capillary GC column. Practical limitations were complicated instrumental arrangements and high pressure drops due to the longer length of the traps (25 – 60 cm). Ortner and Rohwer [21] constructed shorter length (10.5 – 12.5 cm) thick film silicone rubber (PDMS) traps in a multi-channel configuration to concentrate semi-volatile organic air pollutants. The traps were desorbed in an inlet similar to a programmable temperature vaporization (PTV) injector. Multi-channel PDMS traps and thermal desorption in a commercial system were successfully used for monitoring of atmospheric polycyclic aromatic hydrocarbons (PAHs) [18, 22-24]. Advantages of the multi-channel PDMS trap over commercial packed or coated sorptive devices are its open tubular structure and low pressure drop associated with laminar multi-channel flow [21, 22, 24]. Compared to multi-channel traps consisting of a bundle of GC capillary columns which contain nonsorptive outer coatings, both the inside and the outside of the multi-channel silicone rubber trap provide sorptive surfaces.

Considerations for transporting of equipment and sampling in rural areas of South Africa are that electricity is not freely available, travel distances from rural areas to city laboratories are considerable, road conditions are rough both

on and off- road, and cargo space is often limited. Simple, small, battery operated, off-line, field monitoring equipment is therefore preferable to bulky, expensive, conventional high flow PUF based equipment. A new solventless method for the determination of DDT in indoor air is described: vapour and particulate phases are collected separately in a single step, with a low pressure-drop denuder configuration of multi-channel open tubular PDMS traps combined with a micro quartz fibre filter. Air is drawn with a small and simple, off-line, battery-operated field sampler at a low air flow sampling rate and short collection time.

2.2 Materials and methods

2.2.1 Chemical standards

A certified organochlorine pesticides standard mixture (*p,p'*-DDT, *o,p'*-DDT; *p,p'*-DDD, *o,p'*-DDD; *p,p'*-DDE and *o,p'*-DDE, purity $\geq 97\%$) and a certified inlet degradation mixture (*p,p'*-DDT and Endrin, purity $\geq 98\%$,) were purchased from Sigma-Aldrich (Pty) Ltd. Kempton Park, South Africa. Solvents used were of analytical grade. The standard stock solution was diluted in hexane (Merck Chemicals (Pty) Ltd., South Africa) to give calibration standard solutions ranging from $0.5 \text{ pg } \mu\text{L}^{-1}$ to $5 \text{ ng } \mu\text{L}^{-1}$. The inlet degradation solution (*p,p'*-DDT) was diluted in hexane to give a concentration of $1 \text{ ng } \mu\text{L}^{-1}$. An isotope-labeled internal standard, ring substituted $^{13}\text{C}_{12}$ – *p,p'*-DDT (purity 99%), was diluted in hexane to give a concentration of $1 \text{ ng } \mu\text{L}^{-1}$ (Cambridge Isotope Laboratories, Inc. imported by Industrial Analytical (Pty) Ltd., South Africa). Technical DDT

powders used in one of the IRS programmes, were kindly donated by FDA Laboratories, Brooklyn, South Africa. The technical DDT powders were each first dissolved in acetone (Merck Chemicals (Pty) Ltd., South Africa) followed by dilution in hexane to give a concentration of $13 \text{ ng } \mu\text{L}^{-1}$. Working standards of the technical DDT solutions were prepared by dilution in hexane to give a concentration of $1.3 \text{ ng } \mu\text{L}^{-1}$.

2.2.2 Denuder sampling device

Multi-channel open tubular PDMS traps containing $0.4 \pm 0.02 \text{ g}$ silicone were prepared based on a technique described by Ortner and Rohwer [21]. The PDMS trap, providing a sample enrichment volume of $600 \mu\text{L}$, was designed to fit a commercial thermal desorber system (TDS) available from Gerstel™. Twenty two silicone elastomer medical grade tubes ($0.64 \text{ mm OD} \times 0.30 \text{ mm ID}$, SIL-TEC™, Technical Products, Georgia, United States of America) were arranged, in parallel, in a 17.8 cm long glass desorption tube (4 mm ID , 6 mm OD)(Fig. 2.1). The PDMS trap inside the desorption tube was 55 mm long (Fig. 2.1).

Micro quartz fibre filters, 5 mm OD , were punched from Ederol Quartz Microfibre sheets (0.43 mm thickness, pore size $0.3 \mu\text{m}$, grade T293) from Munktell & Filtrak GmbH Bärenstein, Germany. Denuder sampling devices were assembled by placing a micro quartz fibre filter flush between two multi-channel PDMS traps. The multi-channel PDMS traps and in-line filter were held firmly in place with a polytetrafluoroethylene (PTFE) sleeve (Fig. 2.1). The ends

of the glass denuder were capped with glass stoppers during storage. The glass stoppers were secured with tight-fitting PTFE sleeves. The trapped analytes inside the multi-channel PDMS trap and quartz micro-fibre filter of the denuder are not directly exposed to the PTFE sleeves, thereby preventing potential adsorption of analytes onto the Teflon®.

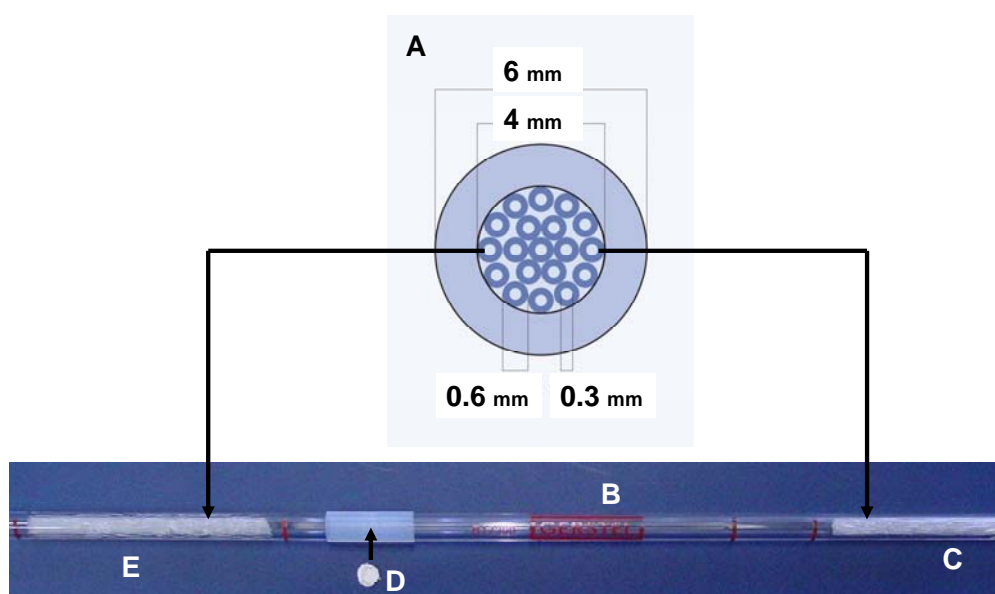


Figure 2.1. (A) Cross-section of a multichannel silicone rubber trap. (B) A novel low pressure-drop miniature denuder. (C) Silicone elastomer (PDMS) tubes are arranged in parallel inside of a commercial glass desorption tube to give a PDMS sorptive volume of 600 μL . The multi-channel PDMS traps and filter are tightly connected in series with a Teflon (PTFE) sleeve. (C) Airborne vapour phase is collected on the first multi-channel PDMS trap and (D) airborne particulate phase is collected on the micro quartz fibre filter. (E) Back-up multi-channel PDMS trap to collect blow-off and potential break-through. Indoor air is sampled with a small and simple battery operated sampling pump at a low air flow sampling rate (200 mL min^{-1}) and a short collection period (20 min).

2.2.2.1 Battery operated field pump

Field gas sampling pumps were designed and built in-house, and included a model G-12/01 pump motor from Rietschle Thomas, Memmingen, Germany. The motor was driven by a constant voltage circuit which made the pump rate independent of battery voltage. Power was supplied by a rechargeable 7 volt-ampere (VA) lead battery (Electronics 123, Pretoria, South Africa).

2.2.3 Indoor air sampling

Indoor air samples were collected from traditional round thatch-roof huts in a rural village (S 23°02'02.3" E 30°51'33.5") in the Vhembe District, Limpopo Province, South Africa. The village is situated within an intermediate-risk malaria area where indoor DDT-spraying is performed annually [5]. A detailed description of the study area was reported in Van Dyk et al. [5]. Sampling was done in November 2007 during the early summer season. The province is a summer rainfall region. Indoor air samples were collected from a total of five huts over a period of five days. A single hut was sampled per day at 4 sampling intervals over a 24 h period. Four litre of indoor air was sampled at approximately 60 cm above ground level with a denuder (multi-channel PDMS trap + micro quartz fibre filter + multi-channel PDMS trap) at 200 mL min⁻¹ for 20 min. Sampling took place prior to indoor DDT application (-1 h), immediately after application of DDT to the walls and ceilings of the rural dwellings (0 h), after 4 h, and after 24 h since DDT-spraying.

2.2.4 Indoor air analyses by GC-MS

The analytes were desorbed from the first multi-channel PDMS traps (gaseous phase airborne contaminants) and the micro quartz fibre filters and back-up multi-channel PDMS traps (particulate phase airborne contaminants) in a Gerstel thermal desorption system (TDS) installed on a Hewlett Packard (HP) GC 1530A coupled to a HP 5973 mass selective detector (MSD) (Chemetrix, Johannesburg, South Africa). The same instrumental conditions were used for analyses of gas phase airborne contaminants and for particulate phase airborne contaminants. The TDS transfer line temperature was 350 °C. During desorption the multi-channel PDMS traps were heated from 30 °C (3 min) at 30 °C min⁻¹ to 280 °C (15 min) with a desorption flow rate of 100 mL min⁻¹ at 65 kPa (Helium, Ultra High Purity, Afrox, Johannesburg), enabling total transfer of analytes to the cold trap. The desorbed analytes were cryogenically focused on a Gerstel cooled injection system (CIS) at -50 °C using liquid nitrogen. The CIS liner was an open deactivated glass liner (Gerstel, Germany). After desorption, a splitless injection (purge on at 5 min, purge flow 80 mL min⁻¹, solvent vent mode) was performed by heating the CIS from -50 °C at 6 °C s⁻¹ to 250 °C maintained for 10 min. GC separation was performed on a Zebron column, ZB1 30 m x 250 µm ID x 0.25 µm film thickness (Phenomenex, SEPARATIONS, Randburg, South Africa), the velocity of the carrier gas (helium) was 33 cm s⁻¹ (0.7 mL min⁻¹) and the column head pressure was 65 kPa in the constant pressure mode. The GC oven temperature programme was 150 °C (5 min) at 10 °C min⁻¹ to 210 °C, at 5 °C min⁻¹ to 280 °C (1 min). The GC run time was 26 min. A post run was performed at 300 °C (5 min). The GC-MS transfer line

was at 300° C, the source (EI+) temperature 230 °C, the MS quadrupole temperature 150 °C, the ionisation energy 70 eV and the electron multiplier (EM) 1700 V.

A chromatogram was recorded in full scan mode (45–450 m/z) to identify the target analytes and to determine their respective retention times. Thereafter, all analyses and quantification were performed in the more sensitive selected ion monitoring (SIM) mode. For DDE the selected ions were 246 m/z, 248 m/z, 318 m/z (100 ms dwell time), whilst for DDD, DDT as well as ¹³C₁₂ – p,p'-DDT (IS) the selected ions were 165 m/z, 235 m/z, 237 m/z, 247 m/z, 249 m/z, 330 m/z (50 ms dwell time). Blanks (PDMS traps and filters) were routinely analysed. Separate GC-MS runs were performed, under the same instrumental conditions, for airborne vapour phase DDT (first multi-channel PDMS trap) and airborne particulate phase DDT (filter and back-up multi-channel PDMS trap).

2.2.4.1 Quantification

GC-MS calibration was performed by addition of 1 µL of each of the calibration standard solutions (0.5 pg µL⁻¹– 5 ng µL⁻¹) to ten blank multi-channel PDMS traps. One microlitre of the isotope-labeled ring substituted ¹³C₁₂ – p,p'-DDT working solution was added as an internal standard (1 ng µL⁻¹) to each of the ten calibration PDMS traps, and as well as to the indoor air enriched PDMS traps and filters. The internal standard (IS) method of quantification was done. Calibration curves (n=10) were constructed by plotting response factors (peak

$\text{area}_{\text{Analyte}}/\text{peak area}_{\text{Internal standard}}$) for each of the compounds. The results of the linear regression analysis are depicted in Table 2.1.

Table 2.1

Linear regression analysis for *p,p'*-DDT, *o,p'*-DDT, *p,p'*-DDD, *o,p'*-DDD, *p,p'*-DDE and *o,p'*-DDE

Compound	Quantification Ion <i>m/z</i>	¹ Regression Equation	R ² (n = 10)	² LOD ng m ⁻³ (pg L ⁻¹)	³ LOQ ng m ⁻³ (pg L ⁻¹)
2,4'-DDE	246	$y = 4.8792x + 0.0856$	0.997	0.0683	0.2277
4,4'-DDE	246	$y = 2.1537x + 0.053$	0.998	0.1196	0.3987
2,4'-DDD	235	$y = 3.1319x + 0.1555$	0.999	0.1337	0.4456
4,4'-DDD	235	$y = 2.5899x + 0.016$	0.998	0.2669	0.8897
2,4'-DDT	235	$y = 2.0905x + 0.0383$	0.999	0.2967	0.9891
4,4'-DDT	235	$y = 0.8885x + 0.0006$	0.998	0.3515	1.1715

Compounds listed in order of elution (apolar separation). Quantification ion for internal standard (¹³C₁₂ - *p,p'*-DDT) is 247 *m/z*. ¹*y* = peak area of compound/peak area of internal standard (¹³C₁₂ - *p,p'*-DDT); *x* = concentration of the compound ng 4L⁻¹. ²Limit of detection (LOD) calculated as the concentration that gives a signal-to-noise ratio of 3. ³Limit of quantification (LOQ) calculated as the concentration that gives a signal-to-noise ratio of 10.

2.3 Results and discussion

2.3.1 Evaluation of *p,p'*-DDT degradation during thermal desorption and CIS injection

It is well known that DDT can degrade to DDD and DDE on a hot inlet surface. DDT degradation is not due to DDT being thermally labile, but due to active sites in the GC inlet. Activity in the injection port liner of a GC is increased at a high inlet temperature. The boiling point of DDT is 260 °C [25] and a typical GC inlet temperature for DDT is 250 °C. Drawing conclusions as to whether DDD and DDE are due to environmental degradation rather than degradation in a GC inlet are therefore problematic. In general, an accepted break-down limit of *p,p'*-DDT degradation in the inlet is 15% [26]. *p,p'*-DDT degradation in the inlet often exceeds 15% and can be as high as 65% [27]. The Gerstel CIS is a programmable temperature vaporising injector (PTV) resulting in injection at a lower temperature. CIS inlet liner dimensions (2 mm ID, 70 mm long) are smaller compared to conventional GC inlet liners (4 mm ID, 78 mm long). Therefore, the potentially active glass surface area of a CIS liner is relatively small compared to a regular inlet liner.

To evaluate the potential for degradation of *p,p'*-DDT during thermal desorption and CIS injection, multi-channel PDMS traps were spiked with 1 ng μL^{-1} of *p,p'*-DDT degradation solution (section 2.2.1). The spiked multi-channel PDMS traps were desorbed using various TDS and CIS heating rates (Table 2.2). The CIS was heated from -50 °C to 250 °C and the TDS from 30 °C to 280 °C for all experiments. Degradation of *p,p'*-DDT (22%) was the greatest at a slow TDS heat rate (10 °C min^{-1}) and a slow CIS heat rate (3 °C s^{-1}) (Table 2.2). Analyte degradation (8%-11%)

decreased at faster TDS and CIS heating rates (Table 2.2). Slower heating rates result in prolonged analyte contact time and an associated increase in degradation. Inlet liners were replaced regularly with new deactivated liners to control DDT degradation.

TDS-CIS injection was then compared to isothermal injection at 250 °C with the same CIS inlet, only now the inlet was in conventional GC inlet mode (septumless samplehead) instead of CIS-PTV mode. Conventional isothermal injection of 1 µL of the inlet degradation solution at 250 °C produced *p,p'*-DDT degradation of 36% (Table 2.2). This confirmed that TDS and cryogenic focusing of analytes prior to injection, followed by injection with ramped heating of the inlet to 250 °C, is a milder sample introduction technique, causing less *p,p'*-DDT degradation, when compared to conventional isothermal injection at 250 °C.

Table 2.2
Comparison of the effect of TDS and CIS heating rates and of conventional injection on % degradation of DDT

Thermal desorption/injection TDS heat rate/CIS heat rate	DDT degradation (%)
10 °C min ⁻¹ /3 °C s ⁻¹	22
30 °C min ⁻¹ /3 °C s ⁻¹	12
60 °C min ⁻¹ /3 °C s ⁻¹	14
30 °C min ⁻¹ /6 °C s ⁻¹	8
60 °C min ⁻¹ /6 °C s ⁻¹	11
30 °C min ⁻¹ /12 °C s ⁻¹	9
60 °C min ⁻¹ /12 °C s ⁻¹	10
Conventional isothermal injection	DDT degradation (%)
250 °C	36

2.3.2 Vapour phase and particulate phase DDT in indoor air

The isotope-labeled internal standard (ring substituted $^{13}\text{C}_{12}$ – p,p' -DDT) method of calibration and linear regression analysis (Table 2.1) were used to quantify p,p' -DDT, o,p' -DDT, p,p' -DDD, o,p' -DDD, p,p' -DDE and o,p' -DDE in contaminated indoor air. Limits of detection were 0.07-0.35 ng m^{-3} for p,p' -DDT, o,p' -DDT, p,p' -DDD, o,p' -DDD, p,p' -DDE and o,p' -DDE (Table 2.1). Should lower LODs be required negative chemical ionisation, instead of EI+, can be used. Figure 2.2 depicts a chromatogram (SIM mode) of a low calibration standard with analyte concentrations ranging from 0.5 $\text{pg } \mu\text{L}^{-1}$ to 2.4 $\text{pg } \mu\text{L}^{-1}$, and overlays of chromatograms of indoor air prior to DDT IRS and after DDT IRS.

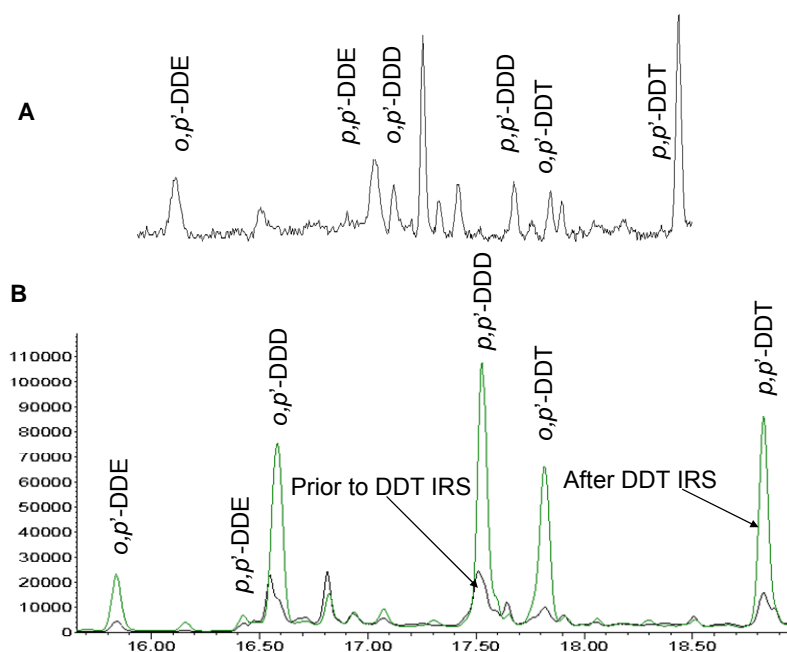


Figure 2.2. (A) SIM chromatogram of the lowest calibration standard with analyte concentrations ranging from 0.5 $\text{pg } \mu\text{L}^{-1}$ to 2.4 $\text{pg } \mu\text{L}^{-1}$. (B) Overlay of SIM chromatograms of 4 L of indoor air: prior to DDT IRS and after DDT IRS. See section 2.2.4 for ions for SIM recording.

Vapour phase and particle bound *p,p'*-DDT, *o,p'*-DDT, *p,p'*-DDD, *o,p'*-DDD, *p,p'*-DDE and *o,p'*-DDE were concentrated from 4 L indoor air using a simple, off-line battery operated, small field sampler consisting of a novel serially fitted low pressure-drop denuder (multi-channel PDMS trap + micro quartz fibre filter + multi-channel PDMS trap) (Section 2.2.2, Fig. 2.1). At the low flow rate (200 mL min^{-1}) employed, the pump motor drew approximately 10 milliampere (mA), which allows for a theoretical pump run time of approximately 700 hours from a battery in good condition, before requiring a recharge. However, batteries were recharged daily. The hydrophobic silicone rubber absorption medium is not sensitive to moist air. A denuder allows simultaneous collection of molecules and transmission of aerosol particles through the silicone rubber tubes based on the large difference in radial diffusion speeds in the axial laminar flow environment [24]. Simply put, molecules diffuse fast enough to reach the absorption medium whereas (heavy) particles are blown straight through because of their slow radial movement. Airborne vapour phase contaminants are collected on the first multi-channel PDMS trap and airborne particulate phase contaminants are collected downstream on a serially fitted quartz micro-fibre filter (Fig. 2.1). A second multi-channel PDMS trap is useful as a back-up trap to collect blow-off and potential break-through (Fig. 2.1). Sampling was performed at a low air flow sampling rate (200 mL min^{-1}) and a short collection time (20 min). Back in the laboratory, solvent extraction of the concentration materials was not required. Instead, thermal desorption allowed solvent-free transfer of the entire collected sample mass to the cryo-cooled (liquid nitrogen) inlet of a GC-MS. To test the desorption efficiency of analytes from multi-channel PDMS traps and filters during TDS, previously analysed multi-channel PDMS traps and filters were immediately redesorbed in consecutive runs. Quantitative removal of analytes from

multi-channel PDMS traps and filters were confirmed, since analytes were not detected during these second runs.

The many benefits of TDS-CIS are depicted in Table 2.3. A disadvantage is that thermal desorption consumes the full sample, preventing repeat injections often performed for liquid extracts (Table 2.3). Storage of an analysed sample is also not possible. The rather substantial cost of a TDS-CIS system may be considered against the cost saving gained by a sample preparation-free and solvent-free system. Instead of liquid nitrogen, a packed liner may be used to focus DDT at room temperature. The advantage of two separate airborne contaminant phases can still be attained by laboratories not equipped with a TDS. In such cases PDMS and filter denuder materials may be solvent extracted.

Table 2.3
Advantages and disadvantages of thermal desorption-injection (TDS-CIS)

Advantage	Disadvantage
Sample preparation not required	Total sample is consumed
-Minimises analyte loss	
-Minimises introduction of artefacts	Cost/Availability
-Cost saving	-TDS-CIS system
Solvent free ("green")	-liquid nitrogen
-No solvent waste disposal	
-No solvent associated artefacts	
-No exposure of staff to solvent	
-Cost saving	
Sample not diluted	
-Enhanced detection limit	
Lower injection temperature minimises DDT conversion	

Figure 2.3 illustrates the mean contribution ($\mu\text{g m}^{-3}$) across five huts of vapour phase and particulate phase *p,p'*-DDT, *o,p'*-DDT, *p,p'*-DDD, *o,p'*-DDD, *p,p'*-DDE and *o,p'*-DDE in indoor air over a 24 h period. Airborne DDT was present in both vapour

phase and in particulate phase in indoor air prior to DDT-spraying (Table 2.4). Directly after indoor residual spraying (IRS) vapour phase and particulate phase mean ($n=5$) Σ DDT increased. A recommendation is that inhabitants should remain outside their dwellings for at least an hour after technical DDT application [28]. However, 24 h after IRS vapour phase mean Σ DDT was at a maximum (possibly due to DDT spray drift from a larger number of huts sprayed in the village within a 24 h period). Particulate phase mean Σ DDT showed a minor decrease over a 24 h period after IRS (under undisturbed dust conditions). Mean ($n=5$) Σ DDT was largely present as vapour phase in indoor air (Table 2.4). Compared to DDT and DDD, vapour phase fractions of p,p' -DDE were lower. p,p' -DDE, a potent endocrine disrupting chemical [29], is reported to show highest bioaccumulation in human fatty tissue when compared to DDD and DDT [29,30]. It is assumed that phase distribution of the compounds depend on the particulate mass concentration and the ambient temperature: the higher the temperature the more the equilibrium shifts to the gas phase [8].

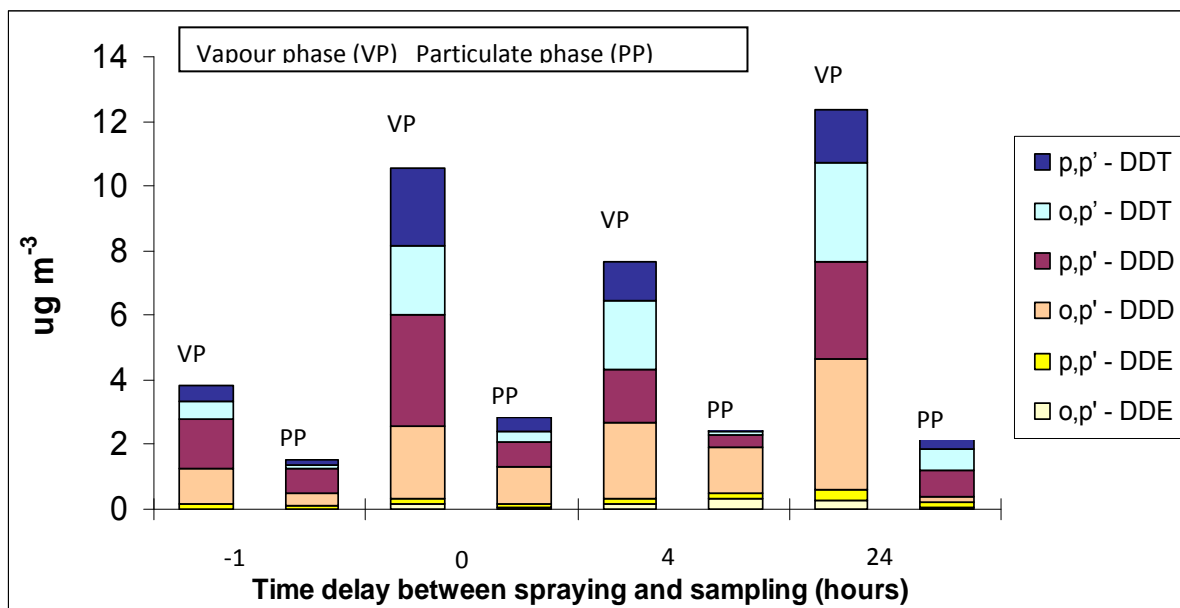


Figure 2.3. Concentrations of *p,p'*-DDT, *o,p'*-DDT, *p,p'*-DDD, *o,p'*-DDD, *p,p'*-DDE and *o,p'*-DDE ($\mu\text{g m}^{-3}$) in vapour (VP) and particulate phases (PP) in indoor air averaged for five huts. Sampling intervals: -1 h prior to DDT-spraying; 0 h directly after DDT-spraying; 4 h after DDT-spraying; 24 h after DDT-spraying. 4 L indoor airborne vapour phase was collected on a multi-channel PDMS trap and airborne particulate phase was collected down-stream on a quartz micro-fibre filter and a second multi-channel PDMS trap. Levels of DDD are higher than DDT across sampling intervals. 4 h after IRS levels of *o,p'*-DDT are higher than *p,p'*-DDT. Vapour phase mean Σ DDT is highest 24 h after IRS, possibly due to DDT spray drift from a larger number of huts sprayed within a 24 h period. Particulate phase Σ DDT showed a minor decrease over a 24 h period after IRS. For details see text 2.3.2.

Table 2.4
DDT, DDD, DDE ($\mu\text{g m}^{-3}$) in indoor air and fraction of the concentration in vapour phase (%) of five huts sampled at intervals prior to IRS, directly after IRS, 4 h and 24 h after IRS

Compound	Vapour phase (VP)			Particulate phase (PP)			VP+PP Total airborne	Vapour phase fraction %
	Mean (n=5)	Range Min Max		Mean (n=5)	Range Min Max			
<u>-1 h prior to IRS</u>								
<i>o,p'</i> - DDE	0.02	0.01	0.03	0.003	<LOD ¹	0.003	0.023	89.1
<i>p,p'</i> - DDE	0.15	0.03	0.26	0.09	<LOD	0.09	0.24	61.4
<i>o,p'</i> - DDD	1.12	0.10	1.92	0.4	0.15	0.61	1.51	73.8
<i>p,p'</i> - DDD	1.48	0.27	3.00	0.77	0.54	1.33	2.25	65.7
<i>o,p'</i> - DDT	0.58	0.36	0.80	0.08	0.12	0.13	0.66	87.5
<i>p,p'</i> - DDT	0.47	0.18	0.63	0.17	0.06	0.37	0.64	73.4
t-DDE ²	0.17			0.09			0.26	
t-DDD	2.60			1.17			3.77	
t-DDT	1.05			0.25			1.30	
Σ -DDT	3.82			1.52			5.33	
<u>0 h after IRS</u>								
<i>o,p'</i> - DDE	0.14	0.09	0.2	0.04	<LOD	0.11	0.18	78.7
<i>p,p'</i> - DDE	0.18	0.13	0.26	0.14	<LOD	0.27	0.32	55.8
<i>o,p'</i> - DDD	2.23	1.69	3.09	1.13	0.31	2.84	3.36	66.4
<i>p,p'</i> - DDD	3.45	1.25	8.21	0.79	0.57	1.25	4.23	81.4
<i>o,p'</i> - DDT	2.13	1.11	4.28	0.28	0.01	0.84	2.41	88.3
<i>p,p'</i> - DDT	2.42	0.74	5.41	0.49	0.14	1.18	2.91	83.2
t-DDE	0.33			0.18			0.51	
t-DDD	5.68			1.91			7.59	
t-DDT	4.55			0.77			5.33	
Σ -DDT	10.56			2.87			13.43	
<u>4h after IRS</u>								
<i>o,p'</i> - DDE	0.17	0.03	0.31	0.33	0.11	0.56	0.5	33.3
<i>p,p'</i> - DDE	0.19	0.14	0.28	0.14	0.02	0.36	0.33	57.3
<i>o,p'</i> - DDD	2.34	0.59	3.73	1.45	0.23	3.75	3.79	61.7
<i>p,p'</i> - DDD	1.63	0.63	2.53	0.4	0.02	0.72	2.03	80.4
<i>o,p'</i> - DDT	2.13	0.65	3.93	0.07	0.01	0.19	2.2	96.6
<i>p,p'</i> - DDT	1.23	0.41	3.11	0.36	0.19	0.85	1.59	77.3
t-DDE	0.35			0.47			0.83	
t-DDD	3.97			1.85			5.82	
t-DDT	3.36			0.44			3.80	
Σ -DDT	7.68			2.76			10.44	
<u>24 h after IRS</u>								
<i>o,p'</i> - DDE	0.27	0.02	0.70	0.06	0.06	0.06	0.33	81.7
<i>p,p'</i> - DDE	0.35	0.06	0.84	0.14	0.001	0.42	0.49	71.3
<i>o,p'</i> - DDD	4.01	0.45	9.72	0.18	0.15	0.21	4.19	95.7
<i>p,p'</i> - DDD	3.03	0.86	6.36	0.83	0.38	1.68	3.86	78.5
<i>o,p'</i> - DDT	3.07	0.59	6.78	0.63	0.004	1.86	3.70	83.1
<i>p,p'</i> - DDT	1.64	1.30	2.01	0.46	0.27	0.63	2.10	78.1
t-DDE	0.62			0.20			0.82	
t-DDD	7.04			1.01			8.05	
t-DDT	4.71			1.09			5.80	
Σ -DDT	12.37			2.30			14.67	

¹Limit of detection ²t-DDT was calculated as the sum of *p,p'*-DDT and *o,p'*-DDT; t-DDD was calculated as the sum of *p,p'*-DDD and *o,p'*-DDD; and t-DDE was calculated as the sum of *p,p'*-DDE and *o,p'*-DDE

2.3.2.1 Ratios of *o,p'*-DDT relative to *p,p'*-DDT

Technical grade DDT (75% wettable powder) used for IRS in South Africa contains 72-75% of *p,p'*-DDT, the active ingredient, and ~22% of *o,p'*-DDT [28, 31]. Prior to, and directly after DDT-spraying, vapour phase *p,p'*-DDT and vapour phase *o,p'*-DDT were present in approximately equal ratios, while particulate phase *p,p'*-DDT was higher than particulate phase *o,p'*-DDT (Fig. 2.3). However, 4 h to 24 h after DDT-spraying vapour phase *p,p'*-DDT (~36%) was considerably lower than vapour phase *o,p'*-DDT, whilst after 4 h particle phase *p,p'*-DDT was considerably greater than particle phase *o,p'*-DDT. Twenty four hours after IRS particle phase *p,p'*-DDT was less than particle phase *o,p'*-DDT. Bouwman et al. [28] demonstrated that relative to *p,p'*-DDT, *o,p'*-DDT constituted ~75%, of the indoor air of huts after IRS. The authors' results support the measurements of higher levels of *o,p'*-DDT relative to *p,p'*-DDT in indoor air reported here, as Bouwman et al.'s [28] sampling was conducted concurrently with the sampling campaign for this study. According to Bouwman et al. [28] two types of IRS products were used during the 2007 season, one product containing significantly higher levels of *o,p'*-DDT compared to *p,p'*-DDT. To the author's knowledge *p,p'*-DDT does not change to *o,p'*-DDT under environmental conditions. This unusual *o,p'*-DDT/*p,p'*-DDT ratio is not typical of technical DDT, instead it is somewhat similar to the ratio of dicofol-associated DDT [32].

Because *p,p'*-DDT degrades to *p,p'*-DDE only under aerobic conditions and to *p,p'*-DDD only under anaerobic conditions [33-35], it can be safely concluded that the DDT products used prior to and during IRS 2007 contained very little *p,p'*-DDT

relative to *o,p'*-DDT. Since it is only *p,p'*-DDT that is effective against the malaria carrying mosquito this diminished insecticidal potency represented by the low levels of *p,p'*-DDT present in DDT products is a major cause for concern. Of interest is that an investigation of POPs in the Southern Hemisphere resulting from atmospheric transport showed that soils from the Eastern coast of Antarctica also contained higher proportions of *o,p'*-DDT relative to *p,p'*-DDT [36].

2.3.2.2 Ratios of DDD and DDE relative to DDT

Total airborne DDT, DDD and DDE was calculated as the sum of vapour and particulate phases (VP+PP) (Table 2.4). The level of total airborne DDD ($3.77 \mu\text{g m}^{-3}$) was higher than total airborne DDT ($1.3 \mu\text{g m}^{-3}$) prior to DDT-spraying, and as well as over a 24 h period after DDT-spraying (Table 2.4, Fig. 2.3). Technical DDT contains, as by-products, less than 1% *o,p'*-DDD, *p,p'*-DDD, *o,p'*-DDE and *p,p'*-DDE [37]. *p,p'*-DDT in the environment degrades to *p,p'*-DDD under anaerobic conditions and to *p,p'*-DDE under aerobic conditions [33-35]. Therefore, DDE formation is favoured in well aerated soil [12]. Because emissions from residues present in soil is a source of pollutants in air [12], DDE rather than DDD is expected to be present in the indoor air of the huts. Thus, the surprisingly elevated level of total (gas+particulate phases) airborne DDD prior to IRS is not the result of weathered DDT, since under the prevailing conditions DDE formation is favoured over DDD. Directly after DDT-spraying total airborne DDD of $7.59 \mu\text{g m}^{-3}$ was double the amount of total airborne DDD just prior to DDT-spraying (Table 2.4). This implies that DDT products used during IRS 2006 and IRS 2007 seasons contained a significant amount of DDD. Prior to DDT-spraying total airborne DDD constituted

71% of total airborne Σ DDT while after DDT-spraying total airborne DDD constituted ~57% of total airborne Σ DDT. Alarming, it appears that the IRS DDT product used at the time of this study contained significantly less than the required ~73% *p,p'*-DDT, and an unusually high level of DDD.

Given that technical grade *p,p'*-DDT should contain very little *p,p'*-DDD and *p,p'*-DDE the presence of *p,p'*-DDD and *p,p'*-DDE in the environment is usually an indication of DDT degradation. *p,p'*-DDE/*p,p'*-DDT and *p,p'*-DDD/*p,p'*-DDT ratios have been used to determine recent or historical *p,p'*-DDT usage [12]. As discussed previously, anaerobic environmental conditions favour *p,p'*-DDD formation over *p,p'*-DDE [33-35]. Degraded residues in well aerated soils therefore generally contain less *p,p'*-DDD than *p,p'*-DDE [12]. Batterman et al. [12] reported a *p,p'*-DDE/*p,p'*-DDT ratio of 0.29 in ambient air in Durban, South Africa. The *p,p'*-DDD/*p,p'*-DDT ratio in ambient air in Durban should then be lower than the reported *p,p'*-DDE/*p,p'*-DDT ratio of 0.29. However, Batterman et al. [12] described airborne levels of *p,p'*-DDD almost equal to *p,p'*-DDT, and in some air samples *p,p'*-DDD exceeded *p,p'*-DDT in ambient air in Durban, South Africa. The authors suggested that this unusual *p,p'*-DDD/*p,p'*-DDT mean ratio of 0.60 for ambient air in Durban may be due to current use of DDT formulations that differ from formulations used in the past [12], which would explain these excessive *p,p'*-DDD levels. Historically, *p,p'*-DDD was produced as an insecticide, although its efficacy was lower compared to *p,p'*-DDT [12], while *o,p'*-DDD has been used medically to treat cancer [38, 39]. The presence of unusual elevated levels of airborne *p,p'*-DDD in South Africa are indeed substantiated by measured ratios of indoor airborne *p,p'*-DDD/*p,p'*-DDT which were 3.52 prior to DDT-spraying, and 1.52 after IRS in Limpopo Province, South Africa.

p,p' -DDD/ p,p' -DDT ratios significantly below 1 are anticipated directly after DDT-spraying. However, even directly after spraying the level of indoor airborne DDD in traditional huts in the Limpopo Province still exceeds that of airborne p,p' -DDT, suggesting that technical DDT contained levels of DDD exceeding the required product composition. It was confirmed that the DDT IRS 2006 product contained more DDD than DDT (personal communication, 2008). Unfortunately, a sample of the commercial DDT product could not be obtained.

A high p,p' -DDE/ p,p' -DDT ratio generally indicates ageing of DDT [12]. As expected, low indoor airborne p,p' -DDE/ p,p' -DDT ratios for Vhembe in Limpopo Province, South Africa were measured. p,p' -DDE/ p,p' -DDT ratios prior to DDT-spraying were 0.37 and after DDT-spraying it was 0.18.

2.3.2.3 Indoor air chemical profile

IRS takes place annually [5]. However, increases in cases of malaria outbreaks following IRS have been reported which then necessitates a second round of IRS (personal communication, 19 August 2009). Ratios of indoor airborne p,p' -DDD/ p,p' -DDT and of o,p' -DDT/ p,p' -DDT in Vhembe are unusually high. In view of the fact that it is only p,p' -DDT that is effective against the malaria carrying mosquito, these unusual ratios suggest that the insecticidal efficacy of the active ingredient in commercial DDT IRS products used prior to and during the 2007 season were reduced. Additionally, technical DDT has oestrogen-like properties, mainly due to o,p' -DDT [29] and therefore levels of o,p' -DDT in IRS products higher than necessary are cause for concern. o,p' -DDT and o,p' -DDD are chiral molecules and

both exist as enantiomeric pairs [26, 40]. *o,p'*-DDT exhibits enantioselective oestrogenicity [39,41,42] and biodegradability [26, 40]. (-)-*o,p'*-DDT enantiomer is a weak oestrogen mimic while (+)-*o,p'*-DDT is inactive [39,41,42]. Airborne enantiomers of R(-)-*o,p'*-DDT and S(+)-*o,p'*-DDT and of S(+)-*o,p'*-DDD and R(-)-*o,p'*-DDD were measured in indoor vapour and particle phases after IRS [40]. Two very different enantiomeric profiles were revealed: indoor air vapour phase displayed a racemic composition, while indoor airborne particulate phase displayed a non-racemic composition [40].

Regrettably, the commercial DDT product used during the IRS 2007 season was not made available to us for analysis. Commercial DDT products supplied to us in 2008, and analysed by us, contained ~73% *p,p'*-DDT relative to Σ DDT with the balance consisting of mainly *o,p'*-DDT and levels of DDD were within specification. However, the chromatogram showed the presence of, amongst others, a pyrethroid and organochlorine compounds other than the target compounds reported in this study. Quality control of IRS products should include a full inspection of the total chromatogram, and not only of *p,p'*-DDT.

2.3.3 Comparison of PUF and denuder (multi-channel PDMS trap + filter + multi-channel PDMS trap) samplers

Indoor air of the huts was sampled concurrently by PUF and denuder (multi-channel PDMS trap+filter+multi-channel PDMS trap) samplers directly after DDT-spraying, after 4 h and after 24 h and the results are shown in Table 2.5. PUF was bulk solvent extracted and analysed by an external laboratory (Agricultural Research

Council's Plant Protection Research Institute of South Africa (ARC-PPRI)) using GC-ECD. In general, a relatively good agreement between total (gas + particulate phases) Σ DDT ($\mu\text{g m}^{-3}$) for PUF and denuder device (multi-channel PDMS trap+filter+multi-channel PDMS trap) sampling was obtained. The relatively larger difference between PUF and denuder values obtained after 24 h is probably due to DDT spray drift from a larger number of huts sprayed within a 24 h period. Spray drift would also explain the elevated levels of Σ DDT observed after 24 h for both PUF and denuder samplers. The total airborne concentrations were slightly higher in samples collected by denuder samplers than those collected by PUF (Table 2.5). This trend was also observed for atmospheric PAHs collected by diffusion denuder+filter vs. filter+PUF [8,9,15]

Because sample preparation steps are completely eliminated, the potential for loss of analyte and introduction of interferences are minimised with a denuder. In contrast, PUF requires solvent extraction followed by evaporation and clean-up which may cause loss of analytes and introduction of interferences and hence may result in lower values obtained with PUF. Disadvantages of PUF are that it is bulky, requires high volume sampling pumps which increases the potential for compound break-through, does not distinguish between vapour and particulate phases, and it requires solvent extraction, clean-up and concentration. In comparison, the denuder sampler used in this study distinguishes between vapour and particulate phases and uses compact, battery operated (an important consideration in rural areas), low volume sampling pumps.

Table 2.5

Comparison of mean indoor airborne Σ DDT ($\mu\text{g m}^{-3}$) values obtained with PUF and a denuder (PDMS trap+filter+PDMS trap) sampler directly after indoor DDT-spraying (0 h), 4 h and 24 h after IRS

Interval	¹ PUF	² Denuder PDMS trap+filter+PDMS trap	² Vapour Phase	² Particulate Phase
0	11	13	10.6	2.9
4	8	10	7.7	2.7
24	9	15	12.4	2.3

¹Bouwman et al. [28] ²Denuder device (multi-channel PDMS trap+filter+multi-channel PDMS trap) distinguishes between air borne vapour phase and airborne particulate phase, whilst PUF does not.

2.4 Conclusions

A new environmental forensic technique was developed for DDT IRS. Indoor airborne vapour phase and particulate phase *p,p'*-DDT, *o,p'*-DDT, *p,p'*-DDD, *o,p'*-DDD, *p,p'*-DDE and *o,p'*-DDE were collected separately by a novel denuder multi-channel PDMS trap+filter+multi-channel PDMS trap combination, at a low air flow sampling rate and a short collection time using a compact, battery operated field pump. The low cost denuder sampler is quick and simple to assemble and it fits commercial thermal desorbers. Solvent extraction of the sampling materials, extract clean-up and concentration are not required. Instead, solventless thermal desorption allows transfer of the entire sample mass to the CIS inlet of a GC-MS. CIS injection is mild compared to conventional isothermal GC injection, minimising the conversion of DDT to DDD during injection. LODs and LOQs of the GC-MS (SIM) EI+ mode method were at ng m^{-3} levels for 4L of air sampled. Vapour phase and particulate phase *p,p'*-DDT, *o,p'*-DDT, *p,p'*-DDD, *o,p'*-DDD, *p,p'*-DDE and *o,p'*-DDE were each quantified separately. Vapour phase mean Σ DDT $3.82 \mu\text{g m}^{-3}$ and particulate phase mean Σ DDT $1.52 \mu\text{g m}^{-3}$ were measured inside traditional huts prior to DDT

spraying. Following a 24 h waiting period after DDT IRS vapour phase mean Σ DDT was $12.37 \mu\text{g m}^{-3}$ and particulate phase mean Σ DDT was $2.30 \mu\text{g m}^{-3}$. Ratios of airborne p,p' -DDD/ p,p' -DDT and of o,p' -DDT/ p,p' -DDT were unusually high and do not match the ideal ingredient composition required of certified commercial DDT. This technique, gentler than conventional injection, reduces uncertainty as to the origin of the unusually high DDD values. Insecticidal efficacy of a DDT IRS product may have been compromised which may explain an incidence of malaria outbreaks following IRS. Since sampling was done under undisturbed conditions it cannot be concluded that particulate phase insecticide presents an unimportant pathway for human exposure. The method is well-suited for use in a follow up study involving the sampling of air during domestic activities (sweeping, dusting). The same sampling method also allows enantiomeric analysis at the concentrations indicated. Enantiomeric analysis would eliminate uncertainties as to whether the fraction of DDD present in the environment is due to dubious IRS products or to the ageing of DDT. The method reported here is not limited to DDT, and can be used for air pollution monitoring of additional POPs and PAHs.

2.5 Acknowledgements

Sincere thanks to Prof Riana Bornman of the Department of Urology, University of Pretoria, for her generous assistance in the collection of air samples during the 2007 IRS season, Dr Fanie van der Walt for designing and building the portable sampling pumps, Sasol and the National Research Foundation (NRF) for funding, Rosy Ocwelwang for laboratory assistance during TDS and GC inlet degradation evaluation, Etienne van der Walt, Ephraim Bafane Malinga and Joel

Matibisi Mooka (ARC-PPRI) for sampling of the indoor air of huts, Azel Swemmer of FDA Laboratories for kindly providing commercial (technical) DDT formulations.

2.6 References

- [1] World Malaria Report, World Health Organisation (2010) [online]. Available: http://www.who.int/malaria/publications/country-profiles/profile_zaf_en.pdf (Accessed 28.06.2011).
- [2] World Malaria Report, World Health Organisation (2011) [online]. Available: http://who.int/malaria/world_malaria_report_2011/en/index.html (Accessed 31.01.2012).
- [3] J. Volckens, D. Leith, *Ann.occup. Hyg.* 47(2) (2003)157-164.
- [4] P. Larsson, O. Berglund, C. Backe, G. Bremle, A. Eklöv, C. Järnmark, A. Persson, *Naturwissenschaften* 82 (1995) 559-561.
- [5] J.C. Van Dyk, H. Bouwman, I.E.J. Barnhoorn, M.S. Bornman, *Sci. Total Environ.* 408 (2010) 2745-2752.
- [6] M. Millet, in: J.L. Tadeo (Ed.), *Sampling and Analysis of Pesticides in the Atmosphere*, CRC Press, Boca Raton, Florida, 2008, pp. 257-286.
- [7] E. Borrás, P. Sánchez, A. Muñoz, L.A. Tortajada-Genaro, *Anal. Chim. Acta* 699 (2011) 57– 65.
- [8] M. Possanzini, V. Di Palo, P. Gigliucci, M.C.T. Scianò, A. Cecinato, *Atmos. Environ.* 38 (2004) 1727-1734.
- [9] M. Possanzini, V. Di Palo, G. Tagliacozzo, A. Cecinato, *Polycycl. Aromat. Comp.* 26(3) (2006) 185-195.
- [10] A.J. Peters, D.A. Lane, L.A. Gundel, G.L. Northcott, K.C. Jones, *Environ. Sci. Technol.* 34 (2000) 5001-5006.
- [11] D.E. Tobias, J.A. Perlinger, P.S. Morrow, P.V. Doskey, D.L. Perram, *J. Chromatogr. A.* 1140 (2007) 1-12.
- [12] S.A. Batterman, S.M. Chernyak, Y. Gounden, M. Matoane, R.N. Naidoo, *Sci. Total Environ.* 397 (2008) 119-130.
- [13] H. Alegria, T.FR. Bidleman, M. Salvador Figueroa, *Environ. Pollut.* 140 (2006) 483-491.
- [14] R. Barro, J. Regueiro, M. Llompарт, C. Garcia-Jares, *J. Chromatogr. A.* 1216 (2009) 540-566.
- [15] M. Goriaux, B. Jourdain, B. Temime, J.-L. Besombes, N. Marchand, A. Albinet, E. Leoz-Garziandia, H. Wortham, *Environ. Sci. Technol.* 40 (2006) 6398-6404.
- [16] E. Baltussen, C.A. Cramers, P.J.F. Sandra, *Anal. Bioanal. Chem.* 373 (2002) 3-22.
- [17] P. Bohlin, K.C. Jones, B. Strandberg, *J. Environ. Monit.* 9 (2007) 501-509.
- [18] P.B.C. Forbes, E.R. Rohwer, *Environ. Pollut.* 157 (2009) 2529-2535.
- [19] D.A. Lane, N.D. Johnson, S.C. Barton, G.H.S. Thomas, W.H. Schroeder, *Environ. Sci. Technol.* 22(8) (1988) 941-947.
- [20] M.S. Kriegler, R.A. Hites, *Environ. Sci. Technol.* 26 (1992) 1551-1555.
- [21] E.K. Ortner, E.R. Rohwer, *J. High Res. Chromatog.* 19 (1996) 339-343.

- [22] P.B.C. Forbes, E.R. Rohwer, *WIT Trans. Ecol. Envir.* 116 (2008) 345-355.
- [23] P.B.C Forbes, A. Trüe, E.R. Rohwer, *Environ. Chem. Lett.* 9 (2011) 7–12.
- [24] P.B.C. Forbes, E.W. Karg, R. Zimmermann, E.R. Rohwer, *Anal. Chim. Acta* 730 (2012) 71–79.
- [25] A.S.Y. Chau, B.K. Afghan, *Analysis of Pesticides in Water. Significance, Principles, Techniques, and Chemistry of Pesticides*, volume 1, CRC Press Inc., Boca Raton, Florida, 1982, p.11.
- [26] J. Muñoz-Arnanz, C. Bosch, P. Fernandez, J.O. Grimalt, B. Jimenez, *J. Chromatogr. A.* 1216 (2009) 6141–6145.
- [27] W.T. Foreman, P.M. Gates, *Environ. Sci. Technol.* 31(3) (1997) 905-910.
- [28] H. Bouwman, R. Bornman, C. van Dyk, I. Barnhoorn, H. Kylin. Dynamics and risks of DDT applied indoors for malaria control. Poster presentation at the 12th EuCheMS International Conference on Chemistry and the Environment, Stockholm, Sweden, 14-17 June 2009.
- [29] R. Bornman, C. de Jager, Z. Worku, P. Farias, S. Reif, *BJUI.* (2009) 1-7.
- [30] S. Hosie, S. Loff, K. Witt, K. Niessen, K.-L. Waag, *Eur. J. Pediatr. Surg.* 10 (2000) 304-309.
- [31] H. Bouwman, B. Sereda, H.M. Meinhardt, *Environ. Pollut.* 144 (2006) 902 – 917.
- [32] X. Qiu, T. Zhu, B. Yao, J. Hu, S. Hu, *Environ. Sci. Technol.* 39 (2005) 4385-4390.
- [33] Y. Naudé, W.H.J. de Beer, S. Jooste, L. van der Merwe, S.J. van Rensburg, *Water SA.* 24(3) (1998) 205-214.
- [34] K.T. Lee, S. Tanabe, C.H. Koh, *Environ. Pollut.* 114 (2001) 207-213.
- [35] T.O. Said, K.M. El Moselhy, A.A.M. Rashad, M.A. Shreadah, *Bull. Environ. Contam. Toxicol.* 81 (2008) 136-146.
- [36] T. G. Negoita, A. Covaci, A. Gheorghe, P. Schepens, *J. Environ. Monit.* 5 (2003) 281-286.
- [37] C. Herrera-Portugal, H. Ochoa, G. Franco-Sánchez, L. Yáñez, F. Díaz-Barriga, *Environ. Res.* 99 (2005) 158-163.
- [38] S. De Francia, E. Pirro, F. Zappia, F. De Martino, A.E. Sprio, F. Daffara, M. Terzolo, A. Berruti, F. Di Carlo, F. Ghezzi, *J. Chromatogr. B.* 837 (2006) 69-75.
- [39] E. Eljarrat, P. Guerra, D. Barceló, *Trends Anal. Chem.* 27 (2008) 847-861.
- [40] Y. Naudé, E.R. Rohwer, *Anal. Chim. Acta*, 730 (2012) 120–126.
- [41] P.F. Hoekstra, B. K. Burnison, T. Neheli, D.C.G. Muir, *Toxicol. Lett.* 125 (2001) 75-78.
- [42] X.-Z. Meng, Y. Guo, B.-I. Mai, E.Y. Zeng, *J. Agric. Food Chem.* 57 (2009) 4299-4304.

Chapter 3

Two multidimensional chromatographic methods for enantiomeric analysis of *o,p'*-DDT and *o,p'*-DDD in contaminated soil and air in a malaria area of South Africa

This chapter was published in Analytica Chimica Acta. The format reflects the style set by the journal.

Naudé, Y. and Rohwer, E.R., 2012. Two multidimensional chromatographic methods for enantiomeric analysis of *o,p'*-DDT and *o,p'*-DDD in contaminated soil and air in a malaria area of South Africa. *Analytica Chimica Acta* 730, 120–126. DOI:10.1016/j.aca.2012.03.028

Author contributions

Conceived and designed the experiments: Yvette Naudé and Egmont Rohwer. Performed experimental work and data analysis, wrote the chapter/article, submitted article to journal, response to reviewers: Yvette Naudé. Initiator of research and study supervisor: Egmont Rohwer.

The work in this chapter was presented at the 34th International Symposium on Capillary Chromatography 2010, Riva del Garda, Italy

Two multidimensional chromatographic methods for enantiomeric analysis of *o,p'*-DDT and *o,p'*-DDD in contaminated soil and air in a malaria area of South Africa

Yvette Naudé* and Egmont R. Rohwer

Department of Chemistry, University of Pretoria, Private Bag X20, Hatfield 0028, Pretoria, South Africa

ABSTRACT

In rural parts of South Africa the organochlorine insecticide DDT (1,1,1-trichloro-2,2-bis(*p*-chlorophenyl)ethane) is still used for malaria vector control where traditional dwellings are sprayed on the inside with small quantities of technical DDT. Since *o,p'*-DDT may show enantioselective oestrogenicity and biodegradability, it is important to analyse enantiomers of *o,p'*-DDT and its chiral degradation product, *o,p'*-DDD, for both health and environmental-forensic considerations. Generally, chiral analysis is performed using heart-cut multidimensional gas chromatography (MDGC) and, more recently, comprehensive two-dimensional gas chromatography (GCxGC). An off-line gas chromatographic fraction collection (heart-cut) procedure was developed for the selective capturing of the appropriate isomers from a first apolar column, followed by reinjection and separation on a second chiral column. Only the *o,p'*-isomers of DDT and DDD fractions from the first dimension complex chromatogram (achiral apolar GC column separation) were selectively collected onto a polydimethylsiloxane (PDMS) multichannel open tubular silicone rubber

trap by simply placing the latter device on the flame tip of an inactivated flame ionisation detector (FID). The multichannel trap containing the *o,p'*-heart-cuts was then thermally desorbed into a GC with time-of-flight mass spectrometry detection (GC-TOFMS) for second dimension enantioselective separation on a chiral column (β -cyclodextrin-based). By selectively capturing only the *o,p'*-isomers from the complex sample chromatogram, 1D separation of ultra-trace level enantiomers could be achieved on the second chiral column without matrix interference. Here, solventless concentration techniques for extraction of DDT from contaminated soil and air are presented, and enantiomeric fraction (EF) values of *o,p'*-DDT and *o,p'*-DDD obtained by a new multidimensional approach for heart-cut gas chromatographic fraction collection for off-line second dimension enantiomeric separation by 1D GC-TOFMS of selected isomers are reported. This multidimensional method is compared to the complementary technique of GCxGC-TOFMS using the same enantioselective column, this time as the first dimension of separation.

Keywords: Polydimethylsiloxane (PDMS) sorptive extraction; Environmental forensics; Persistent organic pollutants (POPs); Chiral chromatography; GCxGC; Heart-cutting

*Corresponding author. Tel.: +27 12 420 2517; fax: +27 12 420 4687.

E-mail address: yvette.naude@up.ac.za

3.1 Introduction

In risk areas of South Africa the organochlorine insecticide DDT (1,1,1-trichloro-2,2-bis(*p*-chlorophenyl)ethane) is still used for malaria vector control. The strict Stockholm Convention on Persistent Organic Pollutants (POPs) allows Indoor Residual Spraying (IRS) of traditional dwellings with DDT. In South Africa, IRS with DDT resulted in a 65% decrease in the number of deaths caused by malaria and an 83% decrease in the number of confirmed malaria cases [1]. Technical grade DDT (75% wettable powder) used for IRS in South Africa contains 72-75% of *p,p'*-DDT, the active ingredient, and ~22% of *o,p'*-DDT [2,3]. Technical DDT has oestrogen-like properties, mainly due to *o,p'*-DDT [4,5]. *o,p'*-DDT and its degradation product *o,p'*-DDD are chiral molecules (*o,p'*-DDE is achiral) and both exist as enantiomeric pairs (-)-*o,p'*-DDT and (+)-*o,p'*-DDT, and (-)-*o,p'*-DDD and (+)-*o,p'*-DDD [6,7]. A chiral compound is produced industrially as a racemic mixture [8]. Fresh treatment with technical DDT will have a chiral signature where enantiomers of *o,p'*-DDT and of *o,p'*-DDD are present as a 1:1 racemic mixture corresponding to an enantiomeric fraction (EF) = 0.5 [9]. In the environment selective breakdown of one enantiomer of a pair can result in non-racemic residues [9] and a deviation of EF from 0.5 in samples may therefore be used to differentiate between recent and past inputs of POPs [7,10,11]. *o,p'*-DDT is reported to show enantioselective oestrogenicity since (-)-*o,p'*-DDT is a weak oestrogen mimic while (+)-*o,p'*-DDT is inactive [5,12,13]. These chiral compounds are separated by using columns with a β -cyclodextrin stationary phase specifically developed for this purpose [7,9,13-18]. However, coelution of compounds in complex environmental mixtures can make forensic

determinations difficult. To overcome the problem of coelution, chiral analysis of POPs is generally performed by heart-cut multidimensional gas chromatography (MDGC) [7,11,15-17,19-22] and comprehensive two-dimensional gas chromatography (GCxGC) [11,15,17,19]. An excellent review of multidimensional chromatography in pesticides analysis can be found in Tuzimski [23]. In the heart-cut MDGC technique two independent GC systems are coupled so that one or more unresolved fractions are transferred directly (on-line) from a first non-enantioselective column (first dimension) to a second enantioselective column (second dimension) where separation of the compounds will occur. In GCxGC the entire sample is separated on two different columns - the first column provides a regular GC elution and the second, shorter, column is fast eluting [16].

Organochlorine pesticides are typically solvent extracted from soil by Soxhlet extraction [9,18,20,21,24,25] and by sonication [7]. Microlitre amounts are injected for analysis. Sensitivity limitations are associated with injection of only a fraction of the final 20 μ L to 1 mL solvent extract [26]. In contrast to extraction procedures using solvents, the procedure applied in this study is a novel solvent free sorptive extraction technique where DDT is concentrated from soil using polydimethylsiloxane (PDMS) loops. PDMS functions as a hydrophobic solvent for the analytes [26]. After extraction the loop is inserted into a commercial thermal desorption tube for solventless introduction into a GC. Chiral columns are sensitive to moisture and matrix components, and therefore desorption-injection rather than liquid extract injection is preferable in order to protect the expensive column.

Taking into consideration that DDT residues in soil are emitted into air (soil-air exchange) [9] and that contaminated airborne dust presents a pathway for exposure to DDT, enantiomeric signatures are also determined for indoor air samples in this study. Here, DDT in indoor air is concentrated with a denuder configuration of a PDMS multichannel open tubular silicone rubber trap (MCT) combined with a micro quartz fibre filter for single-step collection of vapour phase and particulate phase DDT [27].

The extraction of DDT and its associated environmental pollutants by novel solventless sorptive extraction techniques using PDMS and a new multidimensional approach for heart-cut gas chromatographic fraction collection (GCFC) from a non-enantioselective column for off-line second dimension isomer selective enantiomeric separation of both isomers, *o,p'*-DDT and *o,p'*-DDD, by GC-TOFMS are reported. This multidimensional procedure is compared to the complementary technique of GCxGC-TOFMS using the same enantioselective column, this time as the first dimension of separation.

3.2 Materials and methods

3.2.1 Sampling site

Outdoor soil and indoor air samples were collected from a rural village (S 23°02'02.3" E 30°51'33.5") in the Vhembe District, Limpopo Province, South Africa. The village is situated within an intermediate-risk malaria area where indoor DDT-spraying is performed annually [24]. A detailed description of the

study area was reported in Van Dyk et al. [24]. The province is a summer rainfall region. Outdoor soil samples (D8, D10, D12) were collected two months after completion of the IRS programme in February 2008 during the summer season [24]. Indoor air samples were collected from traditional round thatch-roof huts (D7 to D10) directly after IRS in November 2007 and details are reported elsewhere by Naudé and Rohwer [27].

3.2.2 Chemicals and equipment

A certified organochlorine pesticides standard mixture (purity $\geq 97\%$) containing *p,p'*-DDT, *o,p'*-DDT, *p,p'*-DDD, *o,p'*-DDD, *p,p'*-DDE and *o,p'*-DDE and a certified inlet degradation mixture (*p,p'*-DDT and Endrin, purity $\geq 98\%$) were purchased from Sigma-Aldrich (Pty) Ltd. Kempton Park, South Africa. Solvents used were of analytical grade. The standard stock solution was diluted in hexane (Merck Chemicals (Pty) Ltd., South Africa) to give working standard solutions of $1 \text{ ng } \mu\text{L}^{-1}$ and $10 \text{ ng } \mu\text{L}^{-1}$. The inlet degradation solution (*p,p'*-DDT) was diluted in hexane to give a concentration of $1 \text{ ng } \mu\text{L}^{-1}$.

Compounds from air and soil were concentrated on SIL-TEC™ silicone elastomer medical grade tubing (0.64 mm OD x 0.30 mm ID) (Technical Products, Georgia, United States of America). Thermal desorption tubes (17.8 cm long glass tubes, 4 mm ID, 6 mm OD), thermal desorber systems (TDS 3), cooled injection systems (CIS 4) and empty baffled deactivated glass CIS liners were all from Gerstel™ (Chemetrix, Midrand, South Africa or LECO Africa (Pty) Ltd., Kempton Park, South Africa). The GC-FID used for apolar heart-cutting

was an Agilent 6890 GC (Chemetrix, Midrand, South Africa). Chiral separation was performed on a LECO Pegasus 4D Agilent 7890 GC system (LECO Africa (Pty) Ltd., Kempton Park, South Africa. Gases were of ultra high purity grade (Afrox, Gauteng, South Africa).

3.2.3 Solventless concentration methods for *p,p'*-DDT, *o,p'*-DDT, *p,p'*-DDD, *o,p'*-DDD, *p,p'*-DDE and *o,p'*-DDE

3.2.3.1 Soil sampling with PDMS loops

A loop was fashioned by taking a 10.5 cm (0.02 g) length of a silicone elastomer medical grade tubing and joining the ends by inserting a 1 cm piece of fused silica capillary column (250 μm ID) (Figure 3.1). A loop arrangement prevents soil from entering the PDMS tube and it facilitates ease of handling [28]. The sorption volume of the loop used for solventless extraction of the soil samples was 26 μL . A 40 mL glass vial, fitted with a solid screw cap coated on the inside with polytetrafluoroethylene (PTFE), was filled with 40 g (heart-cut GCFC) soil or 10 g soil (GCxGC-TOFMS). A PDMS loop was submerged in the soil. The vial was placed in an oven at 50 $^{\circ}\text{C}$ for 90 min. Thereafter, the PDMS loop was inserted into a glass desorption tube for thermal desorption into a gas chromatograph – flame ionisation detector (GC-FID) or, alternatively, a gas chromatograph – time-of-flight mass spectrometer (GC-TOFMS).

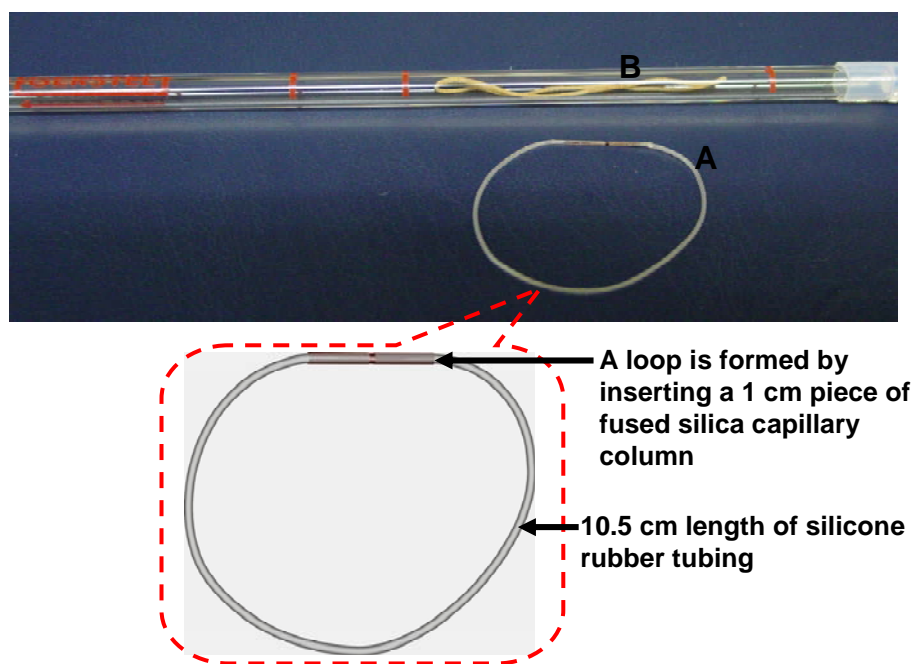


Figure 3.1. PDMS loop prior to (A) and after extraction (B) of soil. A loop arrangement prevents soil from entering the silicone rubber tubing.

3.2.3.2 Denuder indoor air sampling

A full description of the methodology is reported elsewhere by Naudé and Rohwer [27]. Briefly, four litre of indoor air was sampled with a denuder device consisting of a multichannel PDMS trap + micro quartz fibre filter + multichannel PDMS trap combination to sample airborne vapour phase DDT (first PDMS trap) and airborne particulate phase DDT (filter and back-up PDMS trap) in a single step. A denuder allows simultaneous collection of molecules and transmission of aerosol particles through the silicone rubber tubes based on the large difference in radial diffusion speeds in the axial laminar flow environment [29].

3.2.4 *Multichannel open tubular PDMS traps (MCTs) for heart-cut collection of GC separated isomer peaks*

Multichannel traps containing 0.099 ± 0.02 g silicone, providing a sample enrichment volume of 106 μ L PDMS, were prepared based on a technique described by Ortner and Rohwer [30]. The MCT was designed to fit a commercial thermal desorber system. A bundle of twenty eight channels of silicone elastomer medical grade tubing were inserted into glass desorption tubes (Figure 3.2). The MCT inside the desorption tube was 15 mm long. The ends of the MCT device were capped with glass stoppers during storage. The glass stoppers were secured with tight-fitting PTFE sleeves. The trapped analytes inside the MCT are not directly exposed to the PTFE sleeves, thereby preventing potential adsorption of analytes onto the Teflon.

3.2.5 *Multidimensional GC techniques*

3.2.5.1 *Apolar separation*

3.2.5.1.1 *TDS-CIS-GC-FID*

p,p'-DDT, *o,p'*-DDT, *p,p'*-DDD, *o,p'*-DDD, *p,p'*-DDE and *o,p'*-DDE were thermally desorbed from the PDMS loops (soil) and PDMS multichannel traps (air) using a TDS installed on a GC-FID. The TDS transfer line temperature was 280 °C. During splitless desorption the PDMS loops were heated from 30 °C (3 min) at 30 °C min⁻¹ to 250 °C (20 min) with a desorption flow rate of 50

mL min⁻¹ at 75 kPa (hydrogen). The desorbed analytes were cryogenically focused on a CIS at -100 °C using liquid nitrogen. The GC inlet was in the solvent vent mode to achieve a high desorption flow rate whilst the purge valve remained closed during desorption to give a splitless-type injection from the CIS. After desorption, a splitless injection (purge on at 27 min, purge flow 50 mL min⁻¹, solvent vent mode) was performed by heating the CIS from -100 °C at 6 °C s⁻¹ to 250 °C and kept there for 27 min. The GC oven temperature programme was 60 °C (5 min) at 10 °C min⁻¹ to 280 °C (1 min). A post run was performed by heating the GC oven to 310 °C (10 min). The hydrogen carrier gas flow rate was 2 mL min⁻¹ (52 cm s⁻¹) and the column head pressure was 75 kPa in the constant pressure mode. The GC column was an apolar Zebron ZB-1 30 m x 250 µm ID x 0.25 µm film thickness (df) (Phenomenex, Separations, Randburg, South Africa). The FID was operated at 300 °C. Flow rates of FID gases were hydrogen 40 mL min⁻¹, air 400 mL min⁻¹ and nitrogen (make-up gas) 50 mL min⁻¹.

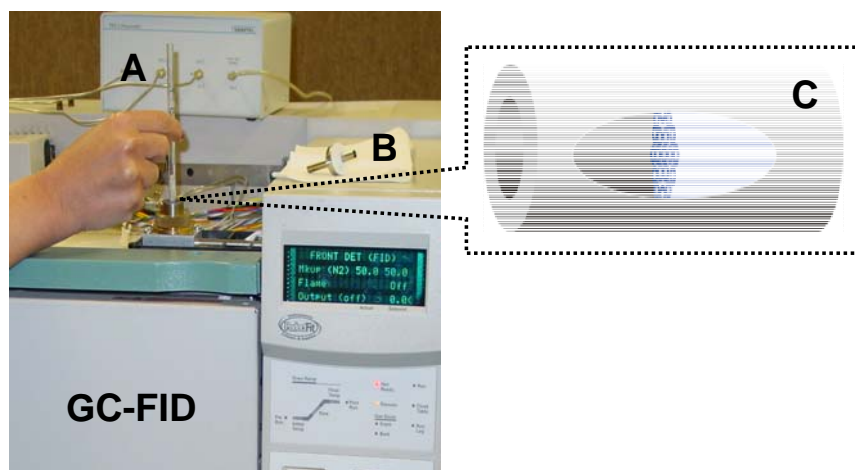


Figure 3.2. Collection of heart-cuts of *o,p'*-DDD and *o,p'*-DDT from the GC effluent onto a multichannel trap. (A) The multichannel trap is simply placed on an inactivated FID flame tip during selected isomer collection. (B) The FID collector is removed prior to heart-cutting. (C) Schematic diagram of a multichannel trap consisting of silicone rubber tubes arranged in parallel inside a commercial glass desorption tube.

3.2.5.1.2 *Novel gas chromatography fraction collection (GCFC) for heart-cut transfer of selected isomers to another off-line GC*

Chromatographic profiles of authentic chemical standards (*p,p'*-DDT, *o,p'*-DDT, *p,p'*-DDD, *o,p'*-DDD, *p,p'*-DDE and *o,p'*-DDE), contaminated soil and indoor air were first obtained using the conditions described in 3.2.5.1.1. Integration results of peak start time and peak end time of the chromatograms were then used to establish the heart-cutting event times. In a subsequent run, different sections of the GC-effluent were selectively recaptured onto MCTs on

a carefully timed basis (Figure 3.2). For isomer selected heart-cutting by GCFC the instrumental conditions were as described in 2.5.1.1, the only difference now was the modification of the detector parameters. The electrometer was switched off. The detector top assembly and the collector are easily removed by loosening the knurled brass nut of the detector assembly and by taking out the collector. Single peaks were collected at the end of the GC column by simply placing a MCT on the inactivated FID flame tip and by supporting the MCT in this position by hand. During collection the FID and flame gases (hydrogen and air) were switched off, the make-up gas (nitrogen) plus carrier gas (hydrogen) flow totalled 50 mL min^{-1} and the detector temperature was at $300 \text{ }^\circ\text{C}$. After selective capturing of *o,p'*-DDT and *o,p'*-DDD heart-cuts onto MCTs, the MCTs were capped with custom-made glass and Teflon stoppers (section 3.2.4) and stored for second dimension 1D chiral separation by GC-TOFMS.

3.2.5.2 *Chiral separation*

3.2.5.2.1 *1D GC-TOFMS analysis of isomer selected heart-cuts from outdoor soil and indoor air collected on MCTs*

The GC-TOFMS used to analyse the isomer selected heart-cuts, *o,p'*-DDT and *o,p'*-DDD, was run in 1D mode. The heart-cut isomers on PDMS multichannel traps were thermally desorbed by heating the traps in a TDS from $30 \text{ }^\circ\text{C}$ (3 min) at $30 \text{ }^\circ\text{C min}^{-1}$ to $250 \text{ }^\circ\text{C}$ (20 min) with a desorption flow rate of 100 mL min^{-1} at a vent pressure of 57 psi (helium). The TDS transfer line

temperature was 280 °C. The desorbed analytes were cryogenically focused on a CIS at –100 °C using liquid nitrogen. After desorption, a splitless injection (purge on at 40 min, purge flow 50 mL min⁻¹, solvent vent mode) was performed by heating the CIS from –100 °C at 6 °C s⁻¹ to 250 °C and held there for the duration of the GC run.

The primary column (¹D) was a β-cyclodextrin-based chiral phase BGB-172 (20% *tert*-butyldimethylsilyl-β-cyclodextrin dissolved in BGB-15 (15% phenyl-, 85% methylpolysiloxane)) 30 m x 0.25 mm ID x 0.25 μm df (BGB Analytik, Switzerland) and the secondary column (²D) was an intermediate polarity Rtx-200 (trifluoropropyl methyl polysiloxane) 1.29 m x 0.18 mm ID x 0.18 μm df (Restek, Bellefonte, PA, USA). The primary oven temperature programme was 120 °C (3 min) at 10 °C min⁻¹ to 200 °C (no hold), 1.5 °C min⁻¹ to 230 °C (10 min). The GC run time was 41 min. The secondary oven was programmed identical to the primary oven, but offset by + 20 °C. The system was unmodulated, i.e. the separation was essentially that provided by the primary column (operated in 1D mode with modulation period set at 0 s). The carrier gas (helium) velocity was 54 cm s⁻¹ (2 mL min⁻¹) in the constant flow mode.

The MS transfer line temperature was set at 280 °C. The ion source temperature was 200 °C, the electron energy was 70 eV in the electron impact ionization mode (EI+), the data acquisition rate was 10 spectra s⁻¹, the mass acquisition range was 40–360 atomic mass units (amu), and the detector

voltage was set at 1700 V. The order of elution of the enantiomers of *o,p'*-DDT and *o,p'*-DDD was obtained from Buser and Muller [6].

3.2.5.2.2 GCxGC-TOFMS analysis of outdoor soil and indoor air

The same GC-TOFMS utilised in 3.2.5.2.1 was now run in GCxGC mode to analyse enantiomers of *o,p'*-DDT and *o,p'*-DDD. The system included a secondary oven and a dual stage modulator. Liquid nitrogen was used for the cold jets and synthetic air for the hot jets. The analytes from contaminated soil (sorbed onto PDMS loops), from vapour phase (on PDMS multichannel trap) and from airborne particulate phase (on a micro quartz fibre filter) contaminants, were thermally desorbed as is described in 3.2.5.2.1. Columns set-up and GC-TOFMS parameters were as described in 3.2.5.2.1. The secondary oven was programmed identical to the primary oven, but offset by + 5 °C. The modulator temperature offset was 30 °C. The modulation period was 4 s with a hot pulse time of 1 s. The data acquisition rate was 100 spectra s⁻¹. Identification of *p,p'*-DDT, *o,p'*-DDT, *p,p'*-DDD, *o,p'*-DDD, *p,p'*-DDE and *o,p'*-DDE was based on comparison of retention times of authentic standards and comparison of mass spectra with a mass spectral library.

3.2.6 Data analysis

Statistical analyses were performed by using the paired t-test set at a 95% level of confidence. Any difference between results was considered not

significant when a probability (two-tailed P value (p)) greater than 0.05 was returned by the t-test.

3.3 Results and discussion

3.3.1 Solventless extraction and desorption-injection

Typically the method for isolating and analysing POPs from soils and air is solvent extraction of the materials followed by the analysis of microlitre amounts of the diluted final extract. A simple, cheap, non-hazardous solventless extraction technique using PDMS for analyte enrichment from soil and air (Figures 3.1 and 3.2) for the introduction of the total amount of sorbed analytes into a GC was developed. A novel multidimensional GC approach was followed where MCTs containing selectively trapped isomers were redesorbed for off-line second dimension separation by 1D GC-TOFMS. For comparison, PDMS loops (outdoor soil samples) and MCTs (indoor air samples) were desorbed for compound separation by the complementary technique of GCxGC-TOFMS. For a fixed desorption time the amount of *o,p'*-DDD and *o,p'*-DDT desorbed from PDMS was dependent on the desorption flow rate of helium. To improve detectability of the target compounds a high desorption flowrate was required. The amount of *o,p'*-DDD and *o,p'*-DDT desorbed from PDMS with a helium vent flow rate of 100 mL min⁻¹ was double the amount desorbed at 60 mL min⁻¹. In contrast, hydrogen did not present the higher desorption yields with increased desorption vent flow rate and 50 mL min⁻¹ was used in this case (3.2.5.1). Desorption and programmable temperature

vaporisation (PTV) injection were optimised to minimise DDT degradation [27] and inlet liners were replaced regularly with new deactivated liners to keep DDT degradation below 10%.

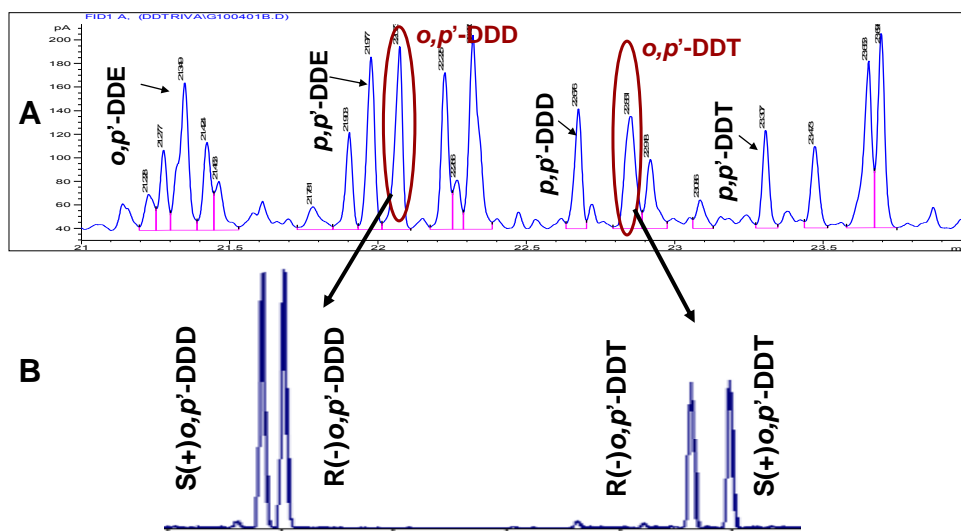


Figure 3.3. Enantiomeric profiling by off-line GCFC–GC-TOFMS. (A) First dimension non-enantioselective separation. (B) Second dimension 1D enantioselective separation (β -cyclodextrin phase) of the heart-cuts of *o,p'*-DDD and *o,p'*-DDT collected from A.

3.3.2 Novel isomer selective off-line heart-cutting by GC fraction collection onto PDMS MCTs

Figure 3.2 depicts selective heart-cutting of the chiral isomers, *o,p'*-DDD and *o,p'*-DDT, from the complex sample achiral chromatogram. Complicated instrumental set-ups, sophisticated equipment or valves were not required. The FID collector was removed prior to heart-cutting. The FID flame gases (hydrogen and air) were switched off. PDMS containing sorbed analytes from

soil or from air was desorbed for achiral (apolar phase) first dimension separation of *o,p'*-DDE, *p,p'*-DDE, *o,p'*-DDD, *p,p'*-DDD, *o,p'*-DDT and *p,p'*-DDT (Figure 3.3A). During this first dimension achiral separation of the complex mixture only *o,p'*-DDD and *o,p'*-DDT were selectively collected from the GC effluent onto a PDMS multichannel trap. The MCT was placed, by hand, on the inactivated flame tip prior to peak elution and removed once the peak had eluted. The two chiral isomers, *o,p'*-DDT and *o,p'*-DDD, were sequentially collected on a single MCT during the same chromatographic run. The MCT with *o,p'*-DDD and *o,p'*-DDT heart-cuts was then desorbed into a GC-TOFMS for second dimension 1D chiral (β -cyclodextrin phase) separation of the enantiomers (Figure 3.3B).

The open tubular structure of the MCT and low pressure drop associated with multichannel flow [28] are characteristics that are particularly suited to the recapturing of chromatographic fractions from the GC effluent during a GC run (Figure 3.2). Most of the effluent of the FID passes through the trap without special sealing arrangement that would otherwise complicate the GCFC procedure. The advantage of a low pressure drop is not offered by conventional packed traps.

3.3.3 Comparison of chiral separation by one dimensional and multidimensional gas chromatography

Figure 3.4 shows the comparison of conventional and multidimensional GC techniques for the enantiomeric separation of *o,p'*-DDD and *o,p'*-DDT.

During conventional 1D chiral separation the achiral isomer, p,p' -DDD, interferes with the enantiomer $(-)$ - o,p' -DDT (Figure 3.4A). In this case, EF values for o,p' -DDT cannot be calculated with accuracy in the presence of an interfering peak. However, the interfering p,p' -DDD peak was successfully eliminated by selective capturing of only the o,p' -DDT isomer during the preceding off-line heart-cut GCFC (Figure 3.4B). Because the complex matrix is purified by heart-cutting of selected isomers from the total chromatogram, second dimension 1D chiral separation of the o,p' -DDT enantiomers was thus achieved without interference by p,p' -DDD. Using the complementary technique of GCxGC-TOFMS p,p' -DDD is similarly well separated from $(-)$ - o,p' -DDT (Figure 3.4C).

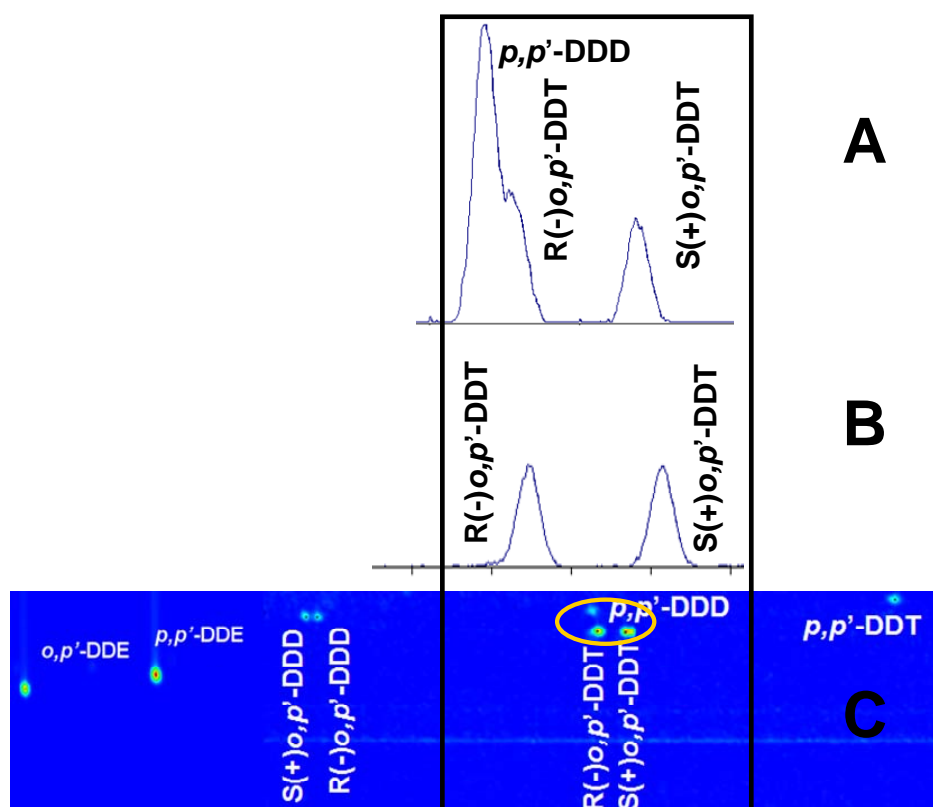


Figure 3.4. Comparison of conventional and multidimensional GC techniques. (A) p,p' -DDD interferes with $R(-)o,p'$ -DDT during conventional 1D chiral separation. (B) Second dimension 1D separation of the o,p' -DDT enantiomers without interference by p,p' -DDD. Off-line heart-cutting eliminated peak

interference. (C) The complementary technique of GCxGC-TOFMS: *p,p'*-DDD is similarly well separated from R(-)*o,p'*-DDT.

3.3.4 Multidimensional chromatographic performance

The EF is used as a descriptor of chiral signatures and is defined by: $EF = \frac{\text{peak area of enantiomer 1}}{\text{peak area of enantiomer 1} + \text{peak area of enantiomer 2}}$, where enantiomer 1 is the first eluting enantiomer and enantiomer 2 is the last eluting enantiomer of a pair [8,31]. Thus, $EF = 0.5$ correlates to a racemic composition of a compound [8,9,31], indicating fresh treatment, whereas a deviation from 0.5 indicates past treatment.

EF values of *o,p'*-DDD and *o,p'*-DDT in a chemical standard, outdoor soil and indoor air samples were determined by 1D heart-cut GCFC–GC-TOFMS and by GCxGC-TOFMS and are given in Table 3.1. Replicate injections ($n=4$) of the chemical standard were performed to determine the precision of the EF values obtained with the two multidimensional techniques (Table 3.1). EF mean values for the chemical standard measured by 1D heart-cut GCFC–GC-TOFMS were 0.494 ± 0.003 (0.69% relative standard deviation (RSD)) for *o,p'*-DDD and 0.498 ± 0.007 (1.38% RSD) for *o,p'*-DDT. The precision of the heart-cut GCFC–GC-TOFMS procedure for replicate injections of the chemical standard, in terms of absolute mass mean values (reported as absolute peak area $\times 10^5$), were 55.49 ± 5.21 (9.39% RSD) for S(+)*o,p'*-DDD; 60.03 ± 4.14 (6.89% RSD) for R(-)*o,p'*-DDD; 28.84 ± 1.93 (6.70% RSD) for R(-)*o,p'*-DDT; and 27.61 ± 2.11 (7.66% RSD) for S(+)*o,p'*-DDT. EF mean values for the chemical standard measured by GCxGC-TOFMS were 0.488 ± 0.011 (2.32% RSD) for *o,p'*-DDD

and 0.490 ± 0.001 (0.27% RSD) for *o,p'*-DDT. The EF mean values for replicate injections of the chemical standard determined by the two methods were not significantly different from 0.5 ($p > 0.05$) and thus the mixture was considered racemic. Statistical evaluation of the EF mean values for the chemical standard measured by the two multidimensional techniques showed that off-line 1D heart-cut GCFC and GCxGC gave results that do not differ significantly for *o,p'*-DDD ($p = 0.421$) and *o,p'*-DDT ($p = 0.100$).

Table 3.1

Comparison of enantiomeric fractions (EF) of *o,p'*-DDD and *o,p'*-DDT in outdoor soil and indoor air from a DDT exposed village determined by off-line GCFC–GC-TOFMS and GCxGC-TOFMS

Sample	Isomer	Concentration	EF _{GCFC–GC-TOFMS}	EF _{GCxGC-TOFMS}
Chemical standard	<i>o,p'</i> -DDD	1 ng or 10 ng on	0.494 (10ng, n=4)	0.488 (1ng, n=4)
	<i>o,p'</i> -DDT	PDMS multichannel traps	0.498 (10ng, n=4)	0.490 (1ng, n=4)
Outdoor soil PDMS loops	<i>o,p'</i> -DDD	1.0 ng g ⁻¹ ^a	0.514 (n=3)	0.493 (n=3)
	<i>o,p'</i> -DDT	0.7 ng g ⁻¹ ^a	0.463 (n=3)	0.508 (n=3)
Indoor air vapour phase on PDMS multichannel traps (IRS 0 h) Air D10	<i>o,p'</i> -DDD	2.23 µg m ⁻³ ^b	0.457	0.491
	<i>o,p'</i> -DDT	2.13 µg m ⁻³ ^b	not detected (< 2.13 µg m ⁻³)	0.512
Air D8	<i>o,p'</i> -DDD		0.523	not determined
	<i>o,p'</i> -DDT		not detected (< 2.13 µg m ⁻³)	not determined
Air D7	<i>o,p'</i> -DDD		0.518	not determined
	<i>o,p'</i> -DDT		not detected (< 2.13 µg m ⁻³)	not determined

^aMean concentration values from Van Dyk et al. [24] ^bMean concentration values for indoor air directly after indoor residual spray (IRS 0 h) from Naudé and Rohwer [27]. Not determined: replicate samples were not available.

3.3.5 *Enantiomeric signatures of outdoor soil and indoor air samples by off-line heart-cut GCFC and GCxGC*

The EF mean values of 0.493 ± 0.044 for *o,p'*-DDD and 0.508 ± 0.033 for *o,p'*-DDT for three outdoor soil samples by GCxGC-TOFMS (Table 3.1) did not differ significantly from the EF mean values for the chemical standard ($p_{o,p'-DDD} = 0.866$, $p_{o,p'-DDT} = 0.563$). However, the EF values for the three individual soil samples showed variability, ranging from 0.451 to 0.539 for *o,p'*-DDD and from 0.475 to 0.542 for *o,p'*-DDT. The individual EF values for *o,p'*-DDD in soil D12 (EF = 0.490) and *o,p'*-DDT in soil D10 (EF = 0.506) displayed racemic profiles. In contrast, EF values for *o,p'*-DDD in soil D8 (EF = 0.539) and in soil D10 (0.451), and for *o,p'*-DDT in soil D8 (EF = 0.542) and in soil D12 (EF = 0.475), were significantly different from that of the chemical standard ($p < 0.05$). IRS with DDT takes place annually. The outdoor soil samples were collected two months after IRS and therefore the variability in EF profiles of the soils reflects both recent and historic treatment with DDT. EF values determined by off-line 1D heart-cut GCFC–GC-TOFMS were 0.514 for *o,p'*-DDD and 0.463 for *o,p'*-DDT (standard deviations were not calculated since residues were high enough for determination by heart-cut GCFC in only one of the three soil samples). EF values for the soil samples measured by the two multidimensional techniques showed that GCxGC and off-line 1D heart-cut GCFC gave results that do not differ significantly for *o,p'*-DDD ($p = 0.502$) and *o,p'*-DDT ($p = 0.147$).

Directly after IRS, EF values for *o,p'*-DDD in indoor air (vapour phase) by off-line 1D heart-cut GCFC ranged from 0.457 to 0.523 (Table 3.1). Due to the low level of *o,p'*-DDT ($< 2.13 \mu\text{g m}^{-3}$) present in indoor air *o,p'*-DDT was not detected by off-line 1D heart-cut GCFC, and therefore EF values for *o,p'*-DDT could not be calculated. The enantiomeric mean profiles of indoor air (vapour phase) directly after IRS by off-line 1D heart-cut GCFC displayed compositions that were not significantly different from the racemic profile of the chemical standard ($p_{o,p'-DDD} = 0.953$). Replicate sets of the indoor air samples (D7 to D9) were not available and hence EFs were determined by heart-cut GCFC only. Two indoor air vapour phase samples were collected in hut D10 and EFs were determined by both multidimensional procedures: $EF_{GC \times GC}$ was 0.491, while EF_{GCFC} was 0.457 for *o,p'*-DDD; for *o,p'*-DDT $EF_{GC \times GC}$ was 0.512, while EF_{GCFC} could not be determined ($< 2.13 \mu\text{g m}^{-3}$) (Table 3.1). Due to past DDT treatment non-racemic residues may be emitted from the soil of the floor into the air of traditional huts. IRS is performed annually and chiral signatures of indoor air may therefore be ambivalent due to the presence of both fresh and past DDT treatment.

Table 3.2

Enantiomeric fractions (EF) of *o,p'*-DDD and *o,p'*-DDT in indoor air vapour phase and indoor airborne particulate phase from a DDT exposed village directly after indoor residual spray (0 h)

Sample	<i>o,p'</i> -DDD		<i>o,p'</i> -DDT	
	EF	Concentration ^a	EF	Concentration ^a
Indoor air vapour phase D9 _{GCFC} on PDMS multichannel trap	0.480	2.23 µg m ⁻³	not detected(< 2.13 µg m ⁻³)	
Indoor air borne particulate phase D9 _{GCxGC} on micro-quartz fibre filter	0.583	1.13 µg m ⁻³	0.527	0.28 µg m ⁻³

^aMean concentration values for indoor air directly after indoor residual spray from Naudé and Rohwer [27].

Enantiomeric fractions of vapour phase (on PDMS multichannel trap) and airborne particulate phase (on micro quartz fibre filter) *o,p'*-DDD and *o,p'*-DDT in indoor air sample D9 are given in Table 3.2. Of particular note is that the chiral signature for *o,p'*-DDD in the vapour phase displayed a racemic composition ($EF_{GCFC} = 0.480$), in contrast to that of *o,p'*-DDD in the airborne particulate phase which showed a non-racemic composition ($EF_{GCxGC} = 0.583$) with enrichment of the (+)- enantiomer (Table 3.2). Also, this EF_{GCxGC} of 0.583 for *o,p'*-DDD in indoor airborne particulate phase was significantly different from the enantiomeric profiles of that of outdoor soil, indoor air vapour phase, and of the chemical standard ($p = 0.000 (4.28 \times 10^{-5})$). Airborne particulate phase pesticide includes dust arising from disturbed surfaces and thus the enantiomeric signature of the particulate phase points to historic DDT treatment. Therefore, two very different enantiomeric profiles are revealed in one sample measurement (single-step denuder sampling distinguishes between vapour phase and particulate phase POPs in air). These first results already indicate the potential importance of investigating EF values of airborne free molecular and particle adsorbed isomers separately.

Compared to off-line GCFC–GC-TOFMS the more sophisticated GCxGC-TOFMS demonstrated enhanced sensitivity of trace level chiral POPs in environmental samples (peaks are narrower in GCxGC). In cases where analytes are present at levels close to detection limits substituting GC-MS (EI+) with negative chemical ionisation (nCI) and selected ion monitoring mode, or with GC-ECD, as a second dimension will greatly improve sensitivity of the off-line heart-cut GCFC method. Muñoz-Arnanz et al. [7] reported

enhancing the limit of detection for *o,p'*-DDT by injection of up to 4 μ L solvent extract for enantiomeric separation by traditional heart-cut MDGC-ECD. However, traditional heart-cut MDGC, although successful, is quite complicated involving two independent GC-ECDs, a temperature controlled transfer line and a stream switching system (Deans switch), compared to the simplicity offered by our off-line GCFC technique. The off-line heart-cut method was selective and the interfering *p,p'*-DDD was successfully eliminated, allowing second dimension 1D enantiomeric separation of *o,p'*-DDT in the absence of interference. Furthermore, chiral columns are sensitive to moisture and dirty matrices, and by eliminating the complex matrix the expensive chiral column is protected and its useful lifetime is prolonged.

3.4 Conclusions

Two multidimensional GC methods, GCxGC-TOFMS and novel off-line GCFC–GC-TOFMS, were evaluated for trace environmental forensic investigations involving solventless sample enrichment with silicone rubber and desorption-injection. Both systems provide sufficient selectivity to perform trace analysis of enantiomers in complex real-life samples. By desorption-injection rather than liquid extract injection, both methods protect the expensive enantioselective column which is sensitive to moisture and matrix components. The off-line GCFC–GC-TOFMS approach provides improved column protection due to injection of only selected isomers from the total complex matrix onto the cyclodextrin column. This procedure has the added advantage of utilising one-dimensional GC and GC-MS equipment

only. The second method using the more sophisticated (and expensive) GCxGC-TOFMS is simpler, providing enhanced sensitivity and fast enantioselective analysis of chiral POPs in environmental samples. First results indicate a significantly different enantiomeric profile for indoor airborne particulate phase compared to the enantiomeric profiles of indoor air vapour phase and of outdoor soil.

3.5 Acknowledgements

Dr Peter Gorst-Allman, LECO Africa (Pty) Ltd., for kindly making available a LECO Pegasus 4D GCxGC-TOFMS and for his valuable guidance on GCxGC separation, Mr Sean Patrick and Prof Riana Bornman of the Department of Urology, University of Pretoria, for providing soil samples, Sasol and the National Research Foundation (NRF) for funding.

3.6 References

- [1] World Malaria Report, World Health Organisation (2010) [online]. Available: http://www.who.int/malaria/publications/country-profiles/profile_zaf_en.pdf (Accessed 28.06.2011).
- [2] H. Bouwman, R. Bornman, C. van Dyk, I. Barnhoorn, H. Kylin. Dynamics and risks of DDT applied indoors for malaria control. Poster presentation at the 12th EuCheMS International Conference on Chemistry and the Environment, Stockholm, Sweden, 14-17 June 2009.
- [3] H. Bouwman, B. Sereda, H.M. Meinhardt, Environ. Pollut. 144 (2006) 902 – 917.
- [4] R. Bornman, C. de Jager, Z. Worku, P. Farias, S. Reif, BJUI. (2009) 1-7.
- [5] A.W. Garrison, V.A. Nzungung, J.K. Avants, J.J. Ellington, W.J. Jones, D. Rennels, N.L. Wolfe, Environ. Sci. Technol. 34 (2000) 1663-1670.
- [6] H.R. Buser, M.D. Muller, Anal.Chem. 67 (1995) 2691-2698.

- [7] J. Muñoz-Arnanz, C. Bosch, P. Fernandez, J.O. Grimalt, B. Jimenez, J. Chromatogr. A. 1216 (2009) 6141–6145.
- [8] T. Harner, K. Wiberg, R. Norstrom, Environ. Sci. Technol. 34 (1) (2000) 218-220.
- [9] K. Wiberg, T. Harner, J.L. Wideman, T.F. Bidleman, Chemosphere 45 (2001) 843-848.
- [10] S. Corsolini, A. Covaci, N. Ademollo, S. Focardi, P. Schepens, Environ. Pollut. 140 (2006) 371-382.
- [11] E. Eljarrat, P. Guerra, D. Barceló, Trends Anal. Chem. 27 (2008) 847-861.
- [12] P.F. Hoekstra, B. K. Burnison, T. Neheli, D.C.G. Muir, Toxicol. Lett. 125 (2001) 75-78.
- [13] X.-Z. Meng, Y. Guo, B.-I. Mai, E.Y. Zeng, J. Agric. Food Chem. 57 (2009) 4299-4304.
- [14] W. Vetter, V. Schurig, J. Chromatogr. A. 774 (1997) 143-175.
- [15] S.P.J. van Leeuwen, J. de Boer, J. Chromatogr. A. 1186 (2008) 161-182.
- [16] L.F. de Alencastro, D. Grandjean, J. Tarradellas, Chimia 57 (2003) 499-504.
- [17] L.R. Bordajandi, L. Ramos, M.J. González, J. Chromatogr. A. 1125 (2006) 220-228.
- [18] F. Wong, M. Robson, M.L. Diamond, S. Harrad, J. Truong, Chemosphere 74(3) (2009) 404-411.
- [19] L.R. Bordajandi, P. Korytár, J. de Boer, M.J. González, J. Sep. Sci. 28 (2005) 163-171.
- [20] T.D. Bucheli, R.C. Brändli, J. Chromatogr. A. 1110 (2006) 156-164.
- [21] M. Kobličková, L. Duček, J. Jarkovský, J. Hofman, T.D. Bucheli, J. Klánová, Environ. Sci. Technol. 42 (2008) 5978-5984.
- [22] H. Hühnerfuss, M.R. Shah, J. Chromatogr. A. 1216(3) (2009) 481-502.
- [23] T. Tuzimski, in: M. Stoytcheva (Ed.), Multidimensional Chromatography in Pesticides Analysis, Pesticides - Strategies for Pesticides Analysis, InTech, 2011, pp. 155-196. Available from: <http://www.intechopen.com/articles/show/title/multidimensional-chromatography-in-pesticides-analysis> (Accessed 23.11.2011).
- [24] J.C. Van Dyk, H. Bouwman, I.E.J. Barnhoorn, M.S. Bornman, Sci. Total Environ. 408 (2010) 2745-2752.
- [25] Y. Naudé, W.H.J. de Beer, S. Jooste, L. van der Merwe, S.J. van Rensburg, Water SA. 24(3) (1998) 205-214.
- [26] E. Baltussen, C.A. Cramers, P.J.F. Sandra, Anal. Bioanal. Chem. 373 (2002) 3-22.
- [27] Y. Naudé, E.R. Rohwer, Anal. Chim. Acta 730 (2012) 112-119.
- [28] Y. Naudé, M.W. van Rooyen, E.R. Rohwer, J. Arid Environ. 75 (2011) 446-456.
- [29] P.B.C. Forbes, E.W. Karg, R. Zimmermann, E.R. Rohwer, Anal. Chim. Acta 730 (2012) 71–79.
- [30] E.K. Ortner, E.R. Rohwer, J. High Res. Chromatog. 19 (1996) 339-343.
- [31] H.-J. de Geus, P.G. Wester, J. de Boer, U.A.T. Brinkman, Chemosphere 41 (2000) 725-727.

Chapter 4

Evidence for a geochemical origin of the mysterious circles in the Pro-Namib desert

This chapter was published in the Journal of Arid Environments. The format reflects the style set by the journal.

Naudé, Y., Van Rooyen, M.W., Rohwer, E.R., 2011. Evidence for a geochemical origin of the mysterious circles in the Pro-Namib desert. *Journal of Arid Environments* 75, 446-456. doi:10.1016/j.jaridenv.2010.12.018

Author contributions

Conceived and designed the experiments: Yvette Naudé and Egmont Rohwer. Performed experimental work and data analysis, wrote the chapter/article, submitted article to journal, response to reviewers: Yvette Naudé. Initiator, contributor and co-supervisor of the fairy circle project: Gretel van Rooyen. Study supervisor: Egmont Rohwer.

See Appendix A for supplementary data not appearing in the journal article.

The work in this chapter was presented at ChromSAAMS 2012, Dikhololo, South Africa

Evidence for a geochemical origin of the mysterious circles in the Pro-Namib desert

Yvette Naudé^{a*}, Margaretha W. van Rooyen^b, Egmont R. Rohwer^a

^a*Department of Chemistry, ^bDepartment of Botany, University of Pretoria, Hatfield, Pretoria 0002, South Africa*

^aYvette.Naude@up.ac.za

^aEgmont.Rohwer@up.ac.za

^bGretel.vanRooyen@up.ac.za

ABSTRACT

The origin of the so-called “fairy circles” has not yet been established. Carbon monoxide (as an indicator of a natural gas microseep) was monitored inside and outside of selected fairy circles in the Namib, Namibia, southern Africa. Hydrocarbons were extracted from the soil by a novel method for trapping analytes onto silicone rubber designed for thermal desorption into a gas chromatograph – mass spectrometer (GC-MS). Unresolved complex mixtures with resolvable alkanes were detected in soil collected from two newly formed circles. Alkenes, the microbial degradation product of alkanes (microbial food source), were more abundant in the circles compared to the levels of alkenes detected in the matrix between circles. Results show a microseepage of gases and hydrocarbons which is expressed at the surface as a geobotanical anomaly of barren circles and circles of altered vegetation. In

addition, this finding may suggest a new approach to the origin of the mima mounds (*heuweltjies*) of the western Cape in South Africa.

Keywords: Fairy circle; Hydrocarbon microseepage; Mima mound (*heuweltjies*); Polydimethylsiloxane sorptive extraction; Termites; Vegetation stress

*Corresponding author at: Department of Chemistry, Natural Sciences 1, Room 2.19, University of Pretoria, Hatfield 0002, South Africa. Tel: + 27 12 420 2517; fax: +27 12 420 4687

E-mail address: yvette.naude@up.ac.za (Y. Naudé).

4.1 Introduction

Traditional Himba folklore holds that beneath the edge of the Namib Desert lies a crack in the earth's crust in which a dragon lives and whenever it exhales bubbles of fire rise to the surface, burning and vaporising the vegetation, forming circles (Carte Blanche, 2004: transcript of televised interview with Dr W. Jankowitz; De Vita, 2006). The origin of the enigmatic pock mark (“fairy circle”) patterned landscape of the Namib Desert has fascinated scientists and the general public for many decades. In many arid and semi-arid environments around the world striking vegetation patterns have developed (Van Rooyen et al., 2004; Rietkerk et al., 2004; Borgogno et al., 2009). Self-organised vegetative patterns of spots, labyrinths, gaps and stripes can arise in response to competition for limiting water and nutrients (Rietkerk et al., 2004). Spots are small round-shaped clusters of vegetation interspersed within a bare soil background while gaps are round-shaped bare soil islands surrounded by homogeneous vegetation (Borgogno et al., 2009). Currently there is no scientifically sound explanation as to the cause of fairy circles: circular depressions (Fig. 4.1a and Fig. 4.1b) which are devoid of vegetation and are often surrounded by a fringe of tall grasses (Van Rooyen et al., 2004). These circles occur in a broken belt in the Pro-Namib zone of the west coast of southern Africa, approximately between 60 and 120 km inland, extending from southern Angola through Namibia to just south of the Gariiep (Orange) River in South Africa (Van Rooyen et al., 2004).

The first reference to the fairy circles was in 1971 when Tinley proposed that the circles were the remains of fossil termitaria (Van Rooyen et al., 2004). In 1978 a group of researchers from the University of Pretoria began investigating the origin of the mysterious circles (Theron, 1979). Eicker et al. (1982) reported on a microbiological study of the barren circles in the Giribes Plain, but did not explain their origin. Theories as to the cause of these circles were related to termite activity, to localised radioactivity and to allelopathic compounds released by dead *Euphorbia damarana* plants, none of which provided conclusive evidence (Van Rooyen et al., 2004). According to Becker (2007) the foraging behaviour of harvester ants and harvester termites are the prime causal factor for the development of fairy circles under certain conditions. The fairy circles have been linked to the mima mounds (“heuweltjies”) of the southern and western Cape in South Africa (Lovegrove, 1993; Albrecht et al., 2001). These mounds are believed to be ancient termite nests. As the calculated dispersion indices for mounds and circles were remarkably close, Albrecht et al. (2001) proposed that termites were involved in both phenomena and that the fairy circles were caused by a substance associated with termite nests. In order to explain the circular shape of the patches, Albrecht et al. (2001) proposed that the biologically active factor central to their hypothesis may be a semi-volatile chemical substance. However, if the factor could diffuse readily to form a circular patch in which inhibition of plant growth occurs, there would need to be an active process whereby the agent is constantly replenished (Albrecht et al., 2001). Jankowitz et al. (2008) concluded that the results of their *in situ* investigation could be interpreted as supporting Albrecht et al.’s (2001) argument that a “semi-volatile gas” produced in the circle inhibits grass growth.

Surface macroseeps (visible hydrocarbon seepage such as oil) and microseeps (invisible, usually detectable by sensitive instrumentation or the visible result of their effect on the near-surface environment) occur because diffusion, effusion and buoyancy (micro-gas bubbles) allow hydrocarbons to escape from sources and migrate to the surface (Mello et al., 1996; Jones et al., 2000; Van der Meer et al., 2000; Yang et al., 2000). The surface expression of a geochemical microseep can take many forms including geobotanical anomalies, anomalous hydrocarbon concentrations in soil, water and atmosphere, microbiological anomalies, anomalous non-hydrocarbon gases, mineralogical changes such as the formation of calcite and certain magnetic iron oxides, and altered magnetic properties of soils (Jones et al., 2000; Yang et al., 2000; Schumacher and LeSchack, 2002). Most geochemical signatures display as apical or halo-like (Schumacher and LeSchack, 2002). An apical anomaly, e.g. hydrocarbons, is greatest above the source and a halo anomaly occurs towards the edge of the source, outside of the anomaly, or forms a circular pattern around an apical anomaly. A general model of hydrocarbon-induced geochemical and geophysical alteration of soils illustrates anomalous surface concentrations (apical or halo formation), carbonate precipitation, bacterial degradation of hydrocarbons, high resistivity anomaly at the surface, magnetic anomaly and oxidising and reducing zones (Schumacher, 1996).

Microseepage rates and surface hydrocarbon concentrations can vary drastically over time. Surface hydrocarbon seeps and soil geochemical anomalies have been shown to appear and disappear in relatively short times, weeks, months or years (Schumacher and LeSchack, 2002). The flux responds

to changes in barometric pressure as well as daily, monthly and yearly cycles. A background seep (noise) can occur around the seepage-induced alteration and hyperspectral remote sensing is generally used to detect trends of circular patterns (halo formation) around a central vent or straight lines (faults) when searching for surface indicators of seeps (Van der Meer et al., 2000; Smith et al., 2004). Near-surface geochemical anomalies are closely associated with faults and fractures (Jones et al., 2000; Van der Meer et al., 2000). Anomalies seemingly not coincident with known faults, fractures or other obvious pathways may present processes not completely understood or recognised (Jones et al., 2000). Although hydrocarbon seepage is more common than is generally believed, it is relatively rare for seeps to overlie major oil or gas fields (Macgregor, 1993). Therefore, the perceived seep anomaly does not necessarily imply the presence of economic recoverable hydrocarbons at depth (Yang et al., 2000). The potential for finding large hydrocarbon accumulations in the Nama Basin is limited as large reservoirs would not be filled due to breaching of possible accumulations (Summons et al., 2008).

Hydrocarbon microseepage is reported to create a chemically reducing zone in the soil column at depths shallower than would be expected in the absence of seepage (Van der Meer et al., 2002). The seep stimulates bacterial activity which further decreases soil oxygen concentration, which, in turn, changes soil chemistry and influences the availability of trace elements to plants (Van der Meer et al., 2002). This environmental change affects the root structure of the vegetation and causes visible stress in plants such as reduced growth, chlorosis of the leaves and plant mortality.

The objectives of this pilot study were to explore, for the first time, a possible geochemical origin of the fairy circles and investigate the hypothesis that fairy circles are the surface expression of geochemical hydrocarbon microseepage.



Figure 4.1a. Pock marked landscape of the Pro-Namib desert.



Figure 4.1b. Circular patch of barren soil in the NamibRand Nature Reserve in Namibia, southern Africa.

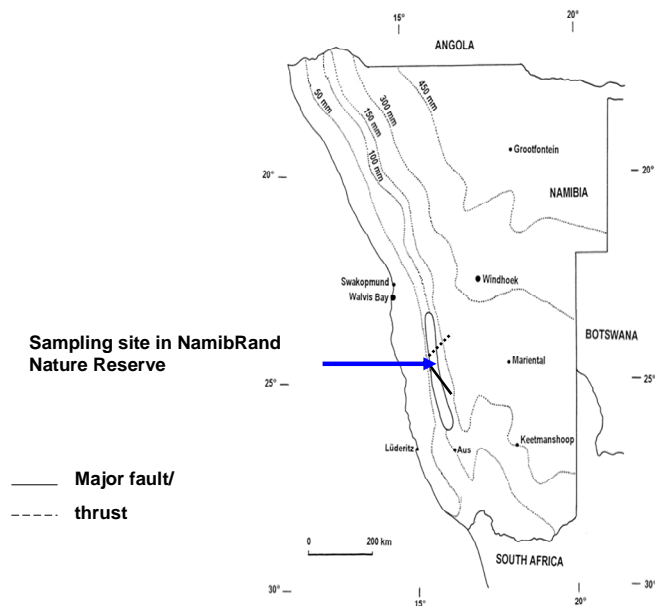


Figure 4.2. Map of Namibia indicating the approximate location where gases were monitored and soil samples were collected in NamibRand Nature Reserve and of some major faults and fault thrusts in the vicinity of the sampling site.

4.2 Materials and methods

4.2.1 Study area

Van Rooyen et al. (2004) collected soil samples from sites, covering a comprehensive region from the Kaokoveld in the north, down to Kubus in the north of South Africa, including the vicinity sampled in this present study. Bioassays conducted on the soils from the different localities revealed the same pattern (Van Rooyen et al., 2004). It is therefore assumed that the causal factor responsible for the fairy circle phenomenon is the same for all circles and hence a single site, based on its relative ease of accessibility, was selected for the current study. Gas measurements were performed from 4 to 6 April 2009 in the

NamibRand Nature Reserve in Namibia, southern Africa (S 24° 58' 37.2" E 15° 56' 55.5") (Fig. 4.2). At this site five fairy circles were selected within a radius of 50 m. Three of the circles (circle 1, 2 and 3) were typical barren patches (Fig. 4.1b), whereas circle 4 was a patch with dead grass tufts and circle 5 contained a mixture of both dead grass tufts as well as live tufts showing severe signs of chlorosis. Gas measurements were also taken in the matrix equidistant between the circles.

Near surface soil was collected at a depth of approximately 50 cm in the centres of circle 4 and circle 5. Soil was also collected in the centres of Circle 1.3 and Circle 2.1, and in the matrix (Matrix 1.3 and 2.1), in the NamibRand Nature Reserve in 2007 (S 24° 58' 44.9"; E 15° 57' 05.9"). Soil samples 1.3 (circle and matrix) were collected at approximately 1 m below the surface and soil samples 2.1 (circle and matrix) were collected at the surface.

4.2.2 *Measurement of CO and O₂*

Gas measurements were recorded between 15:00 and 16:00 on day 1, between 17:00 and 18:00 on day 2, and between 11:40 and 12:05 and 16:30 and 16:50 on day 3 in circles 1 to 3. Gas measurements of the relatively newly formed circles (circles 4 and 5) occurred between 12:12 and 12:30, 15:50 and 16:15, and 17:50 and 18:50 on day 3.

A GreenLine 8000 Portable gas analyser (Elemental Analytics (Pty) Ltd, Boksburg, Johannesburg, South Africa) equipped with a gas sampling probe,

electrochemical (EC) sensors for CO, H₂S, NO₂ and O₂ and non-dispersive infra-red (NDIR) sensors for CO and CO₂ were used for sampling in the field. Detector response time to 90% of readings for the electrochemical sensors (EC) was 40 s for CO and 20 s for O₂. The CO non-dispersive infra-red (NDIR) adsorption response time was 50 s to 90% of reading. Regrettably, the gas analyser was not equipped with sensors for methane and combustible gases (C_xH_y) and thus CO was selected as a marker for the presence of natural gas.

Two litre funnels were buried upside down in the soil at a depth of 20 - 30 cm so that only part of the funnel stem was visible above the soil. The stem of the funnel was covered loosely by a centrifuge tube to allow an unrestricted flow of gases. Initial measurement of gases (day 1) commenced after a waiting period of two hours after the funnels were buried. For days 2 and 3 the funnels were left in place overnight. The presence of gases was monitored by inserting the gas sampling probe of the gas analyser into the buried funnels in the centre of the circles, as well as equidistant between the circles (controls) in the matrix.

4.2.3 Extraction of compounds from soil

Stir bar sorptive extraction (SBSE) with Twisters™ (Gerstel™, Chemetrix, Midrand, South Africa) was initially used for the solventless extraction of hydrocarbon analytes from the soil. However, when the Twister™ was removed from the soil it was discovered that a black seemingly tar-like substance covered the ends of the Twister™. Because the Twister™ is a magnetic stir bar coated with a volume of polydimethyl siloxane (PDMS) the

substance had to possess magnetic properties for it to cling to the poles of the stir bar. Inspection of the substance with a magnifying glass clearly showed a glut of magnetic particles. The particles clinging to the Twisters™ were problematic during sample desorption. An alternative solventless extraction method was therefore developed to specifically avoid magnetising soil minerals.

A 10.5 cm (0.02 g) length of a silicone elastomer medical grade tubing (0.64 mm OD x 0.3 mm ID., Sil-Tec, Technical Products, Georgia, USA) with a sorption volume of 26 µl was used for solventless extraction of the soil samples (Fig. 4.3). To prevent sand from entering the PDMS tube and to facilitate ease of handling the length of PDMS tubing was joined at the ends with a 1 cm piece of capillary column (250 µm ID) to form a loop. A 40 ml glass vial, fitted with a solid screw cap coated on the inside with polytetrafluoroethylene (PTFE), was filled with 40 g soil. A PDMS loop was submerged in the soil. The vial was placed in an oven at 50 °C for 60 min. After extraction of the soil the PDMS loop was inserted into a 17.8 cm long glass desorption tube (4 mm ID, 6.00 mm OD) from Gerstel™ (Chemetrix, Midrand, South Africa) for thermal desorption into a gas chromatograph – mass spectrometer (GC-MS).

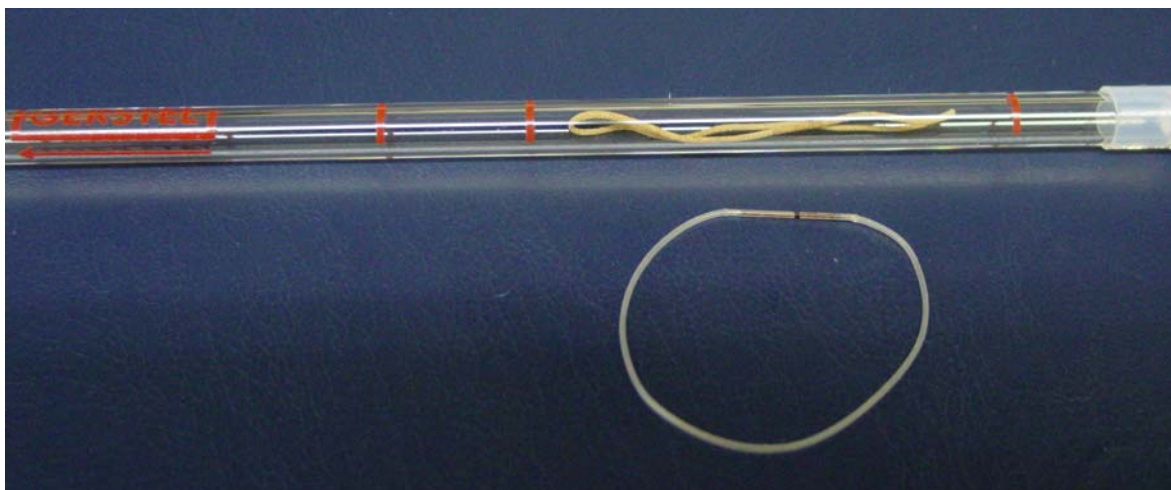


Figure 4.3. PDMS loop (tube ends joined with a piece of capillary column) used for the extraction of soil (bottom), PDMS loop after extraction and inserted inside a TDS tube for desorption into a GC-MS (top). See 4.2.3 for details.

4.2.4 Identification of compounds by GC-MS

The hydrocarbon analytes were thermally desorbed from the PDMS loop using a thermal desorber system (TDS) from Gerstel™ installed on a Hewlett Packard (HP) GC 1530A coupled to a HP 5973 mass selective detector (MSD) (Chemetrix, Midrand, South Africa). Splitless desorption was from 30 °C (2 min) at 30 °C/min to 250 °C (10 min). The desorption flow rate was 50 ml/min (Helium, Ultra High Purity, Afrox, Johannesburg, South Africa) at 65 kPa. The TDS transfer line temperature was 350 °C. The analytes were cryogenically focused, using liquid nitrogen, at –10 °C on a cooled injection system (CIS). The CIS liner contained silicone rubber to improve retention of the volatile analytes during desorption. After desorption, a splitless injection (purge on at 30 min, purge flow 60 ml/min, solvent vent mode) was performed by heating the CIS from –10 °C at 6 °C/s to 250 °C for 10 min. The GC oven temperature programme was –10 °C (2 min) at 10 °C/min to 300 °C (10 min). The GC

column was a Zebron, ZB1 30 m x 250 µm ID x 0.25 µm film thickness (Phenomenex, SEPARATIONS, Randburg, South Africa), the velocity of the carrier gas (helium) was 42 cm/s (1.3 ml/min) and the column head pressure was 65 kPa in the constant pressure mode. The GC-MS transfer line was at 280 °C, the mass scan range was 35-350 atomic mass units (amu) in full scan mode, the source (EI+) temperature 230 °C, the MS quadrupole temperature 150 °C, the ionisation energy 70 eV and the electron multiplier voltage (EM) 1700 V. Compounds were tentatively identified by mass spectral comparison of the samples to that of the mass spectra found in a commercial library (Wiley). Matches of the mass spectra of the components to that of the library were ≥80%.

4.3 Results and discussion

4.3.1 Gas detection

4.3.1.1 Plant stress response to natural gas seeps

Several studies have reported a relationship between microseepage from subsurface sources and the stress response of plants to long term anaerobic conditions and its use in gas/hydrocarbon exploration (Mello et al., 1996; Jones et al., 2000; Van der Meer et al., 2000; Noomen et al., 2003; Smith et al., 2004; Xu et al., 2008). Hydrocarbon seepage influences the soil and the vegetation around the seep. The seepage alters the soil atmosphere and the mineralogy. The gases that seep to the surface partially displace the soil atmosphere,

including soil oxygen and consequently the soil atmosphere is depleted of oxygen. An oxygen poor environment surrounding roots can severely damage plant growth in the seep migration pathway, causing visible plant stress (Smith et al., 2004). Although natural gas is considered not toxic to plants, visible symptoms due to natural gas seepage are reduced plant growth, chlorosis of the leaves and plant mortality. Noomen et al. (2003) reported a circle of bare soil occurring at the centre of a gas leak, and on the edge of the necrotic circle a ring of healthy vegetation flourished. Van Rooyen et al. (2004) reported lower biomass in the fairy circles and the highest biomass at the edge (ringing vegetation) of the patches.

Smith et al. (2004) experimented with the effect of natural gas on germinating seeds and on a fully established grass crop. Injection of natural gas into soil beneath an established grass crop caused a circle of chlorosis: a region of lighter green grass which became more yellow as the experiment progressed, and a reduction of growth of the grass around the area of gas injection. For seedlings, most plants germinated but did not grow in the gas seep.

Certain plant species appear to be less sensitive to anaerobic soil conditions than others (Yang et al., 2000). An anomalous distribution of maple trees occurs in an area of maximum methane seepage and minimum soil oxygen conditions where typically oak-hickory vegetation is expected to occur (Lost River gas field, Appalachian Mountains, West Virginia, United States of America) (Yang et al., 2000). This vegetation anomaly seems to relate to

anaerobic soil conditions that influence the mycorrhizal fungi living on the root hairs of the trees. Fungi on maple trees appear to tolerate the anaerobic soil conditions better than the mycorrhizal fungi living on the roots of oak trees (Yang et al., 2000). Joubert (2008) reported the absence of vesicular arbuscular mycorrhizae (VAM) in the roots of plants collected from within the fairy circles. In contrast, VAM occurred in most of the roots of plants collected between the circles and on the edge of circles (Joubert, 2008). Mycorrhiza are aerobic organisms (Torti et al., 1997) and soil that becomes anaerobic for considerable periods of time generally loses its mycorrhizal component (Ingham, online 01 March 2010). The absence of mycorrhizal fungi in the roots of plants from within circles suggests anaerobic soil conditions within the circles. Soil conditions favouring anaerobic bacteria in the circles were indeed implicated by Eicker et al. (1982) who reported a greater density of anaerobic bacteria and a lower density of aerobic bacteria within barren circles compared with the matrix.

Hydrocarbon microseepage creates a chemically reducing zone in the soil at depths shallower than would be expected in the absence of seepage (Van der Meer et al., 2002). Such leakage stimulates the activity of hydrocarbon-oxidising bacteria, which further decreases soil oxygen concentration while increasing CO₂ and organic acids (Van der Meer et al., 2002). These changes can affect the pH and the redox potential (E_h) in soils which in turn affect the solubility of trace elements and consequently their availability to plants (Schumacher, 1996; Van der Meer et al., 2002). Changes in the soil chemistry environment can therefore affect plant vigour, resulting in

vegetation anomalies (Van der Meer et al., 2002). Van Rooyen et al. (2004) and Joubert (2008) demonstrated that plants failed to flourish when grown in soil collected from within fairy circles, compared to the vitality of plants grown in soil collected from the edge of the circle (stimulated growth) and the matrix (intermediate growth). An anaerobic soil environment in the seep chimney can alter the soil chemistry which leads to the dissolution or precipitation of minerals and the mobilisation or immobilisation of certain elements in the seep chimney (Van der Meer et al., 2002). Results of Joubert's study suggest that the altered soil, when removed from the circle, retained its altered state causing an adverse effect on plant vitality. Seepage induced geobotanical anomalies appear to be primarily related to anaerobic soil conditions.

4.3.1.2 *Bare soil circles*

Figure 4.4 illustrates the simultaneous recording of oxygen (O_2) and carbon monoxide (CO) inside circles and at control sites. Levels of O_2 and CO were 20.9% (EC) and 0.000% (NDIR) respectively prior to insertion of the probe into the funnel (-1s). A drop in O_2 from 20.9% to 20.8% followed by an emission of CO of 0.001% was detected inside of the barren soil circles 1 and 2 on day 1. Although CO was not measured a drop in O_2 from 20.9% to 20.8% was observed in barren soil circle 3. On day 2, CO emissions of 1 part per million (ppm) (EC) was detected after a drop in O_2 of 0.1% was observed inside barren soil circles 1 and 2 and a 0.2% drop in O_2 was observed inside barren soil circle 3 although CO was not detected. The level of O_2 was constant at 20.9% and CO was not detected for a control site ($n = 2$) in between the barren

soil circles. During the midday session on day 3 a 0.2% drop in O₂ was observed followed by a CO emission of up to 0.005% for circle 1. A 0.2% drop in O₂ was observed although CO was not detected inside circle 2. A 0.2% drop in O₂ was measured, followed by a CO emission of up to 0.007% inside of circle 3. The O₂ was constant at 20.9% and no CO was observed for the control site monitored at 12:05. During the late afternoon session a 0.1 – 0.2% drop in O₂ but no CO was detected inside of circles 1, 2 and 3.

A drop in O₂ levels was not observed during three previous measurements in the matrix, the only exception was on day 3 when the site was monitored at 16:45, a 0.2% drop in O₂ was observed, but CO was not detected (Fig. 4.4).

Concentrations of CO, when greater than zero, were always measured after first observing a drop in O₂ (Fig. 4.4).

4.3.1.3 *Newly formed circles*

The two new circles, one being a perfectly circular patch of dead vegetation and another patch consisting of a mixture of both dead vegetation and mature, alive, yellowed plants, were pointed out to us at the end of day 2 and thus the two new circles were monitored on day 3 only. The two patches were bordering each other. A 0.2% drop in O₂ followed by CO of up to 0.028% was observed at 12:12 – 12:30, a 0.2% drop in O₂ followed by CO of 0.001% was detected at 15:50, while a 0.3% drop in O₂ and 0 ppm CO were measured at 17:55, whereas at 18:50 the O₂ remained constant at 20.9% and CO was not detected inside the circle of dead vegetation (Fig. 4.5). The patch consisting of a mixture of both dead and stressed vegetation was monitored and a 0.1% drop in O₂ followed by CO of up to 0.032% was observed at 16:03 – 16:15, while a 0.1% drop in O₂ and 0 ppm CO were detected at 17:50. The control site (15:57) for the newly formed circles measured a constant 20.9% O₂ and CO was not detected.

The results show that CO emissions are of an episodic nature and not continuous. The highest CO emissions were measured at 12:00 and 16:00. Gas flux is dependent on atmospheric pressure changes. Gas flux is at its highest when barometric pressure is at its lowest. The 0.1 - 0.3% drop in O₂ does not fully account for the levels of CO detected at 0.000 - 0.032%. This discrepancy between the displacement of O₂ and the emission of CO indicates the presence of gases other than CO. Contrary to expectation, the gas analyser was not equipped with sensors for methane and combustible gases

(C_xH_y). However, CO attributed to natural sources is not only an indicator of natural gas but it may also result from the oxidation of hydrocarbons, notably methane. Therefore, the measurement of CO in the circles points to the presence of natural gas. Determining the composition of the gases within the seeps will need further investigation. Also, it is anticipated that during peak gas seepage the depletion of O_2 in the subsurface soil (as opposed to the somewhat small drop observed in the rather unsophisticated set-up of inverted funnels with loosely covered stems) will be dramatically more than 0.3%. No NO_2 or changes in CO_2 were detected and levels may be indistinguishable from ambient values. Abnormal CO_2 concentrations in soils are non-specific for petroleum and can result from processes other than microbial oxidation of hydrocarbons (Schumacher, 1996).

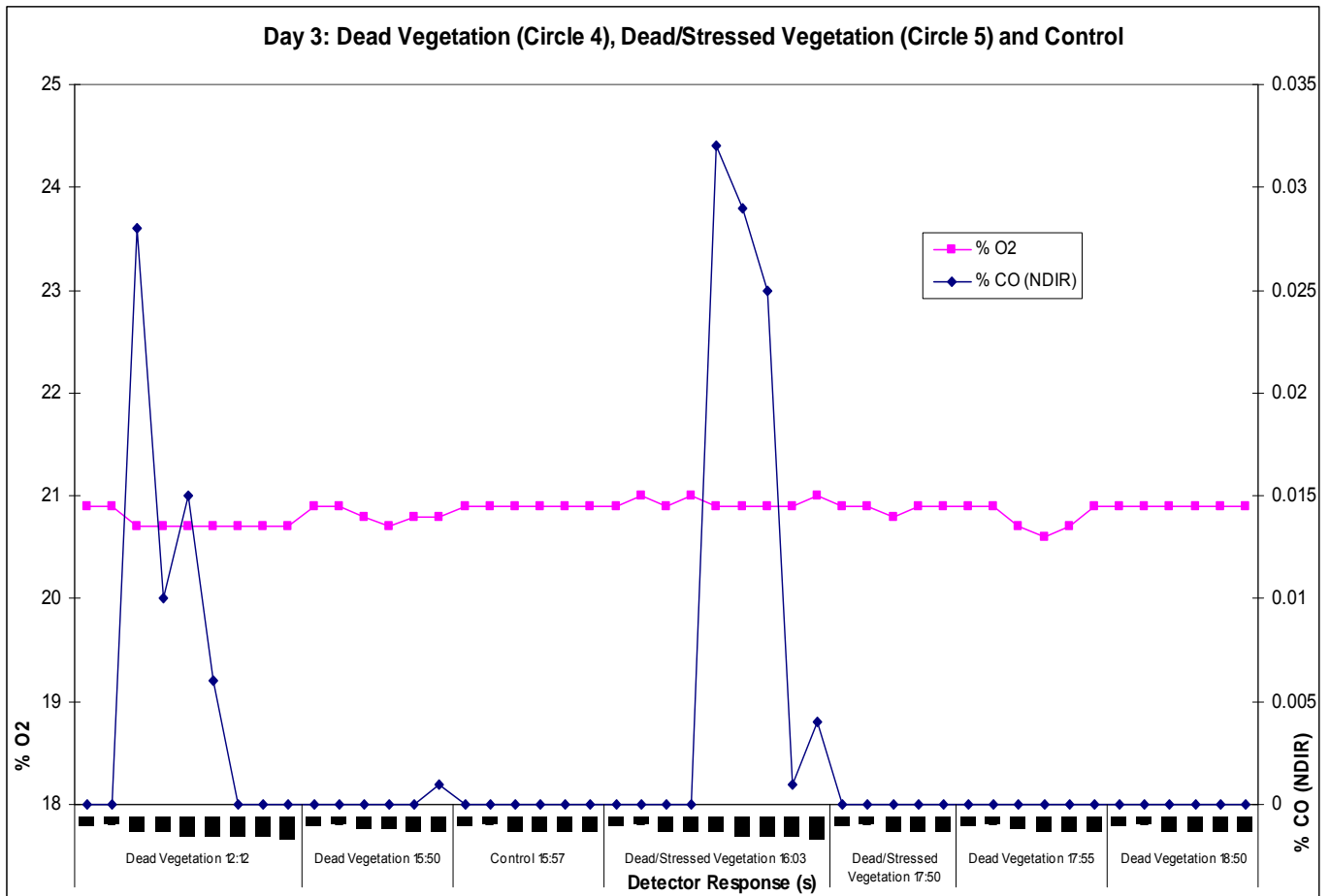


Figure 4.5. Field measurement of O₂ and CO in the soil of a patch of dead vegetation, control (matrix) and a patch of dead and yellowed vegetation. Detector response (s) monitoring period. (-1 s): observation prior to insertion of gas probe. (0 s): insert gas probe. CO and O₂ were recorded simultaneously using a single gas probe. Levels of O₂ and CO were 20.9% and 0.000% respectively prior to inserting the gas probe into the funnel submerged in soil. A drop in oxygen was observed 20 s after insertion of the probe into the funnel buried in the soil (detector response time is 20 s for O₂) and CO (> 0.000%) was observed after 20 – 45 s (detector response time 40-50 s to 90% of reading for CO) after probe insertion. Gas probe was removed from the funnel when no further flux was observed (CO returned to 0.000% and O₂ returned to 20.9%). Dead vegetation: a 0.2% drop in O₂ followed by CO of up to 0.028% was observed at 12:12 – 12:30, a 0.2% drop in O₂ followed by CO of 0.001% was detected at 15:50, a 0.3% drop in O₂ and 0 ppm CO were measured at 17:55, at 18:50 the O₂ remained constant at 20.9% and CO was not detected. Dead/stressed vegetation: a 0.1% drop in O₂ followed by CO of up to 0.032% was observed at 16:03 – 16:15, a 0.1% drop in O₂ and 0 ppm CO were measured at 17:50. Control site (15:57): O₂ was constant at 20.9% and CO was not detected.

4.3.2 TDS-CIS-GC-MS of extracted soil samples

Typically the method for isolating and analysing hydrocarbons from seep-soils is Soxhlet extraction of, often, a sizeable soil sample with large volumes of hazardous (chlorinated) solvents which have the potential for artefact (e.g. hydrocarbons) introduction, followed by the analyses of microlitre amounts of the diluted final extract (Rangel et al., 2003; Summons et al., 2008). In contrast, a simple, cheap, nonhazardous solventless extraction technique for the introduction of the total amount of sorbed analytes into a GC-MS was developed. Because the method is solventless the potential for artefact introduction is minimised and smaller sized soil samples can be extracted.

4.3.2.1 Saturated alkanes

Soil samples containing active (fresh) migrated hydrocarbons produce a gas chromatogram of undegraded *n*-alkanes, branched alkanes, biomarker signatures and a minor naphthenic hump (unresolved complex mixture of hydrocarbon compounds) (Rangel et al., 2003; Abrams, 2005). Soil samples containing passive (dormant stage) migrated hydrocarbons produce a gas chromatogram showing severe degradation characterised by only an elevated unresolved complex mixture (UCM) (Abrams, 2005). Hydrocarbon-degrading bacterial populations preferentially utilise *n*-alkanes relative to branched alkanes (Hamamura et al., 2005). The signature of soils from dormant stage migrated hydrocarbons, recharged with a recent seepage, is similar to the passive seep but with the addition of resolvable compounds C₁₂ - C₂₀ (Abrams, 2005). An

unresolvable hump < C₂₃ is representative of a migrated thermogenic portion (Abrams, 2005).

Chromatograms of soils from the newly formed patches display some resolved peaks on an elevated unresolved hump (Fig. 4.6). Poorly resolved *n*-alkanes in the C₁₃ - C₁₈ range are present while the resolvable compounds consist of almost entirely branched saturated alkanes (C₁₂ – C₂₀). These features are consistent with a dormant stage seep recharged with seepage at some stage. This chemical signature of an elevated unresolved hump (dormant stage degraded seep) with the addition of resolvable saturated alkanes (active seep) is substantiated by the visual appearance of notably the patch containing both dead (past seep activity characterised by an UCM) and yellowed vegetation (a dormant stage permits new plant growth, while chlorosis is the consequence of relatively recent seepage resulting in the addition of resolvable compounds in the C₁₂ – C₂₀ range) (Fig 4.6).

The ratio of the acyclic C₁₉ and C₂₀ isoprenoid hydrocarbons, pristane (Pr) and phytane (Ph), generally reflects the nature of the organic matter (maturity of the seep source) and the redox potential in the depositional environment during early diagenesis of chlorophyll (phytol chain), the main precursor of pristane and phytane (Osuji and Antia, 2005). Ph was detected in the soil of the two newly formed circles, while the presence of Pr could not be confirmed (for subsequent confirmation of pristane and phytane by GCxGC-TOFMS see section 4.7 Appendix A). Both seeps are degraded as are evidenced by their chromatograms showing elevated unresolved humps (Fig. 4.6).

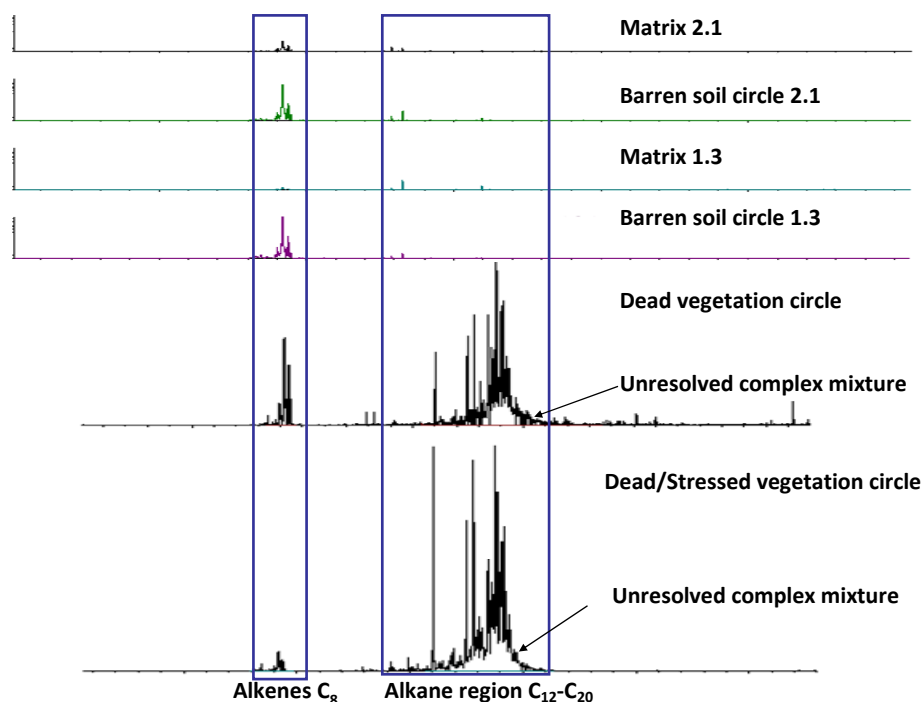


Figure 4.6. Reconstructed ion chromatogram (112 amu) of alkenes (microbiological degradation product of alkanes) relative to alkanes measured in soils collected from barren soil circles (Circles 2.1 and 1.3), between barren soil circles (Matrix 2.1, 1.3) and two newly formed circles (dead and stressed vegetation; dead vegetation). Samples 2.1: soil collected at surface. Samples 1.3: soil collected approximately 1m below surface. Newly formed circles: soil collected approximately 50 cm below surface. Barren soil circles and the two newly formed circles have relatively more alkenes present compared to the alkenes present in the matrix. Bare soil circles and matrix: UCM absent. Two newly formed circles: UCM (degraded seepage) present with addition of resolvable alkanes (active seepage).

4.3.2.2 Alkenes

Bacteria are ubiquitous in the environment but will concentrate where a food source, such as a hydrocarbon seep, is available (Schumacher and LeSchack, 2002). Microorganisms feeding on hydrocarbons will degrade the hydrocarbons. Also, microbial degradation of alkanes to alkenes can occur under anaerobic conditions (Morikawa et al., 1996; Jones et al., 2000; Grossi et al., 2008).

Figure 4.6 shows the reconstructed ion chromatograms (112 amu) of acyclic alkenes (*n*-Octene, branched olefins (C₈H₁₆)) present in the soil samples. The soil collected from inside (centre) the barren soil circles (Circle 1.3, Circle 2.1) has relatively more alkenes (total peak areas of 104 and 86 (arbitrary units indicated in the alkene window)) present when compared to the alkenes (total peak areas of 5 and 22) present in the matrix (Matrix 1.3, Matrix 2.1). For the newly formed circles the soil from the patch of dead vegetation contained alkenes with a total peak area of 52 and the patch with both dead and yellowed vegetation contained alkenes with a total peak area of 26 (Fig. 4.6).

The higher levels of alkenes detected in soil collected inside (centre) the barren circles compared to the lower levels of alkenes present in soil collected between the barren circles (matrix) point to the availability of a more abundant food source for microbial consumption inside the circle relative to outside the circle (matrix). Eicker et al. (1982) recorded the highest activity of anaerobic bacteria in the barren patch and the lowest at the edge. In contrast, Eicker et al. (1982) reported that the lowest aerobic microbial density occurred in the patch and the highest on the edge inferring the presence of a diminished O₂ zone in the seep. These distinct microbial patterns support the geochemical signature of a reducing microseep area above the hydrocarbon source with an outside edge of an oxidised area. Bacterial activity inside a hydrocarbon microseep can cause changes leaving the near-surface materials more dense and resistant to erosion (Xu et al., 2008). Moll (1994) found that the fairy circle soils were slightly more compact than those in the matrix.

Van Rooyen (2004) noted that soil resistance was highest in the barren patch soil and lowest in the edge soil (ringing vegetation). The hydrocarbon microseepage model shows a higher resistivity anomaly at the surface (Schumacher and LeSchack, 2002). Potassium (K) precipitates in a halo anomaly in high pH soils over a seep (Monson and Surr, 2003). The pH of the soil is raised due to bacterial activity resulting in the addition of bicarbonate to pore water (Schumacher, 1996). Van Rooyen et al. (2004) reported alkaline soil pH values of mostly 8 – 9, higher levels of K (mg/kg) at the edge (ringing vegetation) of barren patches and lower levels of K (mg/kg) within barren patches. Mineral alteration related to hydrocarbon microseepage can result in low K anomalies in soils (Van der Meer et al., 2002).

Active hydrocarbon migration may be identified by ratios of alkanes to alkenes (Harbert et al., 2006). High saturate to olefin (unsaturated compound) values (>1) are anomalous and imply an active seep (Harbert et al., 2006). The alkane/alkene ratios for the two newly formed circles were calculated as $\frac{\text{total peak area}_{\text{alkanes}}}{\text{total peak area}_{\text{alkenes}}}$ of the reconstructed ion chromatograms 112 amu (Fig. 4.6). The circular patch of dead vegetation has an alkane/alkene ratio of 7 and the circular patch of both dead and yellowed vegetation has an alkane/alkene ratio of 72. These high values indicate very active seepage, notably so in the case of the circular patch of both dead and yellowed vegetation (chlorosis is indicative of new seep activity). The displacement of O_2 and the release of CO were also the highest for this patch. These two newly formed circular patches are of particular interest. The patch of dead vegetation is evidence of the birth of a vent. The patch of both stressed and dead

vegetation is evidence not only of the birth of a vent but also that the seep had a period of activity (dead plants), followed by a dormant period which allowed plants to germinate and reach maturity until the seep became newly active once again, leading to the current state of the patch consisting of mature yellowed vegetation amongst the dead vegetation.

In contrast to the high alkane/alkene ratios of the two newly formed circles the alkane/alkene ratios for the barren soil circles were 0. An elevated unresolved hump was absent and saturated alkanes were below detectable levels (Fig. 4.6). The flux of hydrocarbon seepage is difficult to measure because seeps may be small, episodic and brief (Van der Meer et al., 2002). Seepage and its associated anomalies can disappear and reappear in response to reservoir depletion and repressuring (Schumacher and LeSchack, 2002).

4.3.3 Seepage-induced stimulation of vegetation growing on the edge of fairy circles

Plants on the edge (fringe of ringing vegetation) of fairy circles grow vigorously compared to the intermediate vitality of plants growing in the matrix. It was suggested that plants growing on the edge of a barren patch have more water and nutrients available to them (Van Rooyen et al., 2004). Noomen et al. (2003) reported a seep with a ring of high biomass surrounding a circle of bare soil, the vegetation cover 15% higher in the ring than in the surrounding area. The authors proposed that the ring of high biomass is most likely due to groundwater collecting at the edge of the halo, since it is known that long-term

gas and oil seepage bring groundwater to the surface (Noomen et al., 2003). Albrecht et al. (2001) found a fivefold higher concentration of water in the inner soil of a barren patch, compared to the outer soil of a fairy circle. However, potting trials with fairy circle soils indicated that the stimulatory effect was not merely due to an increased water supply (Van Rooyen et al., 2004). Growth of plants receiving equal amounts of water was still promoted in soil from the edge of the barren patch, thus the soil retained its stimulatory factor (Van Rooyen et al., 2004). Eicker et al. (1982) reported the highest aerobic microbial density at the edge, the lowest aerobic microbial density in the patch and an intermediate microbial density occurred in the matrix, whilst a lower density of anaerobic bacteria occurred at the edge and the highest density of anaerobic bacteria occurred in a barren patch. The presence of a greater anaerobic microbial density occurring in the patch confirms that the patch is a diminished O₂ zone. The elevated aerobic microbial population in the edge not only shows that the edge is outside of the diminished O₂ zone, but also that the edge retains residual hydrocarbons from the seep, providing for a richer food source to support an aerobic microbial population of higher density when compared to the matrix. The matrix supporting an intermediate microbial density confirms the presence of a less abundant food source compared to the edge (residual seepage) and circle (maximum seepage). The hydrocarbon flux is indeed lower at the edge than in the central vent (Noomen et al., 2003). Van der Meer et al. (2000) reported that hydrocarbon microseepage can act as a fertiliser to the growth of crops. Soil enrichment at the edges of circles is supported by the findings of Van Rooyen et al. (2004) who reported a pronounced stimulation in growth of plants grown in soil collected from the edge of circles in comparison to

the plants grown in soil collected from the matrix and inside the circles. The decrease in soil O₂ within a seep alters the soil chemistry, creating an unfavourable environment for plant growth. Van Rooyen et al. (2004) and Joubert (2008) reported that plants performed poorly in soil collected from within circles, confirming that the soil within circles retained an antagonistic factor. However, the pronounced stimulation in growth of plants in the edge (ringing vegetation) clearly shows that the edge is outside of the unfavourable soil chemistry zone. The presence of an elevated aerobic microbial population in the edge confirms the availability of a richer food source in the edge when compared to the matrix. Since hydrocarbons can act as a fertiliser to plants, stimulatory plant growth at the edge, outside of the antagonistic soil chemistry zone created by peak seepage (circle), is therefore due to residual hydrocarbons enriching the soil at the edge of the fairy circles. In contrast, plants in the circles are disadvantaged by the unfavourable soil chemistry environment induced by peak hydrocarbon microseepage.

4.3.4 Hydrocarbon-induced magnetic anomalies

The presence of shallow magnetic anomalies over oil and gas fields has been noted for several decades (Eldmore et al., 1987; Schumacher, 1996; Schumacher and LeSchack, 2002; Stone et al., 2004; Schumacher and Foote, 2006; Liu et al., 2006). Approximately 80% of oil and gas discoveries are associated with hydrocarbon-induced magnetic anomalies (Schumacher and Foote, 2006). The near-surface magnetic deposits are generated predominantly from microbial alteration of magnetic minerals and iron-bearing

minerals within the hydrocarbon seep. For example, haematite is altered to magnetite under anaerobic conditions in the presence of hydrocarbon microseepage (Eldmore et al., 1987; Schumacher, 1996; Schumacher and LeSchack, 2002; Stone et al., 2004; Schumacher and Foote, 2006; Liu et al., 2006). In addition, hydrogen sulfide (H_2S) is created by bacterial activity. H_2S reacts with goethite to produce magnetite and sometimes goethite is altered to magnetic forms of haematite (Van der Meer et al., 2002). Walden et al. (1999) reported both haematite and goethite within Namib dune sediments.

Figure 4.7a shows a magnetic stir bar with magnetised soil particles accumulated from 40 g soil collected in the patch of dead and yellowed vegetation and Fig. 4.7b shows a magnetic stir bar with magnetised soil particles accumulated from 40 g soil collected between the circles (matrix). Overall, the soil (matrix and circles) contains a considerable amount of easily magnetised particles. The newly formed circle appears to have a higher amount of magnetised soil particles. This could be a consequence of the hydrocarbon seep providing for a greater bacterial energy source resulting in an enhanced alteration of the magnetic minerals within the seep.

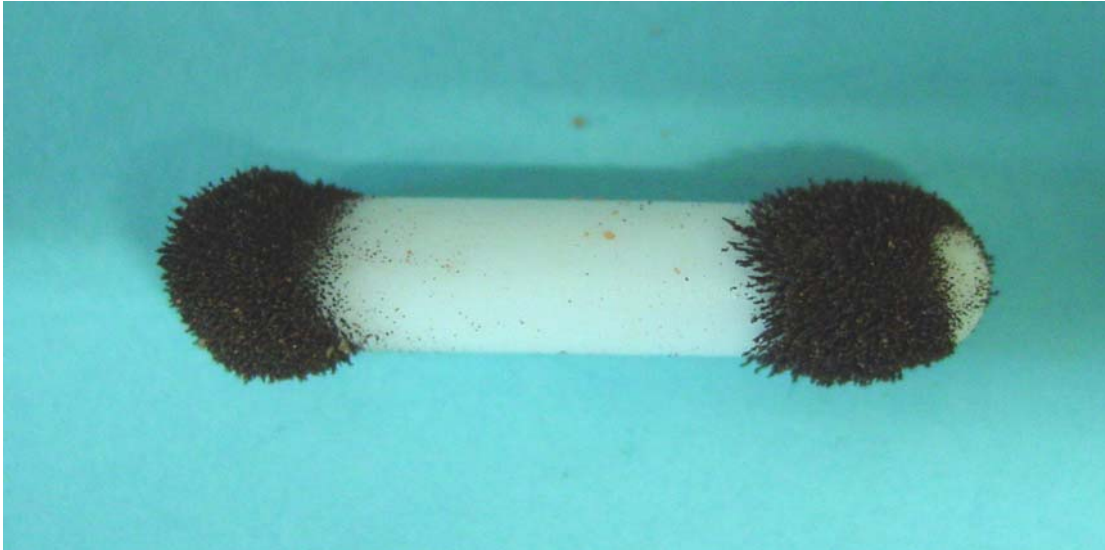


Figure 4.7a. Magnetic stir bar with magnetic soil particles accumulated from 40 g soil collected from a circular patch of dead and yellowed vegetation. See section 4.3.4 for details.



Figure 4. 7b. Magnetic stir bar with magnetic soil particles accumulated from 40 g soil collected between the circles (Matrix 1.3). See section 4.3.4 for details.

4.3.5 Relationships between mima mounds (“heuweltjies”) and fairy circles

The fairy circles have been linked to the mima-like mounds of the Northern and Western Cape in South Africa (Albrecht et al., 2001). The circles

are regarded as the northern counterpart of these unusual earth mounds (Van Rooyen et al., 2004). It is generally thought that mima mounds are fossil features of biogenic origin and were produced by termites (Potts et al., 2009). Berg (1990) proposed that mima mounds formed as a result of seismic activity (Moore and Picker, 1991). The distribution of earth mounds in the western Cape coincides with an area of increased natural seismic hazard (Moore and Picker, 1991). However, Moore and Picker (1991) stated that the earth mounds have an internal stratification that indicates progressive growth by deposition of successive sand layers over a considerable period of time and not in a single event required by the seismic hypothesis. The soils of *heuweltjies* relative to surrounding soils are finer textured, more alkaline and have better water holding capacity that favour a very different community of plants (Desmet, 2007). According to Turner (2003) water retention in the fossil *heuweltjie* soil is enhanced permanently by an impermeable calcareous basement layer at depths of 2-3 m, a consequence of calcite deposition from biogenic production of methane by bacteria in the intestines of termites. The soil chemistry of the mounds differs significantly from surrounding soils with enrichments in Ca, Mg, K, P and N (Moore and Picker, 1991).

Hydrocarbon induced topography is often characterised by conical or volcano-like forms, carbonate crusts, slabs, mounds or chimneys and pock mark-like features (Keller et al., 2007). Conical mounds may have a small central crater (Keller et al., 2007). Moore and Picker et al. (1991) reported that the majority of earth mounds in the Clanwilliam district (South Africa) displayed a central depression. Schwarz (1906) described natural mounds in the

Worcester area (South Africa) as “hillocks with slopes of varying angles and often as acute as a volcanic cone” and mounds in Malmesbury (South Africa) are described as “usually have a depression in the centre”. Dietz (1945) described mima mounds related to barren soil circles in the Gulf Coastal Plain (oil/gas heartland) in the United States of America as such “Commonly associated with the mounds are circular patches of sand which are commonly referred to locally as “sinks” or “slick spots”. No vegetation grows upon these sandy spots and consequently they appear as prominent white scars from the air”. Albrecht et al. (2001) reported a remarkably close correlation between the R-value for spatial distribution of the barren fairy circles ($R = 1.68$) and the R-value recorded for the mima mounds ($R = 1.7$). Because mima mounds are believed to be fossil termitaria, this close correlation of R-values suggested that termites were also involved in the fairy circle phenomenon.

Potts et al. (2009) reported calcite content values of 23.2 – 65.2% for on-mound samples collected from a mound near Worcester, South Africa. No calcite was detected for off-mound samples. The authors pointed out that the calcite content for on-mound samples show that the calcrete is a mound-associated phenomenon, as off-mound samples contained no traces of calcite. Their conclusion was that calcrete formation in the mound stopped 22 000 yr ago and since then the local climatic conditions surrounding the mounds have not been suitable for calcrete formation. Of particular interest pertaining to calcite detected in-mound, but not off-mound, is that hydrocarbon induced alteration in a geochemical seep precipitates calcite (CaCO_3) (Schumacher, 1996). Mineral alteration related to hydrocarbon seepage can result in

enrichment in carbonates with a concentration of calcium and secondary enrichment in calcite around the edge of the seep (Van der Meer et al., 2002). Seep-related carbonates are generally patchy and complex with an irregular network of fractures and cavities present (Cavagna et al., 1999). Moore and Picker (1991) described the basal portions of the mounds as highly calcified and the calcification was patchy. In view of this, the near-surface slab of calcite associated with the fossil *heuweltjies* described by Turner (2003) may, instead, have derived from a geochemical source and not, as was suggested by the author, from termites.

It is the opinion of Becker (2007) that the foraging behaviour of harvester ants and harvester termites are the prime causal factor for the development of fairy circles. However, the author reported that specific conditions need to exist in order for fairy circles to develop, and even when these conditions are met, harvesting activity does not necessarily result in the development of a fairy circle. The results of Jankowitz et al.'s (2008) *in situ* study can not be explained by termites or ants consuming plant material, nor can it be explained by self-organised vegetation pattern formation as causal factors for the development of fairy circles, but it can be interpreted as support for the proposed theory of episodic air displacement by natural gas and the residual effect of traces of low volatility hydrocarbons in the circles. Grass plants growing in open containers inside the circle performed poorly, irrespective of the origin of the soil, while plants growing in sealed containers in the circle showed improved vitality (Jankowitz et al., 2008). A factor not considered by any of the studies reporting on the origin of the fairy circles is that termites are a source of methane which,

potentially, could produce an anaerobic soil environment resulting in a zone of altered soil chemistry which may cause plant stress. However, the detection of unresolved complex mixtures and saturated alkanes $C_{12} - C_{20}$ are totally unrelated to termite activity.

Microseep migration is formed by the diffusion of gases passing through seemingly impenetrable barriers (Van der Meer et al., 2002). Colloidal size gas bubbles ascend through a network of interconnected groundwater filled “microfractures” (Mello et al., 1996; Jones et al., 2000; Van der Meer et al., 2000; Yang et al., 2000; Van der Meer et al., 2002). The cross-sectional shape of the hydrocarbon leaking pattern has been labelled a “chimney effect”, providing channels for seep migration (Van der Meer et al., 2002). Oxidation in the chimney above leaking hydrocarbon accumulations not only leads to the precipitation of carbonates (e.g. calcite) but also to a concentration of calcium with secondary enrichment of calcite around the edge of the seep to form ring structures. The circular shape of the fairy circles correlates with the surface expression of a seep. Fairy circles may be associated with “chimneys” which may explain the perceived patterning distribution of the circles. The circles seem as if uniformly spread, but this is not necessarily so, because the two newly formed circles were adjoining each other.

Results show that the fairy circles are a surface expression of geochemical seepage. If a causal link exists between circles and fossil mounds, as it is indeed suggested by the close correlation between the two phenomena, then mima mounds are not exclusively fossilised termite nests.

Instead, the mounds may be fossilised geochemical seep relics. The significantly different soil chemistry of the mounds compared to surrounding soil suggests correlation with the hydrocarbon induced alteration of soils in a geochemical seep. The particle size and sorting effect in the mound, mudflow event, mound soil enrichment, the cessation of calcite formation in-mound and the absence of calcite off-mound, together with the fact that mound formation did not take place in a single event, but rather, over a considerable period of time may be explained in terms of a fossil hydrocarbon-seep. The hypothesis that mounds may be fossil seep relics, of course, needs investigation.

4.4 Conclusions

It is proposed that the origin of the fairy circle is of a geological nature. Results show a microseepage of gases and hydrocarbons which manifests at the surface as a geobotanical anomaly of barren circles and circles of altered vegetation. Seepage may be minor venting and an anomaly does therefore not necessarily imply an economic hydrocarbon accumulation. The evidence of geochemical seepage is provided by:

- **Geobotanical anomalies.** Elevated natural gas concentrations in soil show as geobotanical anomalies of circular patches of stressed and dead vegetation and circles of barren soil.
- **The presence of natural gases.** Measured amounts of the non-hydrocarbon gas, CO (indicator of natural gas), do not fully account for the relatively small displacement of O₂. Additional gases are therefore present in the seep.

- **Microbiological anomalies.** Alkenes, the microbiological degradation product of alkanes, were detected. Higher levels of alkenes were detected in soil collected from inside barren circles when compared to the relatively lower levels of alkenes detected in soil collected from between the barren circles (matrix). The relatively higher levels of alkenes detected inside the circles are indicative of the presence of a richer microbial food source inside the circles. The relatively lower levels of alkenes detected in soil collected from between the barren circles (matrix) are indicative of the presence of a less abundant microbial food source in the matrix.
- **Anomalous hydrocarbons.** Saturated alkanes were detected in both of the newly formed circles. An alkane/alkene ratio of >1 indicates an active seep. The two newly formed circles had ratios of 7 and 72, suggesting very active seepage.
- **Magnetic susceptibility.** The soil exhibits strong magnetic properties.

The solventless method of extraction of hydrocarbons from soil was simple and successful and can be useful for the sampling of small sized soil samples.

See Appendix A for supplementary data not appearing in the journal article.

4.5 Acknowledgements

Prof N. Grobbelaar for suggesting many years ago that gases should be analysed, NamibRand Nature Reserve in Namibia for granting an entry permit

to the park, Namibian Ministry of Environment and Tourism for a research permit, Dr Willem Jankowitz for assistance with obtaining the permit at the ministry, Dr Noel van Rooyen of Ekotrust and Dr Sieglinde Bauermeister of the Department of Chemistry, University of Pretoria, for assisting during field sampling.

4.6 References

- Abrams M., 2005. Significance of hydrocarbon seepage relative to petroleum generation and entrapment. *Marine and Petroleum Geology* 22, 457-477.
- Albrecht C.F., Joubert J.J., De Rycke P.H., 2001. Origin of the enigmatic, circular, barren patches ('Fairy Rings') of the pro-Namib. *South African Journal of Science* 97, 23-27.
- Becker T., 2007. The phenomenon of fairy circles in Kaokoland (NW Namibia) *Basic and Applied Dryland Research* 1(2), 121-137.
- Borgogno F., D'Odorico P., Laio F., Ridolfi L., 2009. Mathematical models of vegetation pattern formation in ecohydrology. *Reviews of Geophysics* 47, 1-36.
- Carte Blanche [online]. Available: <http://www.mnet.co.za/Mnet/Shows/carteblanche/story.asp?id=2603> [06 September 2010].
- Cavagna S., Clari P., Martire L., 1999. The role of bacteria in the formation of cold seep carbonates: geological evidence from Monferrato (Tertiary, NW Italy). *Sedimentary Geology* 126, 253-270.
- Desmet P.G., 2007. Namaqualand-A brief overview of the physical and floristic environment. *Journal of Arid Environments* 70, 570-587.
- De Vita V., 2006. African desert has its own X-files [online]. Available: http://www.iol.co.za/index.php?from=rss_Travel&set_id=14&click_id=0&art_id=vn20060729094938616C147804 [07 September 2010].
- Dietz R.S., 1945. The small mounds of the Gulf Coastal Plain. *Science* 102(2658), 596-597.
- Eicker A., Theron G.K., Grobbelaar N., 1982. 'n Mikrobiologiese studie van "kaal kolle" in die Giribesvlakte van Kaokoland, S.W.A.-Namibië. *South African Journal of Botany* 1, 69-74.
- Eldmore R.D., Engel M.H., Crawford L., Nick K., Imbus S., Sofer Z., 1987. Evidence for a relationship between hydrocarbons and authigenic magnetite. *Nature* 325, 428-430.
- Grossi V., Cravo-Laureau C., Guyoneaud R., Ranchou-Peyruse A., Hirschler-Réa A., 2008. Metabolism of *n*-alkanes by anaerobic bacteria: A summary. *Organic Geochemistry* 9, 1197-1203.
- Hamamura N., Olson S.H., Ward D.M., Inskeep W.P., 2005. Diversity and functional analysis of bacterial communities associated with natural hydrocarbon seeps in acidic soils at Rainbow Springs, Yellowstone National Park. *Applied and Environmental Microbiology* 5943-5950.

- Harbert W., Jones, V.T., Izzo J., Anderson T.H., 2006. Analysis of light hydrocarbons in soil gases, Lost River region, West Virginia: Relation to stratigraphy and geological structures. AAPG Bulletin 90, 715-734.
- Ingham E.R. Undated. Soil Biology Primer, Chapter 4: Soil Fungi [online]. Available: soils.usda.gov/sqi/concepts/soil_biology/biology.html [01 March 2010].
- Jankowitz W.J., Van Rooyen M.W., Shaw D., Kaumba J.S., Van Rooyen N., 2008. Mysterious circles in the Namib Desert. South African Journal of Botany 74, 332–334.
- Jones V.T., Matthews M.D., Richers D.M., 2000. Light hydrocarbons for petroleum and gas prospecting, in: Hale, M., Govett, G.J.S. (Eds.), Handbook of exploration geochemistry Vol. 7, Chapter 5, Elsevier Science Publishers, Amsterdam, pp. 133-212.
- Joubert A., 2008. Investigation on selected biotic and abiotic factors in the maintenance of the “fairy circles” (barren patches) of southern Africa. MSc. dissertation, University of Pretoria, Pretoria, South Africa.
- Keller E.A., Duffy M., Kennett J.P., Hill T., 2007. Tectonic geomorphology and hydrocarbon induced topography of the Mid-Channel Anticline, Santa Barbara Basin, California. Geomorphology 89, 274-286.
- Liu Q., Liu Q., Chan L., Yang T., Xia X., Cheng T., 2006. Magnetic enhancement caused by hydrocarbon migration in the Mawangmiao oil field, Jiangnan Basin, China. Journal of Petroleum Science and Engineering 53, 25-33.
- Lovegrove, B., 1993. The Living Deserts of Southern Africa. Fernwood Press, Vlaeberg.
- Macgregor D.S., 1993. Relationships between seepage, tectonics and subsurface petroleum reserves. Marine and Petroleum Geology 10, 606–619.
- Mello M.R., Babinski N.A., Gonçalves F.T., Miranda F.P., 1996. Hydrocarbon prospecting in the Amazon rain forest: Application of surface geochemical, microbiological, and remote sensing methods. In: Schumacher, D., Abrams, M.A. (Eds.), Hydrocarbon migration and its near-surface expression: AAPG Memoir 66, pp. 401-411.
- Moll, E.J., 1994. The origin and distribution of fairy rings in Namibia. In: Seyani, J.H., Chikuni, A.C. (Eds.), Proceedings of the 13th Plenary Meeting AETFAT, Malawi, pp. 1203–1209.
- Monson L.M., Shurr G.W., 2003. Assessment of hydrocarbon seepage on Fort Peck Reservation, Northeast Montana: A comparison of surface exploration techniques. AAPG Annual Convention, Salt Lake City, Utah.
- Moore J.M., Picker M.D., 1991. *Heuweltjies* (earth mounds) in the Clanwilliam district, Cape Province, South Africa: 4000-year-old termite nests. Oecologia 86, 424-432.
- Morikawa M., Kanemoto M., Imanaka T., 1996. Biological oxidation of alkane to alkene under anaerobic conditions. Journal of Fermentation and Bioengineering 82, 309-311.
- Noomen M.F., Skidmore A.K., Van der Meer F.D., 2003. Detecting the influence of gas seepage on vegetation, using hyperspectral remote sensing. Third EARSeL workshop on Imaging Spectroscopy, Herrsching.
- Osuji L., Antia B.S., 2005. Geochemical implication of some chemical

- fossils as indicators of petroleum source rocks. *Journal of Applied Sciences and Environmental Management* 9, 45-49.
- Potts A.J., Midgley J.J., Harris C., 2009. Stable isotope and ^{14}C study of biogenic calcrete in a termite mound, Western Cape, South Africa, and its paleoenvironmental significance. *Quaternary Research* 72, 258-264.
- Rangel A., Katz B., Ramirez E., Vaz dos Santos Neto E., 2003. Alternative interpretations as to the origin of the hydrocarbons of the Guajira Basin, Colombia. *Marine and Petroleum Geology* 20, 129-139.
- Rietkerk M., Dekker S.C., De Ruyter P.C., Van de Koppel J., 2004. Self-organised patchiness and catastrophic shifts in ecosystems. *Science* 305, 1926-1929.
- Schumacher D., 1996. Hydrocarbon-induced alteration of soils and sediments, in: Schumacher, D., Abrams, M.A. (Eds.), *Hydrocarbon migration and its near-surface expression: AAPG Memoir 66*, pp. 71-89.
- Schumacher D., LeSchack L.A., 2002. Surface exploration case histories, applications of geochemistry, magnetics, and remote sensing. *AAPG Studies in Geology No. 48*, Tulsa, OK, USA, pp. 1-486.
- Schumacher D., Foote R.S., 2006. Seepage-induced magnetic anomalies associated with oil and gas fields: onshore and offshore examples. *CSPG-CSEG-CWLS Convention*, Canada.
- Schwarz E.H.L., 1906. Natural mounds in Cape Colony. *The Geographical Journal* 27 (1), 67-69.
- Smith K.L., Steven, M.D., Colls J.J., 2004. Use of hyperspectral derivative ratios in the red-edge region to identify plant stress responses to gas leaks. *Remote Sensing of Environment* 92, 207-217.
- Stone V.C.A., Fairhead J.D., Oterdoom W.H., 2004. Micromagnetic seep detection in the Sudan. *The Leading Edge* 23 (8), 734-737.
- Summons R.E., Hope J.M., Swart R., Walter M.R., 2008. Origin of Nama Basin bitumen seeps: Petroleum derived from a Permian lacustrine source rock traversing southwestern Gondwana. *Organic Geochemistry* 39, 589-607.
- Theron G.K., 1979. Die verskynsel van kaal kolle in Kaokoland, SuidWes-Afrika. *Journal of the South African Biological Society* 20, 43-53.
- Torti S.D., Coley P.D., Janos D.P., 1997. Vesicular-Arbuscular Mycorrhizae in Two Tropical Monodominant Trees. *Journal of Tropical Ecology* 13 (4), 623-629.
- Turner J.S., 2003. Trace fossils and extended organisms: a physiological perspective. *Palaeogeography, Palaeoclimatology, Palaeoecology* 192, 15-31.
- Van der Meer F., Van Dijk P., Kroonenberg S., Yang H., Lang H., 2000. Hyperspectral hydrocarbon microseepage detection and monitoring: potentials and limitations. *Second EARSeL workshop on Imaging Spectroscopy*, Enschede, The Netherlands.
- Van der Meer F., Van Dijk P., Van der Werff H., Yang H., 2002. Remote sensing and petroleum seepage: a review and case study. *Terra Nova* 14 (1), 1-17.
- Van Rooyen M.W., Theron G.K., Van Rooyen N., Jankowitz W.J., Matthews W.S., 2004. Mysterious circles in the Namib Desert: review of hypotheses on their origin. *Journal of Arid Environments* 57, 467-485.
- Walden J., White K.H., Kilcoyne S.H., Bentley P.M., 1999. Analyses of iron

- oxide assemblages within Namib dune sediments using high field remanence measurements (9 T) and Mössbauer analysis. *Journal of Quaternary Science* 15, 185–95.
- Xu D.-Q., Ni G.-Q., Jiang L.-L., Shen Y.-T., Li T., Ge S.-L., Shu X.-B., 2008. Exploring for natural gas using reflectance spectra of surface soils. *Space Research* 41, 1800-1817.
- Yang H., Meer F.V.D., Zhang J., Kroonenberg, S.B., 2000. Direct detection of onshore hydrocarbon microseepages by remote sensing techniques. *Remote Sensing Reviews* 18, 1-18.

4.7 Appendix A

Confirmation of the presence of fossil fuel biomarkers, pristane and phytane, in fairy circle soil by GCxGC-TOFMS

Since publication of this chapter in the Journal of Arid Environments the laboratory has acquired a GCxGC-TOFMS. Comprehensive two dimensional gas chromatography achieved separation of a complex mixture (Fig. 4.8) that could not be resolved with one dimensional GC (Fig. 4.6).

Certified reference standard. An authentic reference standard (2000 µg/ml in methylene chloride) containing *n*-heptadecane, pristane, *n*-octadecane and phytane (purity 99%) was purchased from Restek (Restek, Bellefonte, PA, USA). The standard was diluted to 1 µg/ml in methylene chloride.

Sorptive extraction and analysis. Soil from a newly developed fairy circle (patch of dead vegetation) was extracted with a PDMS loop as is described in 4.2.3. The PDMS loop was desorbed in a thermal desorber as is described in 4.2.4. Separation of the desorbed compounds was performed on a LECO Pegasus 4D GCxGC-TOFMS including an Agilent 7890 GC (LECO Africa (Pty) Ltd., Kempton Park, South Africa) (Table 4.1).

Confirmation of target compounds. One microlitre of the diluted reference standard was added to a PDMS loop. The loop was desorbed as is described in 4.2.4. Separation of the desorbed compounds was performed by GCxGC-TOFMS (Table 4.1). Compound confirmation was done by comparing two dimensional retention times and mass spectra of the target compounds in the

soil sample with that of the standard. Figure 4.8 shows the contour plot of hydrocarbons in soil from a newly developed fairy circle (patch of dead vegetation). The presence of the fossil fuel biomarkers, pristane and phytane, confirms a geochemical origin of the fairy circles.

Table 4.1

GCxGC-TOFMS method parameters

First dimension column	Rxi-17SiIMS (15 m x 0.25 mm ID x 0.25 μ m df)
Second dimension column	Rtx-5 (0.99 m x 0.18 mm ID x 0.20 μ m df)
Carrier gas	Helium
Flow mode	Constant flow
Flow rate	1.5 ml/min
Inlet purge time	120 s
Inlet purge flow	30 ml/min
¹ D column temperatures	30 °C for 3 min, ramp at 5 °C/min to 280 °C, hold for 1 min
² D column temperatures	50 °C for 3 min, ramp at 5 °C/min to 300 °C, hold for 1 min
Transfer line temperature	300 °C
Modulator temperature offset	35 °C
Modulation period	5 s
Hot pulse time	1.20 s
Cool time between stages	1.3 s
Acquisition rate	100 spectra/s
Mass range	40-450 amu
Detector voltage	1700 V
Electron energy	70 eV

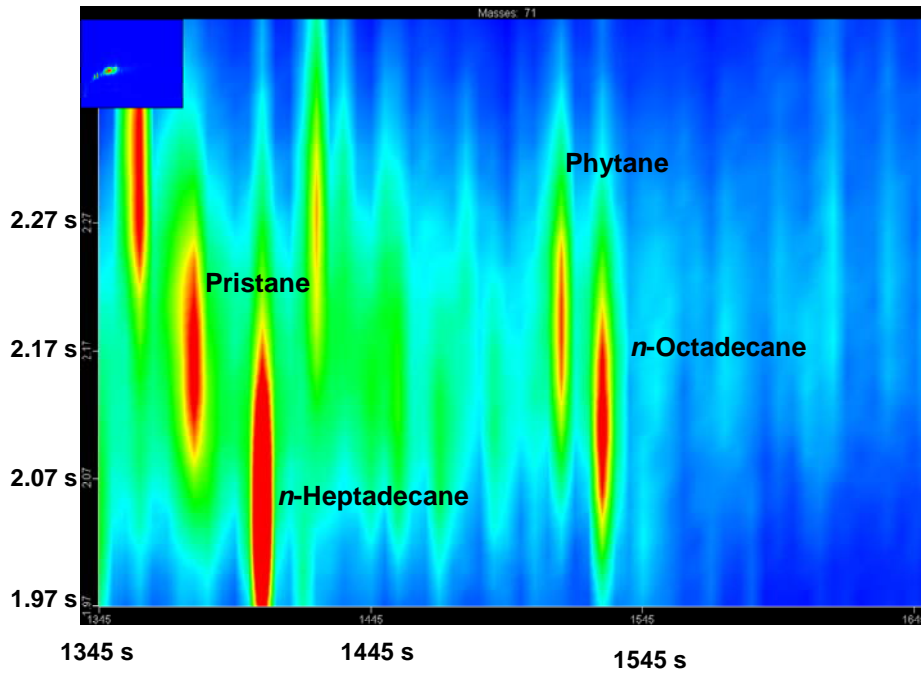


Figure 4.8. Contour plot of hydrocarbons in soil from a newly developed fairy circle (patch of dead vegetation). The presence of the fossil fuel biomarkers, pristane and phytane, confirms a geochemical origin of the fairy circles. See Table 4.1 for instrumental parameters.

Chapter 5

Multi-channel open tubular traps for headspace sampling, gas chromatographic fraction collection and olfactory assessment of milk volatiles

This chapter was published in Journal of Chromatography A. The format reflects the style set by the journal.

Naudé, Y., Van Aardt, M., Rohwer, E.R., 2009. Multi-channel open tubular traps for headspace sampling, gas chromatographic fraction collection and olfactory assessment of milk volatiles. *Journal of Chromatography A*, 2798–2804. doi:10.1016/j.chroma.2008.09.065

Author contributions

Conceived and designed the experiments: Yvette Naudé and Egmont Rohwer. Performed experimental work and data analysis, wrote the chapter/article, submitted article to journal, response to reviewers: Yvette Naudé. Provision of food chemistry context, training and guidance in olfactory assessment: Marleen van Aardt. Initiator of research and study supervisor: Egmont Rohwer.

The work in this chapter was presented at the 32nd International Symposium on Capillary Chromatography 2008, Riva del Garda, Italy and at ChromSAAMS 2008, Bela Bela, South Africa

Multi-channel open tubular traps for headspace sampling, gas chromatographic fraction collection and olfactory assessment of milk volatiles

Yvette Naudé^{a,*}, Marleen van Aardt^b, Egmont Richard Rohwer^a

^aDepartment of Chemistry, ^bDepartment of Food Science, University of Pretoria, Hatfield 0002, South Africa

ABSTRACT

A headspace sampling method is described for concentrating milk volatiles onto a multi-channel open tubular silicone rubber trap (MCT) for thermal desorption into a GC-FID. Sections of the chromatographic profile, single peaks or combinations of compounds are recaptured with secondary MCTs during a subsequent run. The recaptured aroma is released in a controlled manner by heating the MCT in a portable heating device. An aroma release window of several minutes allows up to six people the opportunity to sniff each aroma fraction more than once. Olfactory results suggest that a synergistic combination of 2-heptanone and 2-nonanone could be responsible for a pungent cheese, sour milk-like aroma. MCTs containing single components or fractions can be desorbed into a GC-MS for compound identification.

Keywords: capillary gas chromatography; sorptive extraction and collection; polydimethyl siloxane; headspace sampling; olfactometry; aroma compounds; milk volatiles.

*Corresponding author: Yvette Naudé, Department of Chemistry, Natural Sciences 1, Room 2.19, University of Pretoria, Hatfield, 0002, South Africa, Tel: +27 (0)12 420 2517; Fax: +27 (0)12 420 4687.

E-mail address: yvette.naude@up.ac.za

5.1 Introduction

The ultra high temperature (UHT) treatment of milk imparts an undesirable cooked (cabbage, sulphurous, stale, heated, sterile milk) flavour to packaged long life milk [1-4]. Analytical methods that have been used to study the aroma of dairy products are gas chromatography mass spectrometry (GC-MS) and gas chromatography olfactometry (GCO) [5-8]. To identify individual odour active gas chromatographic fractions, GCO is traditionally used: a human record of aroma perception - in real time - of the GC effluent at the olfactometer outlet. GCO can cause nose fatigue and requires utmost concentration. The rapid elution of compounds is problematic in terms of recalling appropriate odour descriptors. Typically one to two trained evaluators perform the sniffing. However, a group of assessors is required for reliable GCO analysis necessitating numerous analyses, multiple gas chromatographs equipped with sniff ports [9], or directing the effluent of a GC to multiple sniff ports. Instrumental analyses are not always performed on the aroma relevant compounds but also on non odorous compounds that may include hazardous chemicals [10]. Single compounds at a time are evaluated and potential synergistic effects cannot be observed [9]. Since the mechanism governing the combination of individual compounds in the generation of odours is not yet fully understood it is hard to determine how individual compounds of a product relate to the perception of its overall aroma when using traditional instrumental techniques [10]. The discovery of a cluster of olfactory cortex cells in mice responding exclusively to paired odorous molecules but not to either of the single odorous component on its own may explain how mammals and

specifically humans sense mixtures of odourants [11]. For example, carnation, a markedly different third scent is perceived when a combination of both eugenol (clove-like aroma) and phenyl ethyl alcohol (rose-like aroma) in a mixture is sniffed [11].

The target compounds chosen for technique evaluation in this study are important thermally derived off-flavour compounds present in UHT milk. Powerful odour active volatiles detected in heated milk include 2-heptanone, 2-nonanone and nonanal, with 2-heptanone and 2-nonanone identified as the most intense volatile flavour compounds of UHT milk [12]. Higher concentrations were found of, amongst others, the sulphur compound dimethyl sulfide, the ketones: 2-hexanone, 2-heptanone, 2-nonanone and the aldehydes: 2-methylpropanal, 3-methylbutanal and decanal in UHT milk when compared to concentrations measured in raw and pasteurised milk [3]. Calculated odour activity values (OAV) for dimethyl sulfide, 2,3-butanedione, 2-heptanone, 2-nonanone, 2-methylpropanal, 3-methylbutanal, nonanal and decanal show that these compounds may well be important contributors to the off-flavour of UHT milk [3]. The formation of 2,3-butanedione is however not only heat-induced but can also point to microbial activity in milk [3].

Extraction techniques for the isolation of volatile components from food matrices include head space solid phase microextraction (HS-SPME), solvent extraction with solvent-assisted flavour evaporation (SAFE), stir bar sorptive extraction (SBSE), headspace solid-phase dynamic extraction (HS-SPDE) and headspace trap technology [4, 13 – 16, 18 - 21]. Headspace sampling provides

solvent-free aroma extracts that are more representative of food aroma when compared to those obtained by solvent extraction. Commercial sorptive extraction techniques, such as SPME, SBSE, SPDE and headspace trap technology, offer efficient concentration and can be used for sampling the headspace [16 – 21]. SPME is a fibre coated with a small sorbent volume of 0.6 – 0.9 μl [16, 18, 21], SBSE is a stir bar coated with volumes of 25 – 200 μl polydimethylsiloxane (PDMS) [18], SPDE is a sorptive coating with a sorbent volume of 6 μl on the inside wall of a stainless steel needle of a gas tight syringe [17 – 21], while headspace trap technology makes use of a headspace sampler and a built-in trap. The built-in trap is a tube filled with a solid sorbent with a volume of 160 μl [21]. In contrast to the commercially available coated fibres, coated capillaries and tubes filled with solid packing material, the headspace traps used in this study are multi-channel open tubular silicone rubber traps (MCTs) prepared in-house [22, 23, 24]. The PDMS tubing is inserted into a commercial empty desorption tube (Fig. 5.1). The MCT has a considerably larger volume of 635 μl PDMS offering greater sample enrichment. The analytes are concentrated by a purge-and-trap method onto MCTs, followed by thermal desorption of the MCTs into a gas chromatograph with flame ionisation detection (GC-FID). The open tubular structure of the MCTs and low pressure drop make it suitable for the recapturing of aroma fractions, or single aroma compounds, from the GC effluent during a run and also for the off-line release of the recaptured aroma compounds from the MCTs for olfactometric evaluation, as previously demonstrated for the evaluation of beer aroma [25, 26]. MCTs containing recaptured compounds of unknown identity are desorbed into a GC-MS for compound identification [26].

MCTs and their applications to the extraction of odour compounds from packaged long life UHT milk, to quantitative gas chromatographic analysis, to fractionation and collection of odour compounds for off-line olfactory assessment, to evaluation of combinations of aroma compounds and to GC-MS compound identification are reported.

5.2 Experimental

5.2.1 Chemical standards

Dimethyl sulfide, 2,3-butanedione, 2-hexanone, 2-heptanone, 2-nonanone, 2-methylpropanal, 3-methylbutanal, nonanal and decanal, purity \geq 98.5%, were purchased from Sigma-Aldrich (Pty) Ltd. (Kempton Park, South Africa).

5.2.2 Milk samples

Three batches of packaged long life UHT milk (2% milk fat) were purchased from a local supermarket (Montana, Gauteng, South Africa) on different days. The milk purchased was the supermarket's own brand. The samples were stored in a refrigerator at 7 °C.

5.2.3 *Extraction of Aroma Compounds*

5.2.3.1 *Multi-channel open tubular PDMS trap*

MCTs containing 0.4 ± 0.02 g silicone were prepared according to the method described by Ortner and Rohwer [23]. The MCT was designed to fit a commercial thermal desorber system (TDS) available from Gerstel™. Twenty two channels of silicone elastomer medical grade tubing (0.64 mm OD x 0.3 mm ID, Sil-Tec, Technical Products, Georgia, USA) were inserted into 17.8 cm long glass desorption tubes (4 mm ID, 6 mm OD) from Gerstel™ (Chemetrix, Midrand, South Africa). The MCT inside the desorption tube was 55 mm long (Fig. 5.1).

5.2.3.2 *Sample preparation*

A purge-and-trap sampling method developed in-house was used to extract the volatiles from packaged long life UHT milk (2% milk fat) by trapping it on a MCT [24]. The volatiles were isolated from 200 ml milk inside a 500 ml flat bottomed glass flask. The flask was immersed for 35 min in a water bath (40 °C) to a level slightly above that of the UHT milk in the flask. The sample was purged with 500 ml nitrogen gas (5.0, Afrox, Gauteng, South Africa) at 25 ml/min. The purged volatiles were collected on a MCT at 45 °C to minimise the condensation of water from the sample onto the MCT. A second sorption tube was connected to the primary MCT for the determination of breakthrough of the volatiles from the primary MCT. A sorption tube filled with 2/3 Tenax TA (60/80)

/ 1/3 Carboxen 1003 (40/60) (Gerstel™, Chemetrix, Midrand, South Africa) and a MCT were both evaluated for suitability as back-up traps for the primary MCT. After extraction of the milk sample, 0.5 g of silica gel (Saarchem uniLAB®, particle size 1 – 3 mm, Merck Chemicals (Pty) Ltd, Gauteng, South Africa) was added, as a drying agent, to the sorption tube containing the MCT. After 60 min the silica gel was removed.

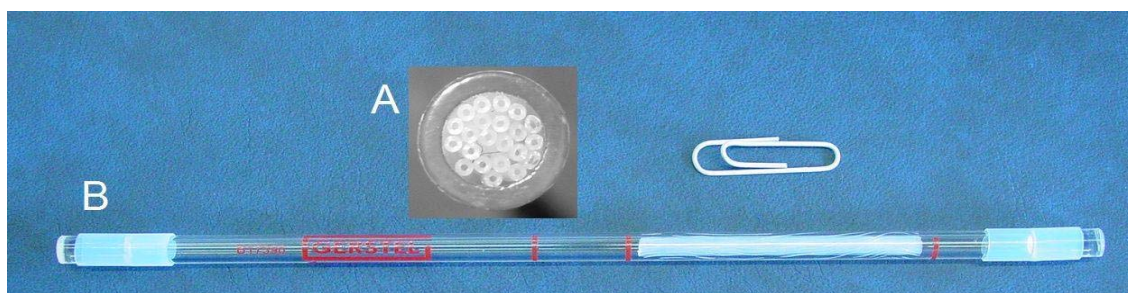


Figure 5.1. (A) Cross section of a MCT. (B) MCT fits a commercial glass desorption tube.

5.2.4 GC-FID with thermal desorption and cryo inlet system

The volatiles were thermally desorbed from the MCT using a TDS from Gerstel™ installed on an Agilent 6890 GC-FID (Chemetrix, Midrand, South Africa). Splitless desorption was from 30 °C (3 min) at 60 °C/min to 210 °C (10 min). The desorption flow rate was 50 ml/min (hydrogen gas, Afrox, Gauteng, South Africa) at 47 kPa. The TDS transfer line temperature was 250 °C. The volatiles were cryogenically focused using liquid nitrogen at –100 °C on a cooled injection system (CIS). The CIS liner contained silicone rubber to improve retention of the extremely volatile dimethyl sulfide. After desorption of the analytes from the MCT, the CIS was heated to 200 °C at 5 °C/s and the

volatiles were analysed by GC-FID (310 °C). The GC oven temperature programme was -50 °C (3 min) at 10 °C/min to 120 °C (10 min), 10 °C/min to 220 °C. Hydrogen carrier gas velocity was 33 cm/s (2.3 ml/min) and the column head pressure was 23 kPa in the constant pressure mode. The GC column was a Zebron ZB-1 30 m x 320 µm ID x 1 µm film thickness (Phenomenex, Separations, Randburg, South Africa).

5.2.5 Quantification

A standard stock solution was prepared in methanol (Saarchem UniVAR, Merck Chemicals (Pty) Ltd., Kempton Park, South Africa) containing dimethyl sulfide, 2,3-butanedione, 2-hexanone, 2-heptanone, 2-nonanone, 2-methylpropanal, 3-methylbutanal, nonanal and decanal to give a concentration of 1 µg/µl. Standard solution was added to 200 ml long life packaged UHT milk (2% milk fat) to give final concentrations of 0.4, 0.8, 4, 8, 16, 40, 70, 85 µg/200ml. Chilled long life UHT milk from the refrigerator was spiked, mixed on a vortex mixer and equilibrated for 20 min in the refrigerator. The spiked samples were extracted as described previously. Calibration curves (matrix-assisted standard addition) for the compounds were constructed and linear regression analysis was used.

5.2.6 Capturing of single compounds and fractions by gas chromatography fraction collection (GCFC)

A chromatographic profile of the packaged long life UHT milk is first obtained using the conditions described previously. Integration results of peak start time and peak end time of the chromatogram of the UHT milk were then used to establish the compound/fraction recapturing event times. In a subsequent run, various sections of the GC-effluent were recaptured, with secondary MCTs on a carefully timed basis. Manual collection commenced 30 s before peak elution and ended 10 s after elution had completed (Table 5.1). For GCFC the instrumental conditions were as previously described, the only difference was the modification of the detector parameters. The electrometer was switched off. The detector top assembly and the collector were removed by loosening the knurled brass of the detector assembly and by lifting the collector out. Single peaks or fractions were collected at the end of the GC column by placing a secondary MCT on the FID flame tip and by supporting the MCT in this position by hand (Fig. 5.2). During collection the FID and flame gases (hydrogen and air) were switched off, the make-up gas (helium) plus carrier gas (hydrogen) flow totalled 50 ml/min and the detector temperature was at 100 °C. After fractions or single compounds were recaptured the MCT was capped and stored for olfactory evaluation and for GC-MS identification.

Table 5.1
GCFC event times – peak capturing time table

Compound	Collection start time (min)	Collection end time (min)
1. Dimethyl Sulfide	12.28	12.91
2. 2-Methylpropanal	13.00	13.62
3. 2, 3-Butanedione	13.70	14.50
4. 3-Methylbutanal	15.20	15.84
5. 2-Hexanone	18.30	19.00
6. 2-Heptanone	20.70	21.50
7. 2-Nonanone	28.20	28.92
8. Nonanal	29.08	29.80
9. Decanal	33.60	34.35



Figure 5.2. Removed detector top assembly and collector. MCT placed on GC-FID flame tip to recapture single peaks or various fractions [25]. Helium was used as the make-up gas.

5.2.7 Olfactory evaluation of captured fractions and single compounds on secondary MCTs

The aroma was released in a controlled manner by heating the secondary MCT containing the recaptured component/s from the GC-effluent in

a portable heating device with a flow of nitrogen gas at a desorption flow rate of 20 ml/min. The MCTs were inserted in the cavity in the portable heating device. The compounds were released from the secondary MCTs at GC column elution temperature for the single compounds. As the aroma eluted from the MCT it was sniffed by a team consisting of six experienced non smoking evaluators (five female, one male). All six of the evaluators participated as a group during the same assessment session. For the evaluation of combinations of compounds the fractions were released at 130 °C and at 160 °C and the aroma was evaluated by a panel of three persons.

5.2.8 Identification of volatile compounds by GC-MS

The recaptured analytes (obtained with GCFC) were desorbed using a Gerstel TDS installed on a Hewlett Packard (HP) GC 1530A coupled to a HP 5973 mass selective detector (MSD) (Chemetrix, Johannesburg, South Africa). The MCTs were desorbed from 30 °C (3 min) at 60 °C/min to 210 °C (10 min), the desorption flow was 60 ml/min at 65 kPa (Helium, Ultra High Purity, Afrox, Johannesburg) in the splitless desorption mode allowing for total transfer of analytes to the cold trap. The TDS transfer line temperature was 250 °C. The desorbed analytes were cryogenically focused on a CIS at –100 °C using liquid nitrogen. The inlet liner contained silicone rubber to improve the retention of the volatile analytes. After desorption, a splitless injection (purge on at 30 min, purge flow 30 ml/min) was performed by heating the CIS from –100 °C at 5° C/s to 200 °C for 10 min. The GC column was a Zebron, ZB1 30 m x 250 µm ID x 0.25 µm film thickness (Phenomenex, Separations, Randburg, South Africa),

the velocity of the carrier gas (helium) was 42 cm/s (1.3 ml/min) and the column head pressure was 65 kPa in the constant pressure mode. The GC oven temperature programme was -50 °C (3 min) at 10 °C/min to 220 °C (1 min). The GC run time was 31 min. The GC-MS transfer line was at 250° C, the mass scan range was 35-300 atomic mass units in full scan mode, the source (EI+) temperature 230 °C, the MS quadrupole temperature 150 °C, the ionisation energy 70 eV and the electron multiplier (EM) 1700 V. The identities of the volatiles were confirmed by comparison of the retention times of the analytes in the sample to the retention times of the standards, by mass spectra comparison of the standards to that of the analytes and to the mass spectra found in a commercial library (Wiley). Matches of the mass spectra of the components to that of the library were ≥90%.

5.3 Results and discussion

5.3.1 Extraction of aroma compounds and GC-FID with thermal desorption and CIS

In order to collect all of the target analytes (C₂-C₁₀) from the UHT milk within a single extraction step a second sorption tube containing 2/3 Tenax TA (60/80) and 1/3 Carboxen 1003 (40/60) was connected as a backup trap to the primary MCT. When the MCT was desorbed for analysis of the C₆-C₁₀ fraction (2-hexanone, 2-heptanone, 2-nonanone, nonanal, decanal) it was found, contrary to expectation, that the C₂-C₅ volatile fraction (dimethyl sulfide, 2-methylpropanal, 2,3-butanedione, 3-methylbutanal) was present on the primary

MCT. The Tenax/Carboxen tube was then desorbed to determine if breakthrough occurred from the primary MCT onto the second backup trap. However, desorption of the Tenax/Carboxen tube was problematic due to the dense packing of the sorption material which caused a high inlet pressure and gas flow shut down, even at very low desorption flow rates. Hence, the use of a Tenax/Carboxen sorption tube as a backup trap for the primary MCT was discontinued. Instead, a second MCT was connected as a backup trap to the primary MCT to determine the level of breakthrough from the first MCT onto the second MCT. Due to the open tubular structure of the MCT, problems with inlet pressure and gas flow were not experienced. For the C₂-C₅ volatile fraction (dimethyl sulfide, 2-methylpropanal, 2,3-butanedione, 3-methylbutanal) breakthrough levels were at 47 – 51% and for the C₆-C₁₀ fraction (2-hexanone, 2-heptanone, 2-nonanone, nonanal, decanal) breakthrough was 0 – 10%.

The inlet liner contained a 7 cm length of silicone rubber tubing (± 10 mg) which dramatically improved the retention and thus focusing of the extremely volatile dimethyl sulfide. Pronounced peak broadening occurred when there was no silicone rubber in the inlet liner, indicating breakthrough from the CIS during desorption of the MCT. Peak broadening of dimethyl sulfide was still observed during the TDS desorption cycle when the GC oven was at ambient temperature. Therefore the oven was cryogenically cooled to -50 °C using liquid nitrogen to obtain narrower GC peaks for dimethyl sulfide. Some residual moisture was collected onto the MCT during extraction of the UHT milk. The moisture caused FID signal instability, shifting the retention times of the early eluting compounds (dimethyl sulfide, 2-methylpropanal, 2,3-butanedione, 3-

methylbutanal) when using a GC column with a 0.25 μm film thickness. To reduce the moisture and to improve retention time repeatability, silica gel was added to the TDS sorption tube containing the MCT. A drying period of one hour was sufficient to dry the MCT. However, when using silica gel a 50% loss from the MCT occurred for dimethyl sulfide and 2-methylpropanal. A thicker film (1 μm) GC column was therefore rather used in this particular application. The thicker film column was less sensitive to any residual moisture which improved FID signal stability and also retention time repeatability of the early eluting compounds.

5.3.2 *Quantification of the aroma compounds*

Table 5.2 shows the results of the linear regression analysis of the calibration ($n=8$) based on the method of standard addition [3]. 2,3-Butanedione was excluded from the quantification results because the purity of the purchased reference standard was compromised. The concentrations of the aroma compounds present in a sample ($n=1$) from the second batch and a sample ($n=1$) from the third batch of packaged long life UHT milk (2% milk fat) used for fraction collection and for the off-line release of the captured aromas are given in Table 5.3. The concentrations were calculated from the regression equations in Table 5.2. The first batch of UHT milk samples was used for technique development.

Table 5.2

Regression equations for UHT milk aroma compounds spiked into long life packaged UHT milk (2% milk fat)

Compound	Regression equation ¹	R ²	LOQ ² (µg/l)
1. Dimethyl Sulfide	y= 2.67x	0.994	3.75
2. 2-Methylpropanal	y= 3.22x	0.998	3.11
3. 2,3-Butanedione	-	-	-
4. 3-Methylbutanal	y= 11.5x	0.997	0.855
5. 2-Hexanone	y= 17.5x	0.988	0.574
6. 2-Heptanone	y= 3.21x	0.999	0.620
7. 2-Nonanone	y= 2.85x	0.995	3.64
8. Nonanal	y= 2.52x	0.997	3.96
9. Decanal	y= 0.803x	0.996	12.8

¹y= Peak Area of compound, x = concentration of the compound µg/l.

²Limit of quantification (LOQ) calculated as the concentration that gives a signal-to-noise (S/N) ratio of 10.

Table 5.3

Concentrations of the aroma compounds in UHT milk (2% milk fat) used for GCFC and olfactory assessment

Compound	UHT batch 2 (µg/l)	UHT batch 3 (µg/l)
1. Dimethyl Sulfide	6.50	15.0
2. 2-Methylpropanal	3.30	< 3.11
3. 2,3-Butanedione	-	-
4. 3-Methylbutanal	1.58	1.11
5. 2-Hexanone	1.23	1.21
6. 2-Heptanone	28.4	37.2
7. 2-Nonanone	29.4	36.3
8. Nonanal	37.9	37.7
9. Decanal	43.9	13.5

5.3.3 Capturing of single compounds and fractions by GCFC

Single compounds or combinations of compounds were collected on secondary MCTs. Figure 5.3 shows the comparison of the primary chromatogram of a primary MCT containing compounds from UHT milk spiked at 195 – 245 µg/l, and the secondary chromatograms of secondary MCTs containing compounds that were recaptured from the GC effluent after desorption of primary MCTs containing spiked (195 – 245 µg/l) and unspiked (1

– 44 µg/l) compounds from UHT milk. The nine compounds were selectively recaptured from the GC effluent so that each secondary MCT contained only the nine target compounds, excluding the remainder of the chromatographic profile. A clean chromatographic secondary profile is thus obtained for the secondary MCTs in contrast to the chromatogram of the primary MCT. The efficiency of recapturing compounds onto secondary MCTs at the GC effluent by this manual method and the re-injection of the fractions were 40 - 70% (Fig. 5.3). This fraction collection method required at least five seconds for the manual exchange of the secondary MCTs. Figure 5.4 shows the secondary chromatograms of compounds that are 23 s apart. The compounds were recaptured individually with 2-nonanone recaptured onto MCT 1 and nonanal recaptured onto MCT 2. Since only a small fraction of the large number of volatiles occurring in a particular matrix contributes to the aroma, a distinction must be made between odour active compounds and the whole range of volatiles present [9]. Thus, for the olfactory assessment, the target compounds were captured exclusively so that each MCT contained a single compound excluding the compounds that make up the remainder of the chromatographic profile.

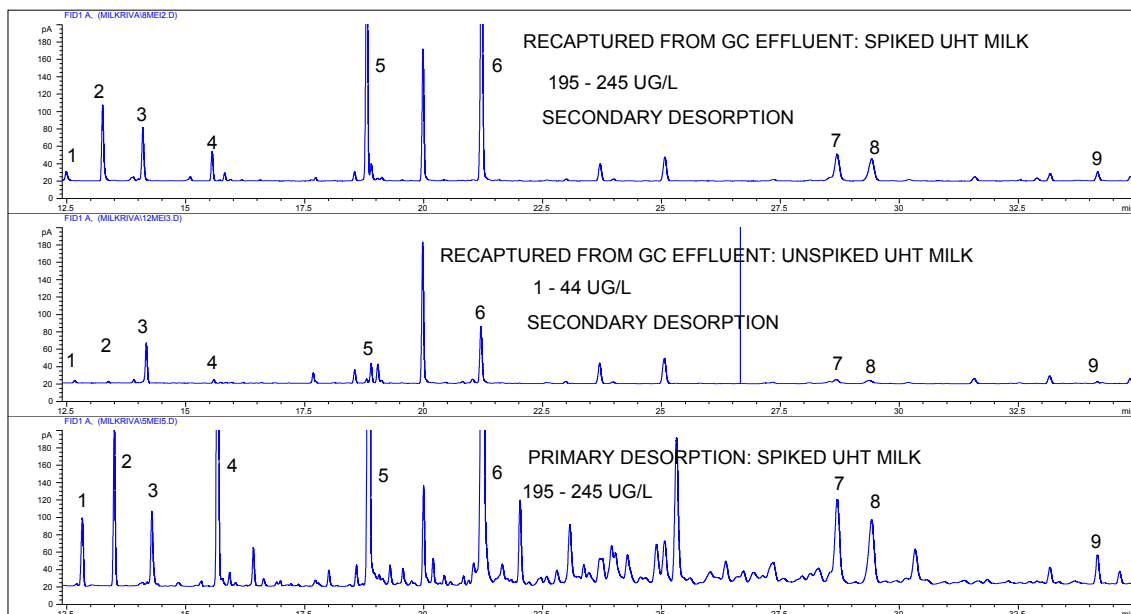


Figure 5.3. Trapping and re-injection efficiency: comparison of the desorption of the secondary MCTs containing the recaptured compounds (single compounds were recaptured from the GC effluent all on the same secondary MCT) of spiked (195 - 245 $\mu\text{g/l}$) and unspiked (1 – 44 $\mu\text{g/l}$) UHT milk (2% milk fat) to the primary chromatogram of UHT milk (2% milk fat) spiked at 195 - 245 $\mu\text{g/l}$. For detail see text; for compound identification see Table 5.1.

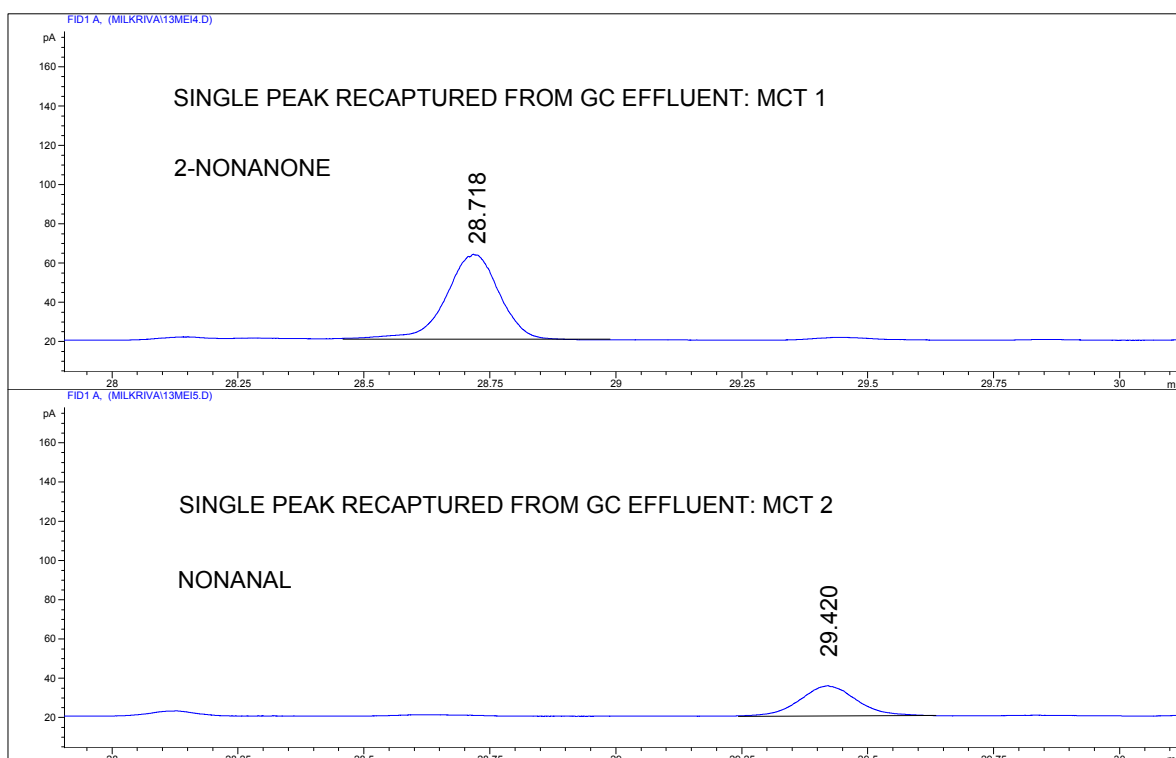


Figure 5.4. Secondary chromatograms of packaged long life UHT milk spiked at 195 – 245 $\mu\text{g/l}$. The single compounds (2-nonanone and nonanal) were separately collected on two different MCTs. The peaks captured were 23 s apart. For detail see text.

5.3.4 GC-MS of a compound recaptured by GCFC

To confirm that dimethyl sulfide was indeed concentrated onto the primary MCT during extraction the peak was recaptured at the end of the GC effluent onto a secondary MCT. The secondary MCT was desorbed into the GC-MS. The retention time and the mass spectrum of the captured peak matched that of the chemical standard and the spectra of the Wiley library. Recapturing of odour active compounds from the GC effluent onto secondary MCTs for analysis by GC-MS can be especially useful when dealing with compounds of unknown identity.

5.3.5 Release of recaptured aroma compounds and the aroma of the overall milk profile from the MCTs for off-line olfactory assessment

Nine odour active compounds (sulfide, aldehydes and ketones) were selected for evaluation and comparison to the aroma of the overall milk profile. Due to the UHT treatment a cooked flavour is imparted when the levels of the compounds in packaged long life UHT milk exceed the levels typically found in freshly pasteurized milk. The low pressure drop of the open tubular channels of the MCT allows most of the effluent of the FID to pass through the trap without special sealing arrangement that would otherwise complicate the GCFC procedure. The advantage of a low pressure drop is not offered by conventional packed traps. After GCFC onto secondary MCTs, the MCTs were desorbed with a flow of nitrogen gas in a portable heating device which resulted in the controlled release of aroma from single compounds or fractions. The aroma

from primary MCTs containing the overall milk profile was also released for comparison to that of the single compounds and fractions. An aroma release window of about three minutes was achieved, allowing up to six people the opportunity to each sniff the aroma more than once during the same release session. This gave ample opportunity for recalling odour descriptors unlike the case for GCO. Quick decisions can impair judgment and attentiveness decreases during a long assessment session. An advantage of GCFC onto MCTs for off-line aroma release is that the olfactory assessment could be terminated and resumed at convenience when the evaluators indicated nose fatigue.

Results of the olfactory assessment of the individual compounds (spike levels of 195 – 245 ug/l in UHT milk) are given in Table 5.4. The aroma descriptors reported by the evaluators for each of the individual compounds generally matched the descriptors reported in the literature [2, 5, 27]. A fairly neutral background was described for the recaptured single compounds and the overall milk profile captured from the unspiked UHT milk (1 - 44 ug/l) (Table 5.4). However, when the overall aroma from the spiked UHT milk (spike level of 79 – 85 µg/l) collected on a single primary MCT was released, the aroma matched the descriptors for the single compounds up to and including 2-hexanone. Thereafter, the aroma observed deviated markedly from the descriptors for the individual compounds. Instead of observing the expected aroma of “soapy” (2-heptanone) and “fruity” (2-nonanone), a sharp, sour milk-like, sweaty aroma was noted. This unexpected and entirely new aroma suggested possible synergistic effects between the compounds, or the

presence of other compounds in the chromatographic profile that are not in the target list of compounds. The unpleasant aroma was absent when the single compounds recaptured during GCFC were sniffed, and when the overall aroma profile of the unspiked milk (1 – 44 µg/l) was sniffed (Table 5.4).

Table 5.4

Olfactory assessment of recaptured single compounds on individual secondary MCTs¹, the overall milk aroma on primary MCTs² and combinations of compounds recaptured onto secondary MCTs³

1. Single compounds captured by GCFC onto secondary MCTs			
Single compounds GCFC	Aroma release temperature °C	¹ Aroma description for single compounds (n=6)	
		Spiked UHT milk 195 – 245 µg/l	Unspiked UHT milk 1 – 44 µg/l
1. Dimethyl Sulphide	21	Sulphurous, rotten egg +++	-
2. 2-Methylpropanal	50	Malty, chemical sweet +++	-
3. 2,3-Butanedione	60	Butter +++	-
4. 3-Methylbutanal	73	Malty, chemical sweet +++	Chemical sweet +
5. 2-Hexanone	103	Feed, hay, field, veld grass ++	-
6. 2-Heptanone	128	Fragrant soap, fruity, floral ++	Fragrant soap +
7. 2-Nonanone	178	Fruity, sweet +++	Fruity, sweet ++
8. Nonanal	185	Biscuit, cotton candy, caramel ++	-
9. Decanal	194	Dusty, musty, rubber ++	Dusty, rubber +

2. Whole milk aroma profile captured by purge-and-trap sampling onto a primary MCT (non-fractionated aroma profile)			
	Aroma release temperature °C	² Aroma description for the overall milk aroma (n=3)	
		Spiked UHT milk 195 – 245 µg/l	Unspiked UHT milk 1 – 44 µg/l
	24 – 40	Rotten egg +, butter +++, sweet +, malty +++	-
	60 – 120	Malty+, feed, pungent, sour milk, sweaty+++	Chemical sweet +
	120 – 185	Sour milk, burnt milk ++	Fragrant soap, floral +

3. Combinations of compounds captured by GCFC onto secondary MCTs			
Binary mixtures	Aroma release temperature °C	³ Aroma description for combinations of compound (n=3)	
		Spiked UHT milk 195 – 245 µg/l	
4. 3-Methylbutanal 5. 2-Hexanone	130	Malty+++ , sweet+	
5. 2-Hexanone 6. 2-Heptanone	160	Milky-sweet, condensed milk ++	
6. 2-Heptanone 7. 2-Nonanone	160	Feta cheese, blue cheese, sweaty, sour, fatty +++	
5. 2-Hexanone 7. 2-Nonanone	160	Cheesy, sweaty, sour +	

+ Intensity indicator. ¹Olfactory evaluation of packaged long life UHT milk (2% milk fat): spiked and unspiked. For each sample nine secondary MCTs each containing heart-cuts of single compounds were individually desorbed in the portable sniffing device at specific temperatures with a flow of nitrogen gas of 20 ml/min.

²Olfactory evaluation of the purge-and-trap extracted overall milk aroma (primary MCT, no GCFC) of long life packaged UHT milk (2% milk fat): spiked and unspiked. The MCTs were desorbed in the portable sniffing device from 24 °C to 185 °C over a period of 60 minutes with a flow of nitrogen gas of 20 ml/min. ³Olfactory evaluation of long life packaged UHT milk (2% milk fat): spiked. For each milk sample four secondary MCTs each containing heart-cuts of binary mixtures of compounds were individually desorbed in the portable sniffing device with a flow of nitrogen gas of 20 ml/min.

5.3.6 Evaluation of combinations of compounds to assess synergistic effects

Combinations of the volatiles were collected onto secondary MCTs during GCFC to determine which compounds were responsible for the modification of the expected fruity, soapy and sweet aroma into the unexpected and wholly new aroma described as pungent, sour milk-like and sweaty. A malty aroma dominated when a combination of the aldehyde 3-methylbutanal (malty, sweet), and the ketone 2-hexanone (“feed”) was sniffed (compounds 4 and 5) (Table 5.4). A milky-sweet, condensed milk aroma was described for the combination of the ketones, 2-hexanone (“feed”) and 2-heptanone (soapy, fruity, floral) (compounds 5 and 6). A pungent, feta cheese, blue cheese, sweaty, sour, fatty aroma was observed when a combination of the ketones, 2-heptanone (soapy, fruity, floral) and 2-nonanone (fruity, sweet), was sniffed (compounds 6 and 7) (Table 5.4). A low intensity cheesy, sweaty, sour aroma was noted when a combination of the ketones, 2-hexanone (“feed”) and 2-nonanone (fruity, sweet), was sniffed (compounds 5 and 7) (Table 5.4).

The results from the olfactory assessment show that the aroma of the individual ketones is distinctly different to the aroma of mixtures of ketones. The combination of 2-nonanone with either 2-heptanone or 2-hexanone, gave a cheesy odour, whilst the combination of 2-hexanone and 2-heptanone did not give a cheesy aroma. The combination of 2-heptanone and 2-nonanone was responsible for the pungent cheese, sour milk-like aroma observed when the overall milk aroma was sniffed. This result seems consistent with the findings of both Vazquez-Landaverde *et al.* (2005) who reported that the odour activity values for 2-heptanone and 2-nonanone suggest that these compounds could

be very important contributors to the aroma of heated milk, and of Moio *et al.* who applied CharmAnalysis® to identify 2-heptanone and 2-nonanone as the two most intense flavour compounds likely to be the main odourants of UHT milk [3,12].

5.4 Conclusions

The headspace sampling technique developed in this study allows for the quantitative analysis of aroma compounds from long life packaged UHT milk (2% milk fat) by concentrating the compounds onto a MCT designed to fit a commercial GC desorber. The GCFC technique can recapture single compounds, sections, or the actual aroma profile (excluding unwanted compounds) of milk for off-line olfactory evaluation by a number of people participating in the same assessment session. The slow release of aroma allows for sufficient time to recall odour descriptors. Combinations of individual compounds can be recaptured to study potential synergistic effects. A mixture of 2-heptanone and 2-nonanone was found to be responsible for a pungent cheese, sour milk-like aroma – descriptors not observed for the single compounds. MCTs containing single components or fractions can be desorbed into a GC-MS for compound identification.

The described instrumentation allows comparison of olfactometric perception of a concentrated overall aroma against that of gas chromatographically separated single compounds, a feature not offered by traditional GCO. In this particular study, the contrast between descriptors of the

overall aroma and the single compounds in the low volatility aroma region could be reconciled by a trial-and-error search for a simple combination of single compounds that matched a descriptor for the whole aroma, not registered for any of the single peaks alone.

Note added in proof: It was only learnt after completion of the study that 2-heptanone and 2-nonanone are the ketones central to the characteristic blue cheese aroma of blue-mould ripened cheese, and that these two compounds are indeed used as additives to impart a cheese aroma [28 - 30].

5.5 Acknowledgements

Sasol for financial support, Mr Musa Lonwabo Kwetana for assistance in sample extractions, the olfactory panel: Dr Marleen van Aardt, Prof Elna Buys, Dr Henriette de Kock, Ms Marise Kinnear and Mr Alex Zabbia of the Department of Food Science, University of Pretoria, Mrs Margaux Lim Ah Tock and Dr Fanie van der Walt for the portable heating device.

5.6 References

- [1] G. Contarini, M. Povolo, R. Leardi, P.M. Toppino, *J. Agric. Food Chem.* 45 (1997) 3171.
- [2] H.E. Nursten, *Int J of Dairy Technol.* 50 (2) (1997) 48.
- [3] P.A. Vazquez-Landaverde, G. Velazquez, J.A. Torres, M.C. Qian, *J. Dairy Sci.* 88 (2005) 3764.
- [4] P.A. Vazquez-Landaverde, J.A. Torres, M.C. Qian, *J. Agric. Food Chem.* 54 (2006) 9184.
- [5] J.E. Friedrich, T.E. Acree, *Int. Dairy J.* 8 (3) (1998) 235.
- [6] J.G. Bendall, *J. Agric. Food Chem.* 49 (2001) 4825.
- [7] S.S. Mahajan, L. Goddik, M.C Qian, *J. Dairy Sci.* 87 (2004) 4057.

- [8] M. van Aardt, S.E. Duncan, J.E. Marcy, T.E. Long, S.F. O' Keefe, S.R. Nielsen-Sims, *J. Dairy Sci.* 88 (2005) 881.
- [9] S. M. van Ruth, *Biomol. Eng.* 17 (2001) 121.
- [10] S. Ampuero, J.O. Bosset, *Sensors and Actuators B* 94 (2003) 1.
- [11] Z. Zou, L. B. Buck, *Science* 311 (2006) 1477.
- [12] L. Moio, P. Etievant, D. Langlois, J. Dekimpe, F. Addeo, *J. Dairy Res.* 61 (1994) 385.
- [13] M. Fabre, V. Aubry, E. Guichard, *J. Agric. Food Chem.* 50 (2002) 1497.
- [14] A. Buettner, *Flavour Fragr. J.* 22 (2007) 465.
- [15] M. van Aardt, E.R. Rohwer, Y. Naudé, E.M. Buys, H.L. de Kock, in preparation for submission to *J. Dairy Sci.* 2008.
- [16] C. Bicchi, C. Cordero, C. Iori, P. Rubiolo, *J. High Resol. Chromatogr.* 23 (9) (2000) 539.
- [17] D.W. Lachenmeier, L. Kroener, F. Musshoff, B. Madea, *Rapid Commun. Mass Spectrom.* 17 (2003) 472.
- [18] C. Bicchi, C. Cordero, E. Liberto, P. Rubiolo, B. Sgorbini, *J. Chromatogr A* 1024 (2004) 217.
- [19] K. Ridgway, S.P.D. Lalljie, R.M. Smith, *J. Chromatogr A* 1124 (2006) 181.
- [20] K. Ridgway, S.P.D. Lalljie, R.M. Smith, *J. Chromatogr A* 1174 (2007) 20.
- [21] K. Schulz, J. Dreßler, E. Sohnius, D.W. Lachenmeier, *J. Chromatogr A* 1145 (2007) 204.
- [22] E.R. Rohwer, M.J. Lim Ah Tock, Y. Naudé, SA provisional patent application ZA 2006/07538, 2006.
- [23] E.K. Ortner, E.R. Rohwer, *J. High Resolut. Chromatogr.* 19 (1996) 339.
- [24] D. Sivakumar, Y. Naudé, E. Rohwer, L. Korsten, *Sci Food Agric.* 88 (2008) 1074.
- [25] M. Lim Ah Tock, E.R. Rohwer, Y. Naudé, Proceedings of the 5th Analitika 2006 Conference, KwaMaritane, Pilanesberg, South Africa, 2006, p.23.
- [26] Y. Naudé, M. van Aardt, E.R. Rohwer, Abstract book of the 32nd International symposium on capillary chromatography and 5th GCxGC symposium, Riva del Garda, Italy, 2008, p.432.
- [27] M. Rychlik, P. Schieberle, W. Gosch, Compilation of odor thresholds, odor qualities and retention indices of key food odorants, Deutsche Forschungsanstalt für Lebensmittelchemie and Institut für Lebensmittelchemie der Technischen Universität München, Garching, Germany, 1998.
- [28] S. Patton, *J. Dairy Sci.* 33 (1950) 680.
- [29] M. Qian, C. Nelson, S. Bloomer, *JAOCS.* 79 (2002) 663.
- [30] L. Moio, P. Piombino, F. Addeo, *J. Dairy Res.* 67 (2000) 273.

Chapter 6

The olfactometric analysis of milk volatiles with a novel gas chromatography based method – a case study in synergistic perception of aroma compounds

This chapter was published in Flavor, Fragrance, and Odor Analysis, Second Edition. The format reflects the style thereof.

Naudé, Y. and Rohwer, E.R., 2012. The olfactometric analysis of milk volatiles with a novel gas chromatography based method – a case study in synergistic perception of aroma compounds. In: Marsili, R. (Ed.), Flavor, Fragrance, and Odor Analysis, Second Edition. Taylor & Francis Group LLC, Boca Raton, Florida, pp. 93-110 (Chapter 5).

Author contributions

Conceived and designed the experiments: Yvette Naudé and Egmont Rohwer. Performed experimental work and data analysis, wrote the chapter, submitted chapter to the Editor, correspondence with publishers: Yvette Naudé. Initiator of research and study supervisor: Egmont Rohwer.

The work described in this chapter originally appeared in Journal of Chromatography A (thesis Chapter 5). Thereafter it was also published with additional information as a book chapter. Information given in thesis Chapter 6, and not appearing in thesis Chapter 5, includes multichannel sorption devices, heart-cutting fraction collection GC based methods, and a figure illustrating offline olfactometric evaluation.

The olfactometric analysis of milk volatiles with a novel gas chromatography based method – a case study in synergistic perception of aroma compounds

Yvette Naudé and Egmont R. Rohwer

University of Pretoria, Pretoria, South Africa

6.1 Introduction

Consumers consider the cooked, cabbage-like, sulfurous and stale notes imparted by the ultra high temperature (UHT) treatment of packaged long life milk undesirable. (Contarini et al. 1997; Nursten 1997; Perkins et al. 2005; Simon et al. 2001; Vazquez-Landaverde et al. 2005, 2006). Analytical methods that have been used to study the aroma of dairy products are gas chromatography mass spectrometry (GC-MS) and gas chromatography olfactometry (GCO) (Bendall 2001; d’Acampora Zellner et al. 2008; Friedrich et al. 1998; Mahajan et al. 2004; Moio et al. 1994, 1998; 2000; Qian et al. 2002; Van Aardt et al. 2005). GCO is traditionally used to identify individual odor active gas chromatographic fractions; a human record of aroma perception, in real time, of the GC effluent at the olfactometer outlet. The rapid elution of compounds is problematic in terms of recalling appropriate odor descriptors. GCO requires utmost concentration and can cause nose fatigue. Typically one to two trained evaluators perform the sniffing. However, a group of evaluators is required for reliable GCO analysis necessitating numerous analyses and multiple gas chromatographs equipped with sniff ports (Van Ruth 2001).

Instrumental analyses are not always performed on the aroma relevant compounds but also on non odorous compounds that may include hazardous chemicals (Ampuero et al. 2003). Co-elution of compounds is a common occurrence in separating complex mixtures, thus the evaluator may not realize that composite peaks, instead of pure compounds, are sniffed. Potential synergistic effects cannot be observed where single compounds are evaluated over time. Many synergistic effects are known to occur between single compounds in complex food matrices (Herrmann et al. 2010). Combinations of single substances can produce enhancing or masking interactive effects. Perceived synergistic sensory effects can arise, not only from a blend of similar volatiles, but also, from a blend of chemically unrelated compounds; for example the sensory threshold for vanillin is lower in the presence of oak lactones (Perez-Coello et al. 1997). Interestingly, the end result of combining single substances in complex food matrices may be the emergence of a strikingly different sensory perception, completely unrelated to that of the individual compounds alone. Herrmann et al. (2010) evaluated the aging of beer and reported a change in the sensory perception of components when in combination. Here, (E)-2-nonenal was described by tasters as cardboard-like when the single substance was evaluated, whilst (E)-2-(Z)-6-nonadienal was described as cucumber-like. However, the combined effect of the two compounds produced a sweet fruity flavor sensory perception distinctly different from the single substances alone. This new sensory perception appears related to both the absolute and relative concentrations of the two compounds. Since the generation of new odors by addition of individual compounds is not yet fully understood it is hard to determine how individual compounds of a product relate

to the perception of its overall aroma when using traditional instrumental techniques (Ampuero et al. 2003).

Addressing the limitation of evaluating single compounds as opposed to mixtures, a heart-cut gas chromatographic fraction collection (GCFC) technique was developed to study, off-line, synergistic perceptions of aroma compounds. The target compounds selected for technique evaluation in this study are important thermally derived off-flavor compounds present in UHT milk. Powerful odor active volatiles detected in heated milk include 2-heptanone, 2-nonanone and nonanal, with 2-heptanone and 2-nonanone identified as the most intense volatile flavor compounds of UHT milk (Moio et al. 1994). Higher concentrations were found of, amongst others, the sulfur compound dimethyl sulfide, the ketones: 2-hexanone, 2-heptanone, 2-nonanone and the aldehydes: 2-methylpropanal, 3-methylbutanal and decanal in UHT milk when compared to concentrations measured in raw and pasteurized milk (Vazquez-Landaverde et al. 2005). Calculated odor activity values (OAV) for dimethyl sulfide, 2,3-butanedione, 2-heptanone, 2-nonanone, 2-methylpropanal, 3-methylbutanal, nonanal and decanal show that these compounds may well be important contributors to the off-flavor of UHT milk (Vazquez-Landaverde et al. 2005). The formation of 2,3-butanedione is, however, not only heat-induced but can also point to microbial activity in milk (Vazquez-Landaverde et al., 2005).

The sorptive extraction of aroma compounds using multi-channel silicone (PDMS) rubber traps (MCTs) for quantitative gas chromatographic analysis; fractionation and collection of aroma compounds from the total chromatogram

for multidimensional gas chromatography (MDGC) and off-line olfactory evaluation of synergistic effects are reported.

6.2 Sorptive extraction

6.2.1 Commercial sample enrichment techniques

Solvent-free approaches to the isolation of volatile components from food matrices include head space solid phase microextraction (HS-SPME), stir bar sorptive extraction (SBSE), headspace solid-phase dynamic extraction (HS-SPDE), headspace trap technology and solid phase extraction-thermal desorption (SPE-tD) (Bicchi et al. 2000; Bicchi et al. 2004; Buettner 2007; Contarini et al. 1997, 2002; Fabre et al. 2002; Markes International 2010a, b; Marsili 1999, 2000; Perkins et al. 2005; Qian et al. 2002; Ridgway et al. 2006; Ridgway et al. 2007; Schulz et al. 2007; Van Aardt et al. 2005; Vazquez-Landaverde et al. 2005, 2006). Headspace sampling provides solvent-free aroma extracts that may be more representative of food aroma when compared to those obtained by solvent extraction (Qian et al. 2002). Commercial sorptive extraction techniques, such as SPME, SBSE, SPDE and headspace trap technology, offer efficient concentration and can be used for sampling the headspace (Bicchi et al. 2000, 2004; Marsili 1999, 2000; Perkins et al. 2005; Ridgway et al. 2006, 2007; Schulz et al. 2007; Tienpont et al. 2000). SPME, pioneered by Janusz Pawliszyn and his group, is a fiber coated with a small sorbent volume of 0.6 – 0.9 μl (Bicchi et al. 2000, 2004; Schulz et al. 2007; Zhang and Pawliszyn 1993); SBSE, introduced by Pat Sandra and his team, is

a glass encapsulated magnetic stir bar coated with volumes of 25 – 200 μl polydimethylsiloxane (PDMS) (Baltussen et al. 1999; Bicchi et al. 2004); SPDE is a sorptive coating with a sorbent volume of 6 μl on the inside wall of a stainless steel needle of a gas tight syringe (Bicchi et al. 2004; Ridgway et al. 2006, 2007; Schulz et al. 2007); while headspace trap technology makes use of a headspace sampler and a built-in trap (Schulz et al. 2007). The built-in trap is a tube filled with a solid sorbent with a volume of 160 μl (Schulz et al. 2007). A SPE-tD cartridge is a titanium tube coated with PDMS on both the inside (1 μm) and the outside (500 μm) of the tube. Two lengths are available with a total exposed PDMS volume of 29.5 μl for the 6 mm length and 147 μl for the 30 mm length respectively.

6.2.2 *Novel multi-channel sample enrichment devices*

Multi-channel configuration devices designed for air pollution studies have been utilised by Lane et al. (1988) who coated a collection of glass tubes on the inside and on the outside with stationary phase, and by Kriegler and Hites (1992) who used a bundle of fused silica tubes cut from a single DB-1 capillary GC column. Practical limitations were complicated instrumental arrangements and high pressure drops due to the longer length of the traps (25 – 60 cm). Ortner and Rohwer (1996) constructed relatively shorter length (10.5 – 12.5 cm) thick film silicone rubber traps in a novel multi-channel configuration to concentrate semi-volatile organic air pollutants. The traps were desorbed in an inlet similar to a programmable temperature vaporization (PTV) injector. McGee and Purzycki (2002) designed the Zenith trap, a bundle of capillary GC

tubes, each coated on the inside with polymers of different polarity. The size of the bundle was made to fit into a thermal desorber. The authors collected the scent of a blue hyacinth flower on the Zenith trap.

6.2.2.1 *Multi-channel silicone (PDMS) rubber traps*

The headspace traps used for the isolation of aroma volatile compounds from UHT milk are multi-channel open tubular silicone rubber traps (MCTs) prepared in-house (Naudé et al. 2009; Ortner and Rohwer 1996; Rohwer et al. 2006; Sivakumar et al. 2008). MCTs containing 0.4 ± 0.02 g silicone were prepared based on a technique described by Ortner and Rohwer (1996). The MCT was designed to fit a commercial thermal desorber system (TDS) available from Gerstel™. A bundle of twenty two channels of silicone elastomer medical grade tubing (0.64 mm OD x 0.3 mm ID, Sil-Tec, Technical Products, Georgia, USA) are inserted into 17.8 cm long glass desorption tubes (4 mm ID, 6 mm OD) (Fig. 6.1). The MCT inside the desorption tube is 55 mm long (Fig. 6.1). The ends of the glass desorption tube are capped with glass stoppers. The glass stoppers are held in place by Teflon® tubing. The MCT with its trapped analytes is not exposed to the Teflon® tubing, thereby preventing potential adsorption of analytes onto the Teflon®. Compared to commercial sorption devices the MCT provides a larger sample enrichment capacity of 600 μ l PDMS. MCTs are not limited to desorption tubes from a single manufacturer, they are constructed to fit into any of the commercial thermal desorption tubes available. Shorter length MCTs are also made to suit specific applications. In contrast to multi-channel traps consisting of a bundle of GC capillary columns

which contain nonsorptive outer coatings, both the inside and the outside of the multi-channel PDMS trap provide sorptive surfaces. Further advantages of the MCT over commercial sorption devices are its open tubular structure and low pressure drop associated with multi-channel flow (Ortner and Rohwer 1996). These characteristics are not only particularly suited to the recapturing of chromatographic fractions - single aroma compounds and their combinations from the GC effluent during a GC run - but also for the off-line release of the heart-cut aroma compounds from the MCTs for olfactometric evaluation. Isolating headspace aroma compounds from beverages onto MCTs and GC fraction collection (heart-cutting) onto MCTs for off-line olfactometry were successfully applied to the aroma studies of beer (Lim Ah Tock et al. 2009) and of novel mocha-styled pinotage wines (Naudé and Rohwer 2010b). Aroma analytes are concentrated from matrices onto MCTs by either a purge-and-trap method, for example when sampling beverages (Lim Ah Tock et al. 2009; Naudé et al. 2009; Naudé and Rohwer 2010b; Potgieter 2006) or liquidized fruit (Sivakumar et al. 2008), or by dynamic head-space sampling using an air sampling pump when sampling live plants. Neat compounds, either single or their combinations, are conveniently trapped onto a MCT by simply drawing with a syringe a volume of their head space through a MCT. After sample enrichment the aroma is released from the MCTs for off-line olfactometric evaluation. In addition, MCTs containing aroma analytes are thermally desorbed into a gas chromatograph with flame ionization detection (GC-FID) or GC-MS.

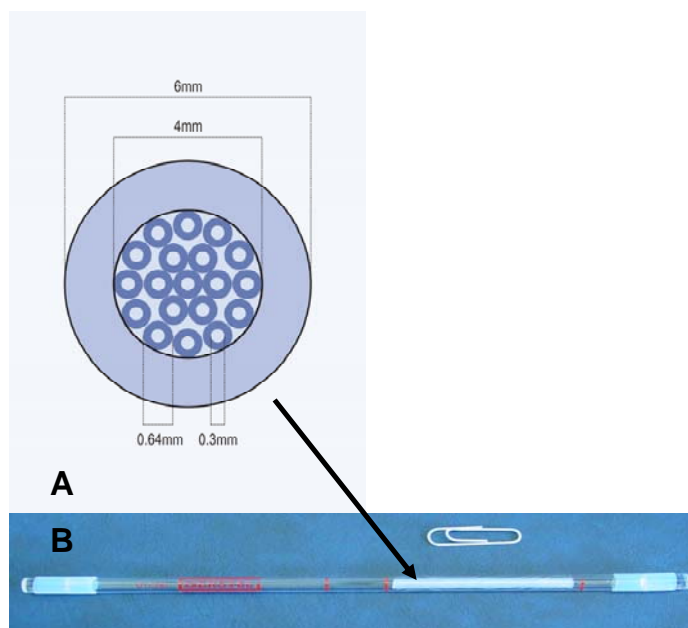


Figure 6.1. Multichannel silicone (PDMS) rubber trap (MCT). (A) Cross-section of an MCT. (B) Twenty two silicone elastomer (PDMS) tubes (sorption volume of 600 μ l) are arranged in parallel inside of a commercial glass thermal desorption tube. The ends of the thermal desorption tube containing the MCT are capped with glass stoppers during storage. Teflon® tubing keep the glass stoppers in position, samples are not in contact with the Teflon®. Reprinted from *Journal of Chromatography A*, 1216, Naudé, Y., Van Aardt, M., Rohwer, E.R., Multi-channel open tubular traps for headspace sampling, gas chromatographic fraction collection and olfactory assessment of milk volatiles, page 2799, Copyright (2009), with permission from Elsevier.

6.3 High capacity headspace sorptive extraction of aroma compounds from milk followed by TDS-CIS-GC-FID

Sample enrichment. A purge-and-trap sampling method developed in-house was used to extract the aroma compounds from packaged long life UHT milk (2% milk fat) by trapping it on a MCT (Naudé et al. 2009). The volatiles were isolated from 200 ml milk inside a 500 ml flat bottomed glass flask. The flask was immersed for 35 min in a water bath (40 °C) and the sample was purged

with 500 ml nitrogen gas at 25 ml/min. The purged volatiles were collected on a MCT at 45 °C to prevent the condensation of water from the sample onto the MCT.

Chemical standards. A standard stock solution was prepared in methanol (Saarchem UniVAR, Merck Chemicals (Pty) Ltd., Kempton Park, South Africa) containing 1) dimethyl sulfide; 2) 2-methylpropanal; 3) 2,3-butanedione; 4) 3-methylbutanal; 5) 2-hexanone; 6) 2-heptanone; 7) 2-nonanone; 8) nonanal and 9) decanal to give a concentration of 1 µg/µl. Standard stock solution was added to 200 ml portions of chilled long life packaged UHT milk (2% milk fat) to give spiking levels of 0.4, 0.8, 4, 8, 16, 40, 70, 85 µg/200 ml milk. The spiked milk portions were thoroughly mixed on a vortex mixer and returned to the refrigerator to equilibrate for 20 min. After the equilibration period the spiked samples were extracted as described previously (sample enrichment).

Instrumentation. The volatiles were thermally desorbed from the MCT using a thermal desorber system (TDS) from Gerstel™ installed on an Agilent 6890 GC-FID (Chemetrix, Midrand, South Africa) (Naudé et al. 2009). Splitless desorption was from 30 °C (3 min) at 60 °C/min to 210 °C (10 min). The desorption flow rate was 50 ml/min (hydrogen gas, Afrox, Gauteng, South Africa) at 47 kPa. The TDS transfer line temperature was 250 °C. The volatiles were cryogenically focused using liquid nitrogen at -100 °C on a cooled injection system (CIS). The CIS liner contained silicone rubber to improve retention of the extremely volatile dimethyl sulfide. After desorption of the analytes from the MCT, the CIS was heated to 200 °C at 5 °C/s and the volatiles were analysed by GC-FID. The GC oven temperature programme was -50 °C (3 min) at 10 °C/min to 120 °C (10 min), 10 °C/min to 220°C. Hydrogen carrier

gas velocity was 33 cm/s (2.3 ml/min) and the column head pressure was 23 kPa in the constant pressure mode. The GC inlet was in the solvent vent mode (to achieve a high desorption flow rate for trapping onto the CIS) whilst the purge valve remained closed to give a “splitless” type injection from the CIS. The GC column was a Zebron ZB-1 30 m x 320 µm ID x 1 µm film thickness (Phenomenex, Separations, Randburg, South Africa).

6.4 Novel heart-cutting fraction collection GC based methods

A fraction collection, heart-cutting, enrichment and two-dimensional GC approach to aroma evaluation of essential oils was described by Sandra et al. (1980). Here, the column effluent was split using an all glass device. For aroma evaluation one splitter arm led to an FID and the second splitter arm led to the nose. For off-line heart-cutting the split effluent was collected on a glass capillary micro-trap coated with OV-101. Co-elution of two or more compounds frequently occurs when separating complex mixtures (Naudé and Rohwer 2010b; Sandra et al. 1980). Using longer GC columns or a different stationary phase is not always ideal (Sandra et al. 1980). Although sophisticated GCxGC offers superior resolving power (Naudé and Rohwer 2010b) similar results may be obtained using one-dimensional GC and GC-MS: a heart-cut of a composite peak from one stationary phase is captured followed by off-line rechromatographing the composite heart-cut on a different GC stationary phase (Naudé and Rohwer 2010a, b; Sandra et al. 1980). Sandra et al.'s (1980) excellent paper describes re-injection on a different stationary phase by either flushing analytes from the micro-trap with solvent or by connecting the micro-

trap between the GC inlet and column followed by heating of the GC oven. Commercial development in GC sample introduction systems dictated a strategy of conveniently desorbing the MCT in a thermal desorber. A novel multidimensional GC (MDGC) approach is followed where MCTs containing selectively trapped compounds are redesorbed for compound identification by off-line second dimension separation by GC-MS (Naudé et al. 2009) or by the complimentary technique of GCxGC-TOFMS (Naudé and Rohwer 2010a, b). Recapturing of odor active compounds from the GC effluent onto secondary MCTs for analysis by GC-MS is especially useful when dealing with compounds of unknown identity (Naudé et al. 2009; Naudé and Rohwer 2010b) (Fig. 6.2). The multidimensional GCFC and off-line olfactometric technique is particularly suited to a directed search approach when confronted with complex aroma chromatograms: heart-cuts of composite peaks obtained from a first dimension apolar separation can be re-injected for a second dimension polar separation followed yet again by the selective heart-cutting of single peaks or their combinations for off-line olfactometric evaluation.

6.4.1 Capturing of single compounds and their combinations by off-line heart-cut gas chromatography fraction collection (GCFC)

A chromatographic profile of the packaged long life UHT milk is first obtained using the conditions described previously. Integration results of peak start time and peak end time of the chromatogram of the UHT milk are then used to establish the heart-cutting event times. In a subsequent run, various sections of the GC-effluent are selectively recaptured onto secondary MCTs on

a carefully timed basis (Fig. 6.2). Manual collection of heart-cut peaks from the complex/total chromatogram commences, as a rule of thumb, 30 s before peak elution and ends 10 s after elution. For GCFC the instrumental conditions were as previously described, the only difference now was the modification of the detector parameters. The electrometer is switched off. The detector top assembly and the collector are easily removed by loosening the knurled brass nut of the detector assembly and by lifting the collector out. Single peaks and their combinations are collected at the end of the GC column by simply placing a secondary MCT on the inactivated FID flame tip and by supporting the MCT in this position by hand (Fig. 6.2). Complex instrumental set-ups, sophisticated equipment or valves are not required. The MCT was placed on the flame tip prior to peak elution and removed once the peak had eluted. To collect single peaks nine MCTs were exchanged one after the other so that each MCT contained a single compound. For combinations of compounds, two peaks were collected on a single MCT. During collection the FID and flame gases (hydrogen and air) were switched off, the make-up gas (helium) plus carrier gas (hydrogen) flow totalled 50 ml/min and the detector temperature was at 300 °C. The low pressure drop of the open tubular channels of the MCT allows most of the effluent of the FID to pass through the trap without special sealing arrangement that would otherwise complicate the GCFC procedure. The advantage of a low pressure drop is not offered by conventional packed traps. After single compounds or their combinations were selectively recaptured the MCTs were capped with custom-made glass and Teflon® stoppers (Fig. 6.1) and stored for olfactory evaluation or for GC-MS identification.

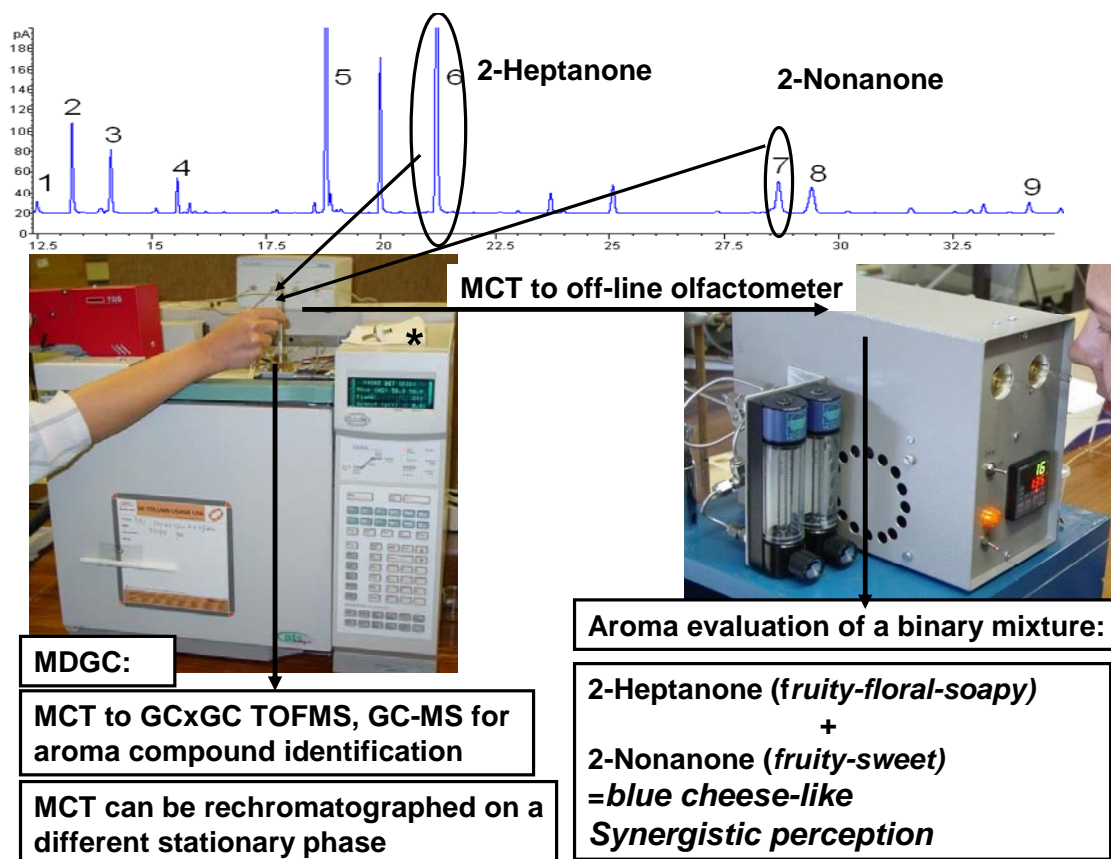


Figure 6.2. Fraction collection and off-line evaluation of synergistic perceptions of aroma compounds. (1) Dimethyl Sulfide, (2) 2-Methylpropanal, (3) 2, 3-Butanedione, (4) 3-Methylbutanal, (5) 2-Hexanone, (6) 2-Heptanone, (7) 2-Nonanone, (8) Nonanal, (9) Decanal. (*) Collector removed from FID. FID conditions: detector 300 °C, make-up gas (He) 50 ml/min, detector gases off. The MCT is simply placed on top of the FID flame tip and held in position during peak elution. The MCT is removed from the flame tip at the end of peak elution. Peaks 6 and 7 were both selectively captured on the same MCT. The combined aroma (6+7) mixture was released from the MCT at 160 °C with a flow of N₂ gas (20 ml/min). The synergistic perception of the combined aroma (6+7) mixture was evaluated by off-line olfactometry. The portable olfactometric device consists of two sniff ports for a blank and a sample, gas flow control and temperature programming. MDGC: MCTs containing fractions can be rechromatographed on a different stationary phase and by GC-MS for compound identification. Chromatogram reprinted from *Journal of Chromatography A*, 1216, Naudé, Y., Van Aardt, M., Rohwer, E.R., Multi-channel open tubular traps for headspace sampling, gas chromatographic fraction collection and olfactory assessment of milk volatiles, page 2802, Copyright (2009), with permission from Elsevier.

6.5 Off-line olfactory evaluation of single compounds and their combinations

Nine odor active compounds (sulfide, aldehydes and ketones) were selected for evaluation and comparison to the aroma of the overall milk profile. The aroma was released in a controlled manner by heating the secondary MCT containing the recaptured component/s from the GC-effluent in a portable heating device with a flow of nitrogen gas at a flow rate of 20 ml/min (Fig. 6.2). The portable olfactometric device was designed and built in-house. The MCTs were inserted in the cavity in the portable heating device (Fig. 6.2). The compounds were released from the secondary MCTs at GC column elution temperature for the olfactory assessment of the single compounds (Table 6.1). As the aroma eluted from the MCT it was sniffed by a team consisting of six experienced non smoking evaluators (five female, one male). All six of the evaluators participated as a group during the same assessment session. For the evaluation of combinations of single compounds the combined fractions were released at 130 °C or at 160 °C and the aroma was evaluated by a panel of three persons. A second device since built contained two sniff ports so that a blank MCT can be sniffed next to an MCT containing the trapped aroma compounds (Naudé and Rohwer 2010b).

6.5.1 Slow release of the aroma of single compounds captured by GCFC on individual secondary MCTs

Results of the olfactory assessment of the individual compounds captured from UHT milk (spike levels of 195 – 245 ug/l) are given in Table 6.1. The aroma descriptors reported by the evaluators for each of the individual compounds generally matched the descriptors reported in the literature (Nursten 1997; Friedrich and Acree 1998; Rychlik et al. 1998). A fairly neutral background was described for the recaptured single compounds collected from the chromatogram of the unspiked UHT milk (Table 6.1).

6.5.2 Slow release of the total milk aroma profile captured by purge-and-trap on primary MCTs

The aroma from primary MCTs containing the total milk profile extracted by purge-and-trap was also released for comparison to that of the single compounds and their combinations captured by GCFC (Table 6.1). The MCT in the olfactometric device was heated from ambient to 185 °C at 2 °C/min. A fairly neutral background was described for the overall milk profile isolated by purge-and-trap from the unspiked (1 - 44 µg/l) UHT milk (Table 6.1). However, when the overall aroma from the spiked UHT milk (195 - 245 µg/l) isolated on a primary MCT by purge-and-trap was released, the aroma matched the descriptors for the single compounds up to and including 2-hexanone (heart-cut 5). Thereafter, the aroma observed deviated markedly from the descriptors for the single compounds. Instead of observing the expected aroma of “soapy” (2-

heptanone (heart-cut 6)) and “fruity” (2-nonanone (heart-cut 7)), a pungent, sour milk-like, sweaty aroma was noted. This unpleasant aroma was absent when the single compounds recaptured during GCFC were sniffed, and it was absent when the overall aroma profile isolated from the unspiked milk on a MCT was sniffed (Table 6.1). This unexpected and entirely new aroma isolated from the spiked milk on a MCT suggested possible synergistic effects between the compounds.

Table 6.1

Olfactory assessment of single compounds captured by GCFC on individual secondary MCTs¹, the overall milk aroma collected on a primary MCT² and binary combinations of compounds captured by GCFC onto secondary MCTs³

1. Single compounds captured by GCFC onto secondary MCTs			
Single compounds GCFC	Aroma release temperature °C	¹ Aroma description for single compounds (n=6)	
		Spiked UHT milk 195 – 245 µg/l	Unspiked UHT milk 1 – 44 µg/l
1. Dimethyl Sulphide	21	Sulphurous, rotten egg +++	-
2. 2-Methylpropanal	50	Malty, chemical sweet +++	-
3. 2,3-Butanedione	60	Butter +++	-
4. 3-Methylbutanal	73	Malty, chemical sweet +++	Chemical sweet +
5. 2-Hexanone	103	Feed, hay, field, veld grass ++	-
6. 2-Heptanone	128	Fragrant soap, fruity, floral ++	Fragrant soap +
7. 2-Nonanone	178	Fruity, sweet +++	Fruity, sweet ++
8. Nonanal	185	Biscuit, cotton candy, caramel ++	-
9. Decanal	194	Dusty, musty, rubber ++	Dusty, rubber +

2. Whole milk aroma profile captured by purge-and-trap sampling onto a primary MCT (non-fractionated aroma profile)			
	Aroma release temperature °C	² Aroma description for the overall milk aroma (n=3)	
		Spiked UHT milk 195 – 245 µg/l	Unspiked UHT milk 1 – 44 µg/l
	24 – 40	Rotten egg +, butter +++, sweet +, malty +++	-
	60 – 120	Malty+, feed, pungent, sour milk, sweaty+++	Chemical sweet +
	120 – 185	Sour milk, burnt milk ++	Fragrant soap, floral +

3. Combinations of compounds captured by GCFC onto secondary MCTs		
Binary mixtures	Aroma release temperature °C	³ Aroma description for combinations of compound (n=3)
		Spiked UHT milk 195 – 245 µg/l
4. 3-Methylbutanal 5. 2-Hexanone	130	Malty+++, sweet+
5. 2-Hexanone 6. 2-Heptanone	160	Milky-sweet, condensed milk ++
6. 2-Heptanone 7. 2-Nonanone	160	Feta cheese, blue cheese, sweaty, sour, fatty +++
5. 2-Hexanone 7. 2-Nonanone	160	Cheesy, sweaty, sour +

+ Intensity indicator. ¹Olfactory evaluation of packaged long life UHT milk (2% milk fat): spiked and unspiked. For each sample nine secondary MCTs each containing heart-cuts of single compounds were individually desorbed in the portable sniffing device at specific temperatures with a flow of nitrogen gas of 20 ml/min. ²Olfactory evaluation of the purge-and-trap extracted overall milk aroma (primary MCT, no GCFC) of long life packaged UHT milk (2% milk fat): spiked and unspiked. The MCTs were desorbed in the portable sniffing device from 24 °C to 185 °C over a period of 60 minutes with a flow of nitrogen gas of 20 ml/min. ³Olfactory evaluation of long life packaged UHT milk (2% milk fat): spiked. For each milk sample four secondary MCTs each containing heart-cuts of binary mixtures of compounds were individually desorbed in the portable sniffing device with a flow of nitrogen gas of 20 ml/min. Reprinted from *Journal of Chromatography A*, 1216, Naudé, Y., Van Aardt, M., Rohwer, E.R., Multi-channel open tubular traps for headspace sampling, gas chromatographic fraction collection and olfactory assessment of milk volatiles, page 2803, Copyright (2009), with permission from Elsevier.

6.5.3 *Slow release of heart-cuts of combinations of single compounds captured by GCFC on individual secondary MCTs*

Combinations of the single volatiles were selectively collected onto secondary MCTs during GCFC (Fig. 6.2) to determine which compounds were responsible for the change in aroma perception from the expected fruity, soapy and sweet aroma into the unexpected and wholly new aroma described as pungent, sour milk-like and sweaty (Table 6.1). For each of the binary sets the combinations were collected on a single MCT (four MCTs, each contained a heart-cut binary set). For example, heart-cuts 4 + 5 (3-methylbutanal + 2-hexanone) were both collected on a single MCT. The MCT was simply placed on the burner jet tip of the inactive FID just prior to the elution of 3-methylbutanal. The MCT was removed from the flame tip once the peak eluted. The same MCT containing 3-methylbutanal was once again placed on the flame tip just prior to the elution of 2-hexanone. The MCT was removed from the flame tip once the peak eluted. The MCT containing the two heart-cuts was capped for storage. The portable sniff device was set to a specific temperature, the MCT containing both compounds was inserted and the combined aroma was released with a flow of nitrogen. A malty aroma dominated when a combination of the aldehyde 3-methylbutanal (malty, sweet), and the ketone 2-hexanone (“feed”) was sniffed (heart-cuts 4 + 5) (Table 6.1). A milky-sweet, condensed milk aroma was described for the combination of the ketones, 2-Hexanone (“feed”) and 2-Heptanone (soapy, fruity, floral) (heart-cuts 5 + 6). A pungent, feta cheese, blue cheese, sweaty, sour, fatty aroma was observed when a combination of the ketones, 2-heptanone (soapy, fruity, floral) and 2-

nonanone (fruity, sweet), was sniffed (heart-cuts 6 + 7) (Table 6.1). A low intensity cheesy, sweaty, sour aroma was noted when a combination of the ketones, 2-hexanone (“feed”) and 2-nonanone (fruity, sweet), was sniffed (heart-cuts 5 + 7) (Table 6.1).

The results from the olfactory assessment show that the aroma of the individual ketones is distinctly different to the aroma of mixtures of ketones. The combination of 2-nonanone with either 2-heptanone or 2-hexanone, gave a cheesy odor, whilst the combination of 2-hexanone and 2-heptanone did not give a cheesy aroma. The combination of 2-heptanone and 2-nonanone was responsible for the pungent, sweaty and sour milk-like note observed when the overall milk aroma captured by purge-and-trap was sniffed. A strong blue cheese-like note was detected for a combination of 2-heptanone and 2-nonanone selectively captured from the total chromatogram by GCFC. These results seem consistent with the impact that 2-heptanone and 2-nonanone has on the aroma of UHT milk and of blue-veined cheese. Moio et al. (1994) applied CharmAnalysis® to identify 2-heptanone and 2-nonanone as the two most intense flavor compounds likely to be the main odorants of UHT milk. Vazquez-Landaverde et al. (2005) reported that the odor activity values for 2-heptanone and 2-nonanone suggest that these compounds could be very important contributors to the aroma of heated milk. Moio et al. (2000) concluded that 2-heptanone and 2-nonanone impart a strong Gorgonzola (Italian blue-veined cheese) cheese note in their study of odor-impact compounds of Gorgonzola cheese. Patton (1950) and Qian et al. (2002) reported that compounds central to the Blue cheese aroma include 2-heptanone

and 2-nonanone, and McGorin (2002) stated that 2-heptanone and 2-nonanone are reportedly the dominant character compounds of Blue cheese flavor.

6.6 Summary

Synergistic sensory effects are known to emerge between single compounds in complex food matrices. To address the limitations of traditional GCO where single compounds are evaluated over time - not providing information on their behavior in mixtures - a heart-cut gas chromatography fraction collection (GCFC) technique was developed to study, off-line, the synergistic perceptions of aroma compounds. Single compounds and their combinations are selectively recaptured from the GC effluent onto a multi-channel configuration of silicone (PDMS) rubber (MCT) without the need for complicated instrumental arrangements. A benefit of the MCT is its low pressure drop not offered by conventional packed traps. The aroma heart-cuts are released off-line in a controlled manner by heating the MCT in a portable device. An advantage of uncoupling the time scale is that the olfactory assessment can be terminated and resumed at convenience when the evaluators indicate nose fatigue. Olfactory results suggest that a synergistic combination of 2-heptanone and 2-nonanone was responsible for a pungent cheese, sour milk-like aroma detected in UHT milk.

6.7 Acknowledgements

Dr Fanie van der Walt for constructing the olfactory device, the olfactory panel: Dr Marleen van Aardt, Prof Elna Buys, Dr Henriette de Kock, Ms Marise Kinnear and Mr Alex Zabbia of the Department of Food Science, University of Pretoria, Pretoria, South Africa, Sasol Fuels and the South African National Research Foundation (NRF) for funding.

6.8 References

Ampuero, S., Bosset, J.O. 2003. The electronic nose applied to dairy products: a review. *Sensors and Actuators B* 94:1-12.

Baltussen, E., Sandra, P., David, F., Cramers, C. 1999. Stir bar sorptive extraction (SBSE), a novel extraction technique for aqueous samples: Theory and principles. *Journal of Microcolumn Separations* 11: 737-747.

Bendall, J.G. 2001. Aroma compounds of fresh milk from New Zealand cows fed different diets. *Journal of Agricultural and Food Chemistry* 49: 4825-4832.

Bicchi, C., Cordero, C., Iori, C., Rubiolo, P., Sandra, P. 2000. Headspace sorptive extraction (HSSE) in the headspace analysis of aromatic and medicinal plants. *Journal of High Resolution Chromatography* 23 (9): 539-546.

Bicchi, C., Cordero, C., Liberto, E., Rubiolo, P., Sgorbini, B. 2004. Automated headspace solid-phase dynamic extraction to analyse the volatile fraction of food matrices. *Journal of Chromatography A* 1024: 217-226.

Buettner, A. 2007. A selective and sensitive approach to characterize odour-active and volatile constituents in small-scale human milk samples. *Flavour and Fragrance Journal* 22: 465-473.

Contarini, G., Povola, M. 2002. Volatile fraction of milk: Comparison between purge and trap and solid phase microextraction techniques. *Journal of Agricultural and Food Chemistry* 50: 7350-7355.

Contarini, G., Povolo, M., Leardi, R., Toppino, P.M. 1997. Influence of heat treatment on the volatile compounds of milk. *Journal of Agricultural and Food Chemistry* 45: 3171-3177.

D'Acampora Zellner, B., Dugo, P., Dugo, G., Mondello, L. 2008. Gas chromatography-olfactometry in food flavour analysis. *Journal of Chromatography A* 1186: 123-143.

Fabre, M., Aubry, V., Guichard, E. 2002. Comparison of different methods: Static and dynamic headspace and solid-phase microextraction for the measurement of interactions between milk proteins and flavor compounds with an application to emulsions. *Journal of Agricultural and Food Chemistry* 50: 1497-1501.

Friedrich, J.E., Acree, T.E. 1998. Gas chromatography olfactometry (GC/O) of dairy products. *International Dairy Journal* 8(3): 235-241.

Herrmann, M., Klotzbücher, B., Wurzbücher, M., et al. 2010. A new validation of relevant substances for the evaluation of beer aging depending on the employed boiling system. *Journal of the Institute of Brewing* 116(1):41-48.

Kriegler, M.S. and Hites, R.A. 1992. Diffusion denuder for the collection of semivolatile organic compounds. *Environmental Science and Technology* 26:1551-1555.

Lane, D.A., Johnson, N.D., Barton, S.C., Thomas, G.H.S., Schroeder, W.H. 1988. Development and evaluation of a novel gas and particle sampler for semivolatile chlorinated organic compounds in ambient air. *Environmental Science and Technology* 22(8):941-947.

Lim Ah Tock, M.J. 2009. Aroma analysis of alcoholic beverages using multi-channel silicone rubber traps, M.Tech. dissertation, Tshwane University of Technology, Pretoria, South Africa.

Mahajan, S.S., Goddik, L., Qian, M.C. 2004. Aroma compounds in sweet whey powder. *Journal of Dairy Science* 87: 4057-4063.

Markes International Thermal Desorption Technical Support Note 88. 2010a. Enhancing olfactory profiling of fruit juices and wine using complementary analytical thermal desorption techniques.

Markes International Thermal Desorption Technical Support Note 94. 2010b. Using Markes' thermal desorption technology to automate high/low analysis of complex beer sample.

Marsili, R. T. 1999. SPME-MS-MVA as an electronic nose for the study of off-flavors in milk. *Journal of Agricultural and Food Chemistry* 47: 648-654.

Marsili, R. T. 2000. Shelf-life prediction of processed milk by solid-phase microextraction, mass spectrometry, and multivariate analysis. *Journal of Agricultural and Food Chemistry* 48: 3470-3475.

McGee, T. and Purzycki, K.L. 2002. Headspace techniques for the reconstitution of flower scents and identification of new aroma chemicals, in:

Flavor, Fragrance and Odor Analysis, ed. R. Marsili, 249-276. Marcel Dekker, Inc., New York, NY.

McGorin, R.J. 2002. Character impact compounds: flavors and off-flavors in foods, in: *Flavor, Fragrance and Odor Analysis*, ed. R. Marsili, 375-413. Marcel Dekker, Inc., New York, NY.

Moio, L., Etievant, P., Langlois, D., Dekimpe, J., Addeo, F. 1994. Detection of powerful odorants in heated milk by use of extract dilution sniffing analysis. *Journal of Dairy Research* 61: 385-395.

Moio, L., Addeo, F. 1998. Grana Padano cheese aroma. *Journal of Dairy Research* 65: 317-333.

Moio, L., Piombino, P., Addeo, F. 2000. Odour impact compounds of Gorgonzola cheese. *Journal of Dairy Research* 67: 273-285.

Naudé, Y., Rohwer, E.R. 2010a. New multidimensional chromatographic methods for enantiomeric analysis of *o,p'*-DDT and associated environmental pollutants, presented at the 34th International Symposium on Capillary Chromatography, Riva del Garda, Italy, May 30 – June 4, 2010.

Naudé, Y., Rohwer, E.R. 2010b. The analysis of pinotage wine aromas by a novel fractionating olfactometric method combined with comprehensive two dimensional gas chromatography – mass spectrometry, presented at the 15th World Congress of Food Science and Technology, Cape Town, South Africa, Aug. 22-26, 2010.

Naudé, Y., Van Aardt, M., Rohwer, E.R. 2009. Multi-channel open tubular traps for headspace sampling, gas chromatographic fraction collection and olfactory assessment of milk volatiles. *Journal of Chromatography A* 1216: 2798–2804.

Nursten, H.E. 1997. The flavour of milk and dairy products: I. Milk of different kinds, milk powder, butter and cream. *International Journal of Dairy Technology* 50 (2): 48-56.

Ortner, E.K., Rohwer, E.R. 1996. Trace analysis of semi-volatile organic air pollutants using thick film silicone rubber traps with capillary gas chromatography. *Journal of High Resolution Chromatography* 19: 339-344.

Patton, S. 1950. The methyl ketones of Blue Cheese and their relation to its flavor. *Journal of Dairy Science* 33(9): 680-684.

Perkins, M.L., D'Arcy, B.R., Lisle, A.T., Deeth, H.C. 2005. Solid phase microextraction of stale flavour volatiles from the headspace of UHT milk. *Journal of the Science of Food and Agriculture* 85:2421-2428.

Perez-Coello, M.S., Sanz, J., Cabezudo, M.D. 1997. Analysis of volatile components of oak wood by solvent extraction and direct thermal desorption-

gas chromatography-mass spectrometry. *Journal of Chromatography A* 778: 427-434.

Potgieter, N. 2006. Analysis of beer aroma using purge-and-trap sampling and gas chromatography. M.Sc. dissertation, University of Pretoria, Pretoria, South Africa.

Qian, M., Nelson, C., Bloomer, S. 2002. Evaluation of fat-derived aroma compounds in Blue Cheese by dynamic headspace GC/Olfactometry-MS. *Journal of the American Oil Chemists' Society* 79: 663-667.

Ridgway, K., Lalljie, S.P.D., Smith, R.M. 2006. Comparison of in-tube sorptive extraction techniques for non-polar volatile organic compounds by gas chromatography with mass spectrometric detection. *Journal of Chromatography A* 1124: 181-186.

Ridgway, K., Lalljie, S.P.D., Smith, R.M. 2007. Use of in-tube sorptive extraction techniques for determination of benzene, toluene, ethylbenzene and xylene in soft drinks. *Journal of Chromatography A* 1174: 20-26.

Rohwer, E.R., Lim Ah Tock, M.J., Naudé, Y. 2006. SA provisional patent application ZA 2006/07538.

Rychlik, M., Schieberle, P., Gosch, W. 1998. Compilation of odor thresholds, odor qualities and retention indices of key food odorants, Deutsche Forschungsanstalt für Lebensmittelchemie and Institut für Lebensmittelchemie der Technischen Universität München, Garching, Germany, ISBN 3-9803426-5-4.

Sandra, P., Saeed T., Redant, G., Godefroot, M., Verstappe, M., Verzele, M. 1980. Odour evaluation, fraction collection and preparative scale separation with glass capillary columns. *Journal of High Resolution Chromatography & Chromatography Communications* 3:107-114.

Schulz, K., Dreßler, J., Sohnius, E., Lachenmeier, D.W. 2007. Determination of volatile constituents in spirits using headspace trap technology. *Journal of Chromatography A* 1145: 204-226.

Simon, M., Hansen, A.P. 2001. Effect of various dairy packaging materials on the shelf life and flavor of ultrapasteurized milk. *Journal of Dairy Science* 84:784-791.

Sivakumar, D., Naudé, Y., Rohwer, E., Korsten, L. 2008. Volatile compounds, quality attributes, mineral composition and pericarp structure of South African litchi export cultivars Mauritius and McLean's Red. *Journal of the Science of Food and Agriculture* 88:1074-1081.

Tienpont, B., David, F., Bicchi, C., Sandra, P. 2000. High capacity headspace sorptive extraction. *Journal of Microcolumn Separations* 12(11): 577-584.

Van Aardt, M., Duncan, S.E., Marcy, J.E., Long, T.E., O' Keefe, S.F., Nielsen-Sims, S.R. 2005. Aroma analysis of light-exposed milk stored with and without natural and synthetic antioxidants. *Journal of Dairy Science* 88: 881-890.

Van Ruth, S.M. 2001. Methods for gas chromatography-olfactometry: a review. *Biomolecular Engineering* 17: 121-128.

Vazquez-Landaverde, P.A., Velazquez, G., Torres, J.A., Qian, M.C. 2005. Quantitative determination of thermally derived off-flavor compounds in milk using solid-phase microextraction and gas chromatography. *Journal of Dairy Science* 88: 3764-3772.

Vazquez-Landaverde, P.A., Torres, J.A., Qian, M.C., J. 2006. Effect of high-pressure-moderate-temperature processing on the volatile profile of milk. *Journal of Agricultural and Food Chemistry* 54: 9184-9192.

Zhang, Z., Pawliszyn, J. 1993. Headspace solid-phase microextraction. *Analytical Chemistry* 65: 1843-1852.

Chapter 7

Investigating the coffee flavour in South African Pinotage wine using novel off-line olfactometry and comprehensive gas chromatography with time of flight mass spectrometry

This chapter was published in Journal of Chromatography A. The format reflects the style set by the journal.

Naudé, Y. and Rohwer, E.R., 2013. Investigating the coffee flavour in South African Pinotage wine using novel off-line olfactometry and comprehensive gas chromatography with time of flight mass spectrometry. *Journal of Chromatography A* 1271, 176-180. DOI: 10.1016/j.chroma.2012.11.019

Author contributions

Conceived and designed the experiments: Yvette Naudé and Egmont Rohwer. Performed experimental work and data analysis, wrote the chapter/article, submitted article to journal, response to reviewers: Yvette Naudé. Initiator of research and study supervisor: Egmont Rohwer.

The work in this chapter was presented at the 36th International Symposium on Capillary Chromatography 2012, Riva del Garda, Italy; and at ChromSAAMS 2012, Dikhololo, South Africa.

Investigating the coffee flavour in South African Pinotage wine using novel off-line olfactometry and comprehensive gas chromatography with time of flight mass spectrometry

Yvette Naudé* and Egmont R. Rohwer

Department of Chemistry, University of Pretoria, Private Bag X20, Hatfield 0028, Pretoria, South Africa

ABSTRACT

Pinotage wine from several South African wine cellars has been produced with a novel coffee flavour. This innovative coffee effect was investigated using in house developed solventless sampling and fractionating olfactometric techniques, which are unique in their ability to study synergistic aroma effects as opposed to traditional gas chromatography olfactometry (GC-O) which is designed to, ideally, evaluate single eluting compounds in a chromatographic sequence. Sections of the chromatogram, multiple or single peaks, were recaptured on multichannel open tubular silicone rubber (polydimethylsiloxane (PDMS)) traps at the end of a GC column. The recaptured fractions were released in a controlled manner for off-line olfactory evaluation, and for qualitative analysis using comprehensive two-dimensional gas chromatography coupled to time of flight mass spectrometry (GCxGC-TOFMS) for compound separation and identification, thus permitting correlation of odour with specific compounds. A combination of furfural and 2-furanmethanol was responsible for a roast coffee bean-like odour in coffee style

Pinotage wines. This coffee perception is the result of a synergistic effect in which neither of the individual compounds was responsible for the characteristic aroma.

Keywords: GCxGC-TOFMS; Heart-cut; Multichannel open tubular trap; Off-line olfactometry; Pinotage wine; Polydimethylsiloxane (PDMS) sorptive extraction

*Corresponding author. Tel.: +27 12 420 2517; fax: +27 12 420 4687.

E-mail addresses: yvette.naude@up.ac.za, egmont.rohwer@up.ac.za

7.1 Introduction

Pinotage is a unique South African red wine cultivar cross-bred from Pinot Noir and Cinsaut (Hermitage). Isoamyl acetate is a key impact odourant responsible for the distinctive character of Pinotage wines [1]. Recently, Pinotage wine from several South African wine cellars has been produced with a novel coffee flavour. This contemporary aroma profile is deliberately derived from a particular combination of Pinotage, alternative toasted wood products and malolactic fermentation.

Traditionally, high-quality red wines are matured in oak barrels [2,3]. Compounds present in the wood are extracted into the wine during the aging process. Volatiles (e.g. oak lactones, guaiacol, 4-methylguaiacol, furfural and 5-methylfurfural) transferred into the wine produce distinctive flavours depending on the type of oak, level of toasting and seasoning [3,4]. Barrels are expensive, have a short lifetime (3-5 years) and maturation is a slow process. Recently, as an alternative to traditional wine aging, the maturation process is accelerated by adding toasted oak chips or staves to wine kept in stainless steel tanks or used barrels [2-4]. By exploiting the larger surface area of these alternative oak products wood derived compounds are transferred rapidly into the wine in relative short periods compared to traditional barrel maturation. A desired flavour profile can be selected depending on the toast level and type of oak product used. For example, descriptions supplied by a manufacturer (XTRAOAK) of these alternative products state that American oak medium toast

(AOMT) products may impart a vanilla flavour, American oak medium toast plus (AOMT+) can impart chocolate and coffee notes, French oak medium toast (FOMT) imparts nuances of spice and tobacco, and French oak medium toast plus (FOMT+) imparts subtle smokiness and coffee characteristics.

Gas chromatography olfactometry (GC-O) is traditionally used to investigate individual odour active substances. Aroma perception of the GC effluent is recorded by the human nose, in real time, at the olfactometer outlet. By comparing olfactometric data with chromatographic data, an individual compound can be matched with an odour [5-8]. However, potential synergistic effects cannot be observed when single compounds are evaluated over time. The result of combining single compounds in a complex matrix may be the emergence of a strikingly different sensory perception, completely unrelated to that of the individual compounds alone [9,10]. Addressing the limitations of evaluating rapidly eluting single compounds as opposed to selective combinatorial mixtures, a heart-cut gas chromatographic fraction collection (GC-FC) technique was developed to study, off-line, synergistic perceptions of odourants.

Sample preparation techniques for isolating compounds from wine for analysis are stir bar sorptive extraction (SBSE) [11-14], solid phase microextraction (SPME) [3,14-17], solid phase extraction (SPE) [18,], or liquid-liquid extraction (LLE) [4,18-20]. In the case of SPE or LLE, sensitivity limitations are associated with analysis of microlitre amounts of the diluted final extract. Solvent free sample enrichment provides aroma extracts that may be

more representative of food aroma when compared to those obtained by solvent extraction. SPME and SBSE are efficient commercial solvent free sorptive extraction alternatives to procedures using solvents. SPME (pioneered by Pawliszyn and co-workers) has a small sorbent volume of 0.6 – 0.9 μl [21], while SBSE (developed by Baltussen and Sandra) provides for sorptive volumes of 25 – 200 μl polydimethylsiloxane (PDMS) [22]. Multichannel open tubular silicone rubber (PDMS) traps, constructed in-house, were used in this study [9,10,23-26] (Fig. 7.1). The multichannel PDMS trap has a considerably larger volume of 0.6 ml PDMS thereby providing for a greater sample enrichment capacity. The analytes are concentrated by a purge-and-trap method onto a multichannel PDMS trap, followed by thermal desorption of the PDMS trap into a gas chromatograph with flame ionisation detection (GC-FID) or GCxGC-TOFMS.

Solvent free sampling using PDMS for high capacity analyte enrichment from Pinotage wines, GC fraction collection (heart-cutting) onto multichannel PDMS traps for off-line olfactory evaluation of synergistic effects, and for qualitative analysis by GCxGC-TOFMS for compound separation and identification, thus allowing correlation of odour with specific compounds are reported.

7.2 Materials and methods

7.2.1 *Wine samples*

Three brands of coffee style Pinotage wines (oak staves in tanks, maturation for three to six months) of vintages 2008 (brand 1), 2009 (brand 2), 2010 (brand 3) and 2011 (brand 2), and one traditional style Pinotage wine (second-fill and third-fill French oak barrel maturation for ten months) of vintage 2007 were purchased during 2009-2012 from local supermarkets (Pretoria, South Africa).

7.2.2 *Chemical standards*

Furfural (2-furancarboxaldehyde) (purity 99%) and 2-furanmethanol (furfuryl alcohol) (purity 99%) were purchased from Sigma-Aldrich (Pty) Ltd. Kempton Park, South Africa. For linear retention index determination *n*-alkanes C₆-C₁₈ were used (Merck, Pretoria, South Africa).

7.2.3 *Sorptive extraction with multichannel open tubular PDMS traps*

Multichannel PDMS traps containing 0.4 ± 0.02 g silicone were prepared based on a technique described by Ortner and Rohwer [23]. The multichannel PDMS trap was designed to fit a commercial thermal desorber system (TDS 3) available from Gerstel™ (Chemetrix, Midrand, South Africa). A bundle of twenty two channels of SIL-TEC™ silicone elastomer medical grade tubing (0.64 mm OD x 0.30 mm ID) (Technical Products, Georgia, United States of America)

were arranged, in parallel, inside a 17.8 cm long glass desorption tube (4 mm ID, 6 mm OD) (Fig. 7.1). The multichannel PDMS trap inside the desorption tube was 55 mm long. The multichannel trap provides a high sample enrichment capacity of 0.6 ml PDMS.

A purge-and-trap sampling method developed in-house [9,10,24] was used to extract the aroma compounds from wines by trapping it on a multichannel PDMS trap. The volatiles were isolated from 50 ml wine inside a 500 ml flat bottomed glass flask. The flask was immersed for 35 min in a water bath (25 °C) after which the sample was purged with 500 ml nitrogen gas at 25 ml/min. The purged volatiles were collected on a multichannel PDMS trap at 35 °C to prevent the condensation of water from the sample onto the trap. The ends of the trap device were capped with glass stoppers during storage. The glass stoppers were secured with tight-fitting polytetrafluoroethylene (PTFE) sleeves. The trapped analytes inside the trap device are not directly exposed to the PTFE sleeves, thereby preventing potential adsorption of analytes onto the Teflon®. The multichannel PDMS traps were desorbed into a GC-FID for heart-cutting, or into a GCxGC-TOFMS for compound identification.

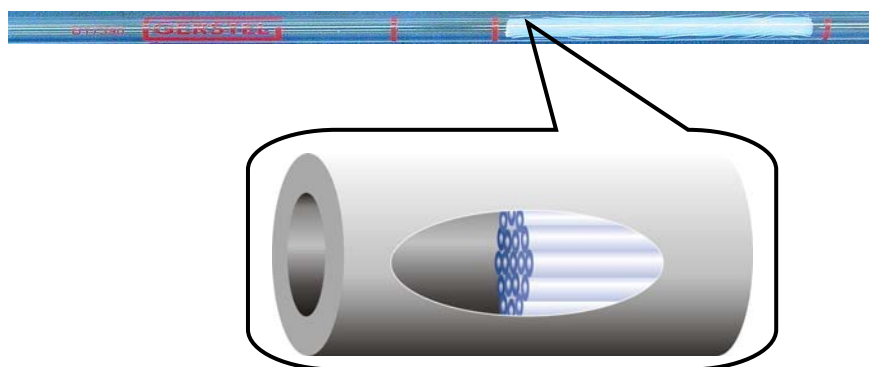


Figure 7.1. Solvent free concentration with silicone rubber (PDMS) tubing. Multichannel trap sampler: a bundle of silicone rubber tubing is inserted, in parallel, into an empty commercial glass desorption tube. The multichannel trap has a sorptive volume of 0.6 ml PDMS.

7.2.4 Heart-cutting with GC-FID: Capturing of single compounds, combinations of compounds, or fractions by GC-FC

The heart-cut procedure followed was previously described [9,10,26]. Briefly, the flame ionisation detector gases are switched off, the FID top assembly and the collector were removed by loosening the knurled brass nut and by taking out the collector prior to heart-cutting; single peaks or fractions were collected from the GC effluent (hydrogen carrier gas) at the end of the GC apolar column by simply placing a multichannel PDMS trap on the inactivated FID burner jet tip [27].

Experimental linear retention indices (RI_{exp}) were calculated according to the method of Van den Dool and Kratz [28]. Once a wine sample chromatogram was obtained sections of a chromatogram were captured during consecutive runs. Firstly, RI_{exp} fractions 600-800 (N), 801-899 (M), 901-1016

(KL), 1017-1250 (C), 1300-1800 (DE) were selectively captured on multichannel PDMS traps (Fig. 7.2) (characters in brackets denote a specific fraction). Thereafter, single peaks and combinations of heart-cuts were collected. After selective capturing of sections, single peaks, or combinations of heart-cuts onto multichannel PDMS traps, the traps were capped with custom-made glass and Teflon® stoppers (section 2.3) and stored for off-line olfactometric evaluation or for qualitative analysis by GCxGC-TOFMS.

7.2.5 Off-line olfactometry

The procedure followed for off-line olfactometric evaluation of aroma compounds captured on multichannel PDMS traps was previously described by Naudé et al. [9,10]. In short, the whole aroma (not fractionated) was released from multichannel PDMS traps at 20 °C to 140 °C (10 °C/min) and with a flow of nitrogen gas at a flow rate of 20 ml/min in an in-house built portable heating device. Heart-cuts (section 2.4) were released from the multichannel PDMS traps at 140 °C. Two evaluators, participating in the same session, recorded the odour thus released from the multichannel traps.

7.2.6 GCxGC-TOFMS

Separation of compounds was performed on a LECO Pegasus 4D GCxGC-TOFMS including an Agilent 7890 GC (LECO Africa (Pty) Ltd., Kempton Park, South Africa). The system included a secondary oven and a dual stage modulator. Liquid nitrogen was used for the cold jets and synthetic

air for the hot jets. Gases were of ultra high purity grade (Afrox, Gauteng, South Africa). Compounds isolated on multichannel PDMS traps were thermally desorbed by heating the traps in a Gerstel™ thermal desorber system (TDS 3) (Chemetrix, Midrand, South Africa) from 25 °C (3 min) at 30 °C/min to 250 °C (30 min) with a desorption flow rate of 80 ml/min at a vent pressure of 13 psi (helium). The TDS transfer line temperature was 350 °C. The desorbed analytes were cryogenically focused at –40 °C using liquid nitrogen and a cooled injection system (CIS 4) with an empty baffled deactivated glass liner. After desorption, a splitless injection (purge on at 3 min, purge flow 50 ml/min, solvent vent mode) was performed by heating the CIS from –40 °C at 10 °C/s to 250 °C and held there for the duration of the GC run.

The column set consisted of a 30 m x 0.25 mm ID x 0.25 µm df Rxi 5SilMS (5% phenyl, 95% dimethylpolysiloxane) apolar column as the primary column (¹D) joined to a 1.8 m x 0.15 mm ID x 0.15 µm df Rtx-200 (trifluoropropyl methyl polysiloxane) intermediate polarity secondary column (²D) (Restek, Bellefonte, PA, USA). The primary column was connected to the secondary column with a presstight column connector (Restek, Bellefonte, PA, USA). The primary oven temperature programme was 40 °C (3 min) at 10 °C/min to 300 °C (1 min). The GC run time was 30 min. The secondary oven was programmed identical to the primary oven, but offset by + 5 °C. The modulator temperature offset was 20 °C. The modulation period was 5 s with a hot pulse time of 1.20 s. The carrier gas (helium) velocity was 30 cm/s (1 ml/min) in the constant flow mode. The MS transfer line temperature was set at 280 °C. The ion source temperature was 200 °C, the electron energy was 70 eV in the electron impact

ionization mode (EI+), the data acquisition rate was 100 spectra/s, the mass acquisition range was 40–350 atomic mass units (amu), and the detector voltage was set at 1700 V. Identification of compounds was based on comparison to authentic standards.

7.3 Results and discussion

7.3.1 *Multichannel PDMS traps*

A simple, cheap, non-hazardous solvent free sampling technique using PDMS for analyte enrichment from wine was developed (Fig. 7.1). The total amount of sorbed analytes was introduced into a GC providing for increased sensitivity. Compared to commercial sorption devices the multichannel PDMS trap provides a larger sample enrichment capacity of 0.6 ml PDMS. Multichannel PDMS traps may be assembled inside any of the commercial thermal desorption tubes available. Additional advantages of the multichannel PDMS traps over commercial sorption devices are their open tubular structure, multichannel flow and associated low pressure drop [23].

7.3.2 *Heart-cutting by GC-FC and off-line olfactometry*

Figure 7.2 depicts selective heart-cutting by GC-FC from the complex sample chromatogram. Complicated instrumental set-ups, sophisticated equipment or valves were not required. The FID collector was removed prior to heart-cutting. The FID flame gases (hydrogen and air) were switched off.

PDMS containing sorbed analytes from wine was desorbed and during this apolar separation of the complex mixture, fractions were selectively collected from the GC effluent onto a secondary PDMS multichannel trap. The secondary multichannel trap was placed, by hand, on the inactivated burner jet tip prior to peak/fraction elution and removed once the peak/fraction had eluted. The multichannel PDMS trap containing a heart-cutted section of a chromatogram was then desorbed in an off-line portable olfactometer for the controlled release of compounds. The open tubular structure of the multichannel PDMS trap and low pressure drop associated with multichannel flow are features that were not only particularly amenable to the recapturing of chromatographic fractions from the GC effluent during a GC run, but also for the controlled release of trapped compounds in an off-line olfactometer (Fig. 7.2). Most of the effluent of the FID passes through the trap without special sealing arrangement that would otherwise complicate the GC-FC procedure. The advantage of a low pressure drop is not offered by conventional packed traps.

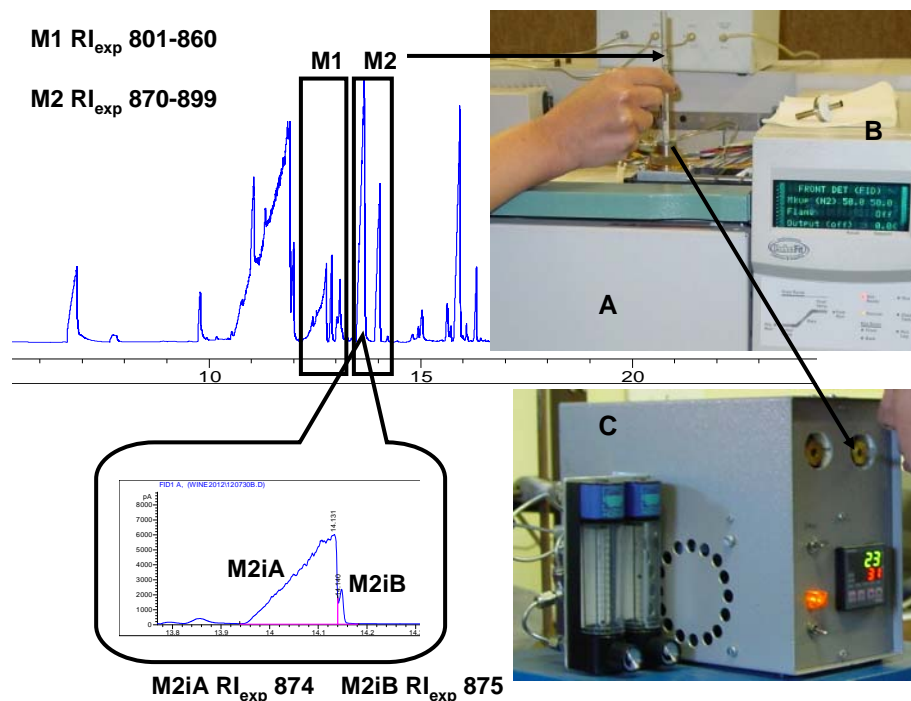


Figure 7.2. Heart-cutting and off-line olfactometry: identifying the fraction of a chromatogram responsible for a coffee odour. Sections of the chromatogram are captured from the GC effluent on a multichannel silicone rubber trap (A). The trap is rested on the burner jet tip of an inactive FID during collection. The collector is removed prior to heart-cutting (B). The odour is released from the trap at 140 °C and with a flow of nitrogen gas (20 ml/min) in an off-line olfactometer (C).

The Pinotage wines were first evaluated for a coffee aroma by releasing the whole aroma (not fractionated), after purge-and-trap sample preparation, from multichannel PDMS traps in an off-line olfactometer (section 2.5). Odour descriptors and the temperature at which an odour was perceived were recorded. The traditional Pinotage wine displayed notes of chocolate box, banana, sweet, fruity, smoky, tobacco and toasty. The coffee style wines had notes of chocolate box, banana peel, smoky, burnt rubber, roast coffee bean, savoury, charred veld and leather. Various heart-cuts of the coffee style wine sample chromatogram were then collected from the GC effluent onto secondary multichannel PDMS traps. GC elution temperatures, corresponding to off-line olfactometric temperatures at which an odour was perceived, served as a

guideline to determine the heart-cut windows. The fractions thus collected represented experimental retention indices (RI_{exp}) 600-800 (N), RI_{exp} 801-899 (M), RI_{exp} 901-1016 (KL), RI_{exp} 1017-1250 (C) and RI_{exp} 1300-1800 (DE) (characters in brackets denote a specific fraction).

For each fraction the heart-cut aroma was released from the secondary multichannel PDMS trap in an off-line olfactometer at 140 °C with a flow of nitrogen gas (20 ml/min). Fruity, sweet, caramel, chocolate notes were described for fraction N (RI 600-800); sweet-fruity, banana peel, sweet-smoky, savoury, roast coffee bean, burnt rubber and charred wood were described for fraction M (RI 801-899); sour cream, cotton candy, smoky, sweet, fruity were described for fraction KL (RI 980-1016); savoury, smoke, cocoa powder-like, leather and tobacco were described for fraction C (RI 1017-1250), while fraction DE (1300-1800) was described as burnt rubber, dusty, citrus, exotic sweet floral, black fruit.

Fraction M (RI_{exp} 801-899), in which the coffee bean-like note was detected, was fractionated further to establish the exact GC range in which the compounds responsible for the coffee note eluted. Fraction M was heart-cut into fractions M1 and M2 (Fig. 7.2). Fraction M1 (RI_{exp} 801-860) was described as sweet-fruity, and fraction M2 (RI_{exp} 870-899) exhibited a roast coffee bean-like note. Fraction M2, the roast coffee bean-like fraction, was again fractionated further into heart-cut M2_{iA} (RI_{exp} 874) and heart-cut M2_{iB} (RI_{exp} 875) (Fig. 7.2). The aroma from heart-cut M2_{iA}, released in the off-line olfactometer, was described as sweet-smoky. The aroma from heart-cut M2_{iB}, released in the off-

line olfactometer, was described as char, burnt. The roast coffee bean perception was not noted for any of the two heart-cuts. A roast coffee bean-like odour was described only for a combination of heart-cuts M2_{iA} and M2_{iB}.

7.3.3 Identification of the compounds in the roast coffee bean-like fraction M2 by GCxGC-TOFMS

GCxGC-TOFMS revealed the presence of furfural and of 2-furanmethanol in heart-cut M2 (Fig. 7.3). The headspace of authentic standards of furfural and 2-furanmethanol was then captured, either separately or in combination, onto multichannel PDMS traps (volumes were sucked through traps with a 60 ml gastight syringe). The odour was released from the traps in an off-line olfactometer (section 2.5). Furfural was described as sweet and almond-like, while 2-furanmethanol was described as savoury, burnt and ether-like. Thereafter, the headspace of furfural and of 2-furanmethanol was combined in varying ratios. The odour of combinations of furfural:2-furanmethanol released from multichannel PDMS traps was described as almond, coffee, smoky and savoury for a ratio of 1:1; almond and dark roasted coffee bean for a ratio of 1:2; and roasty-dusty and coffee beans for a ratio of 1:4.

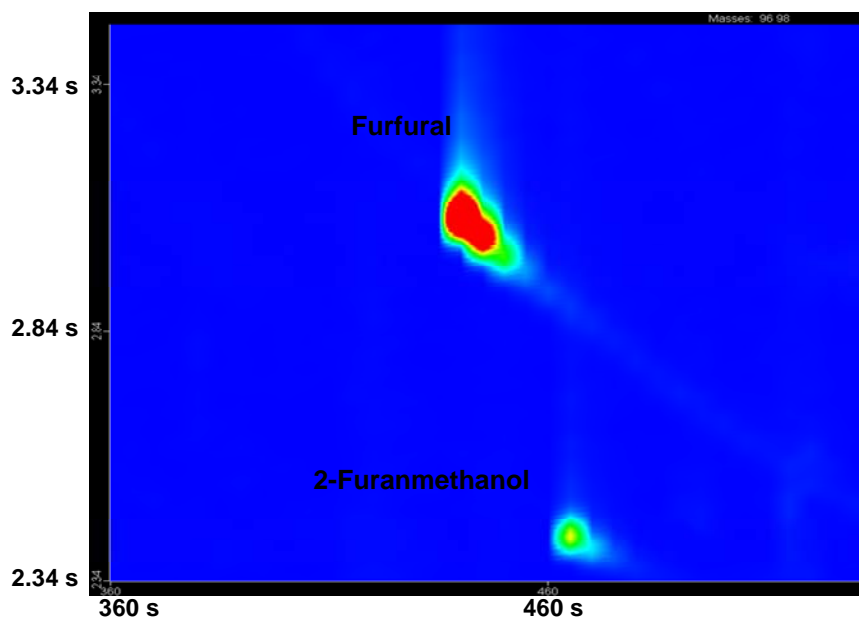


Figure 7.3. Contour plot of a reconstructed ion chromatogram (96 + 98 amu) shows the presence of furfural (440 s, 3.070 s) and 2-furanmethanol (465 s, 2.430 s) in heart-cut M2. See 7.2.6 for instrumental conditions.

Furfural and 2-furanmethanol are amongst the key odourants thought to be particularly responsible for a coffee aroma in brewed coffee [29]. In brewed coffee furfural is described as cooked pea, smoky; and 2-furanmethanol is described as burnt, unpleasant [29]. In general, furfural is described as pungent, but sweet and almond-like [30], while in oak extracts it is described as caramel-like [8]. 2-Furanmethanol is well associated with the burnt and bitter note of dark-roasted coffees [30]. Thus, furfural was responsible for the sweet-smoky note in heart-cut M2i_A, and 2-furanmethanol was responsible for the burnt note in heart-cut M2i_B.

As is to be expected, furfural was relatively higher in the wines exposed to toasted wood staves, compared to the wine aged in a used barrel (Fig. 7.4).

Relative high levels of 2-furanmethanol were present in Pinotage wines exposed to alternative wood products (chips or staves), while it was not detected in the used barrel aged Pinotage wine (Fig. 7.4). Furfural in wine is oak-derived, whilst 2-furanmethanol does not directly originate from oak [4,31]. In wine furfural may, chemically or microbiologically, convert to 2-furanmethanol [4]. Although 2-furanmethanol was reported to occur in Spanish red wine exposed to toasted oak chips [31], in traditional aged Shiraz [13], in Shiraz exposed to oak chips and micro-oxygenation [32] and in Merlot [17], there are no reports of 2-furanmethanol occurring in Pinotage wines (possibly because published studies [11-13,15,16,18] did not include Pinotage wines exposed to alternative wood products). A roast coffee aroma of certain red Bordeaux wines was attributed to the presence of 2-furanmethanethiol [33]. However, this chemical compound was not detected in the Pinotage wines analysed here.

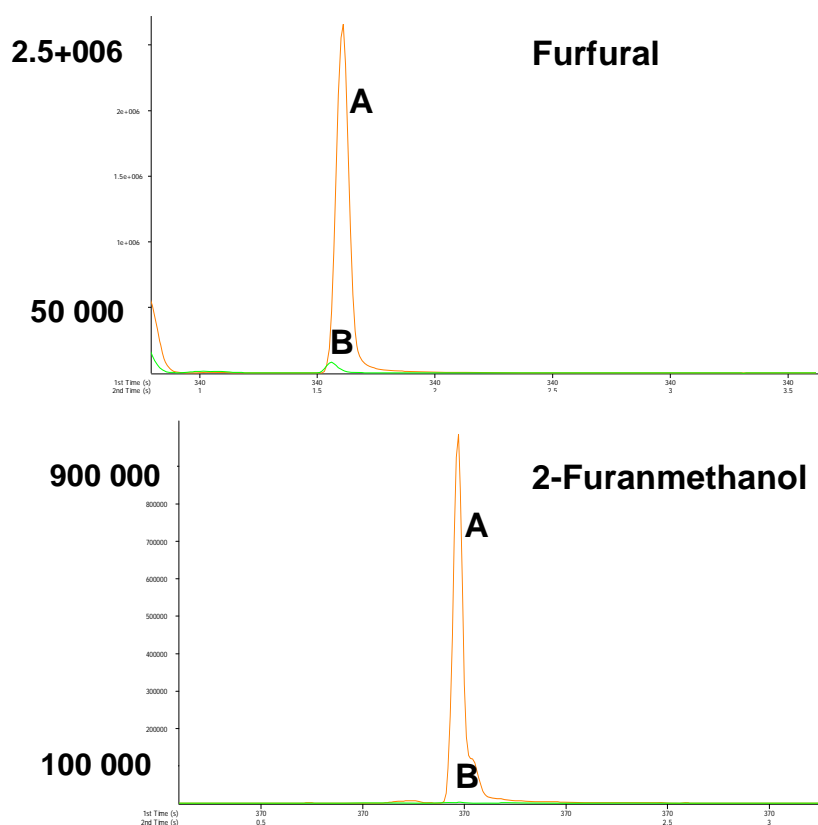


Figure 7.4. Reconstructed first dimension ion chromatograms of furfural (96 amu) and 2-furanmethanol (98 amu) in a coffee style Pinotage wine (oak staves in tanks, maturation for three months) (orange chromatogram A) compared to a traditional style Pinotage wine (used French oak barrel maturation for ten months) (green chromatogram B). See 7.2.6 for instrumental conditions.

7.4 Conclusions

Multichannel PDMS traps were used for solvent free extraction of compounds from wines and for collection of heart-cuts at the end of a GC column. Heart-cuts thus collected were released from the multichannel PDMS traps in an off-line olfactometer which permitted the study of synergistic aroma effects. Heart-cuts were desorbed into a GCxGC-TOFMS for compound identification, thereby allowing correlation of aroma with specific compounds. A

simple combination of furfural and 2-furanmethanol was, for the first time, shown to contribute to a roast coffee bean-like odour in coffee style Pinotage wines. This coffee bean-like perception is the result of a synergistic effect in which no individual compound was responsible for this particular aroma.

7.5 Acknowledgements

Gerhard Overbeek for assisting in the extraction of wine and aroma evaluation, Phakama Botha for assistance in wine extraction, Dr Fanie van der Walt for the custom-built olfactometer, David Masemula for the assembly of multichannel PDMS traps, Dr Peter Gorst-Allman from LECO Africa (Pty) Ltd. for use of a LECO Pegasus 4D GC×GC–TOFMS, Philip Langenhoven from LECO Africa (Pty) Ltd. for sponsorship, Jack Cochran from Restek for kind donation of GC columns and consumables, SASOL and the National Research Foundation (NRF) for financial support.

7.6 References

- [1] C.J. van Wyk, O.P.H. Augustyn, P. de Wet, W.A. Joubert, *Am. J. Enol. Vitic.* 30(3) (1979) 167.
- [2] D. de Beer, E. Joubert, J. Marais, W. du Toit, B. Fourie, M. Manley, S. Afr. J. Enol. Vitic. 29(1) (2008) 39.
- [3] E. Koussissi, V.G. Dourtoglou, Ageloussis, Y. Paraskevopoulos, T. Dourtoglou, A. Paterson, A. Chatzilazarou, *Food Chem.* 114 (2009) 1503.
- [4] A.B. Boutista-Ortín, A.G. Lencina, M. Cano-López, F. Pardo-Mínguez, J.M. López-Roca, E. Gómez-Plaza, *Aust. J. Grape Wine Res.* 14 (2008) 63.
- [5] T.E. Acree, J. Barnard, D.G. Cunningham, *Food Chem.* 14 (1984) 273.
- [6] W. Grosch, *Flav. Fragr. J.* 9 (1994) 147.
- [7] L. Moio, E. Chambellant, I. Lesschaeve, S. Issanchou, P. Schlich, P. Etiévant, *Ital. J. Food Sci.* 3 (1995) 265.
- [8] M. Consuelo Díaz-Maroto, E. Guchu, L. Castro-Vázquez, C. de Torres, M. Soledad Pérez-Coello, *Flavour Fragr. J.* 23 (2008) 93.

- [9] Y. Naudé, M. van Aardt, E.R. Rohwer, J. Chromatogr. A 1216 (2009) 2798.
- [10] Y. Naudé, E.R. Rohwer, in: R. Marsili (Ed.), Flavor, Fragrance, and Odor Analysis, Second Edition, Taylor & Francis Group LLC, Boca Raton, Florida, 2012, pp. 93.
- [11] B.T. Weldegergis, A.G.J. Tredoux, A.M. Crouch J. Agric. Food Chem. 55 (2007) 8696.
- [12] B.T. Weldegergis, A.M. Crouch, J. Agric. Food Chem. 56 (2008) 10225.
- [13] A. Tredoux, A. de Villiers, P. Majek, F. Lynen, A. Crouch, P. Sandra, J. Agric. Food Chem. 56 (2008) 4286.
- [14] A. de Villiers, P. Alberts, A.G.J. Tredoux, H.H. Nieuwoudt, Anal. Chim. Acta 730 (2012) 2.
- [15] J. Vestner, S. Malherbe, M. du Toit, H.H. Nieuwoudt, A. Mostafa, T. Górecki, A.G.J. Tredoux, A. de Villiers, J. Agric. Food Chem. 59 (2011) 12732.
- [16] B.T. Weldegergis, A. de Villiers, C. McNeish, S. Seethapathy, A. Mostafa, T. Górecki, A.M. Crouch, Food Chem. 129 (2011) 188.
- [17] J.E. Welke, V. Manfroi, M. Zanus, M. Lazarotto, C.A. Zini, J. Chromatogr. A 1226 (2012) 124.
- [18] B.T. Weldegergis, A.M. Crouch, T. Górecki, A. de Villiers, Anal. Chim. Acta 701 (2011) 98.
- [19] P. Schreier, F. Drawert, A. Junker, J. Agric. Food Chem. 24(2) (1976) 331.
- [20] A. Rapp, Nahrung 42 (1998) 351.
- [21] Z. Zhang, J. Pawliszyn, Anal. Chem. 65 (1993) 1843.
- [22] E. Baltussen, P. Sandra, F. David, C. Cramers, J. Microcolumn Sep. 11 (1999) 737.
- [23] E.K. Ortner, E.R. Rohwer, J. High Resolut. Chromatogr. 19 (1996) 339.
- [24] M.J. Lim Ah Tock, M.Tech. dissertation (2009) Aroma analysis of alcoholic beverages using multi-channel silicone rubber traps, Tshwane University of Technology, Pretoria, South Africa [online]. Available: http://libserv5.tut.ac.za:7780/pls/eres/wpg_docload.download_file?p_filename=F485852604/Lim,%20M.J.%20Ah%20Tock.pdf (Accessed 30 July 2012).
- [25] Y. Naudé, E.R. Rohwer, Anal. Chim. Acta 730 (2012) 112.
- [26] Y. Naudé, E.R. Rohwer, Anal. Chim. Acta 730 (2012) 120.
- [27] E.R. Rohwer, M.J. Lim Ah Tock, Y. Naudé, SA provisional patent application ZA 2006/07538 (2006).
- [28] H. van den Dool, P.D. Kratz, J. Chromatogr. 11 (1963) 463.
- [29] S-T. Chin, G.T. Eyres, P.J. Marriott, J. Chromatogr. A 1218 (2011) 7487.
- [30] I. Flament, Coffee Flavour Chemistry, John Wiley & Sons, West Sussex, England, 1st ed., 2002, pp. 81.
- [31] B. Fernández de Simón, E. Cadahía, M. del Álamo, I. Nevares, Anal. Chim. Acta 660 (2010) 211.
- [32] L.M. Schmidtke, thesis (2011) Effects of Micro-oxygenation on Shiraz Wine, Agricultural and Wine Sciences, Charles Sturt University, Australia [online]. Available: http://researchoutput.csu.edu.au/R/-?func=dbin-jump-full&object_id=29361&local_base=GEN01-CSU01 (Accessed 25 October 2012).

- [33] T.Tominaga, L.Blanchard, P. Darriet, D. Dubourdieu, J. Agric. Food Chem. 48 (2000) 1799.

Chapter 8

Conclusion

To meet real world challenges, and to overcome the problems associated with solvent extraction, novel silicone rubber (PDMS) samplers were constructed in-house for solvent free enrichment of trace level analytes from indoor air, contaminated soil, desert soil, ultra high temperature (UHT) milk and Pinotage wine. A unique off-line multidimensional GC approach involving heart-cut gas chromatographic fraction collection and an off-line olfactometric method for the evaluation of synergistic odour effects were developed.

Compared to bulky polyurethane foam (PUF) samplers that collect total air (*i.e.*, vapour and particulate phases), and therefore do not distinguish between contributions from each phase, the miniature denuder accomplished separate concentration of vapour phase and of particulate phase fractions of DDT from indoor air, in a single step. Indoor airborne vapour phase and particulate phase pollutants were collected at a lower air flow sampling rate and a shorter collection time using a compact battery operated field pump. Since sampling was done under undisturbed conditions one cannot conclude that particulate phase insecticide presents an unimportant pathway for human

exposure. Ratios of airborne p,p' -DDD/ p,p' -DDT and of o,p' -DDT/ p,p' -DDT are unusual and do not match the ideal certified ingredient composition required of commercial DDT. Results suggest that technical DDT used for indoor residual spraying may have been compromised with regards to insecticidal efficacy, demonstrating the power of this new environmental forensics tool.

Unlike laborious Soxhlet extraction, PDMS loop samplers are convenient to use for the fast, solvent free extraction of trace level POPs and geochemical hydrocarbons from soil samples. A possible geochemical origin of the enigmatic fairy circles of Namibia was investigated for the first time. PDMS loop samplers, a simple, cheap, nonhazardous solvent free enrichment technique for the introduction of the total amount of sorbed analytes into a GC-MS, was prepared in-house to specifically manage the easily magnetised desert soil. It is proposed that microseepages of natural gas and low volatility hydrocarbons are expressed at the surface as a geobotanical anomaly of barren circles and circles of altered vegetation.

Multichannel PDMS trap samplers were employed for sampling of the headspace of UHT milk and of Pinotage wine. The multichannel trap samplers offered high sample enrichment capacity due to their considerably larger volume of PDMS when compared to SPME or SBSE.

A unique heart-cut technique, involving gas chromatographic fraction collection onto multichannel PDMS traps to physically resolve complex samples thereby offering versatile off-line multidimensional capability, was presented.

Compounds are selectively captured from the complex sample chromatogram onto multichannel traps from the GC effluent without the need for instrumental modifications. The open tubular structure, multichannel flow and associated low pressure drop of the multichannel traps are not offered by conventional packed traps. This new approach for heart-cut gas chromatographic fraction collection was utilised to capture selected chiral isomers from a non-enantioselective column for off-line second dimension enantiomeric separation of *o,p'*-DDT and *o,p'*-DDD in air and soil by GC-TOFMS. Cyclodextrin columns are sensitive to moisture and dirty matrices. By eliminating the complex matrix the expensive chiral column is protected and its useful lifetime is prolonged. It was demonstrated that this new multidimensional GC approach could be used as an alternative to the more expensive GCxGC-TOFMS. First results indicate a significantly different enantiomeric profile for indoor airborne particulate phase compared to the enantiomeric profiles of indoor air vapour phase and of outdoor soil.

The same heart-cutting technique used to capture selected chiral isomers was also employed to address the limitations of traditional gas chromatography olfactometry (GC-O). Evaluating rapidly eluting single compounds over time does not provide information on their behaviour in mixtures. The heart-cut gas chromatography fraction collection technique was utilised for the off-line assessment of selective combinatorial mixtures to explore synergistic aroma perceptions. The recombined aroma heart-cuts are released off-line in a controlled manner by heating the multichannel trap in a portable olfactometer. The slow release of aroma allows for sufficient time to recall

odour descriptors. An advantage of uncoupling the time scale is that the olfactory assessment can be terminated and resumed at convenience when nose fatigue is indicated. The described instrumentation permits comparison of olfactometric perception of a concentrated overall aroma against that of gas chromatographically separated single compounds, a feature not offered by traditional GC-O. The disparity between descriptors of an overall aroma and the single compounds could be reconciled by a trial-and-error search for a simple combination of single compounds that matched a descriptor for the whole aroma, not registered for any of the single peaks alone. Heart-cutting onto multichannel PDMS traps for off-line second dimension analysis by GC-MS or GCxGC-TOFMS enables correlation of odour with specific compounds. A synergistic combination of 2-heptanone and 2-nonanone was responsible for a pungent cheese-like odour in UHT milk, while a synergistic combination of furfural and 2-furanmethanol was responsible for a roast coffee bean-like odour in coffee style Pinotage wines.

The versatility of PDMS as a loop sampler, a multichannel trap, or a miniature denuder for environmental forensics, geochemical and aroma investigations were demonstrated. The small, low cost samplers are quick and easy to assemble and they fit commercial thermal desorber systems. The PDMS samplers are reusable and only require baking out in a flow of gas prior to the next sampling event. Solvent extraction of the sampling materials, extract clean-up and pre-concentration are not required. Thus, potential loss of analyte, introduction of contaminants and waste disposal are minimised, and laboratory staff are protected against exposure to solvents. Thermal desorption

permits transfer of the entire sample mass to the cooled injection system (CIS) inlet of a GC resulting in greater sensitivity when compared to injection of microlitre amounts of a solvent extract. Enhanced sensitivity enabled sampling of smaller sized soil samples, shorter air sampling times and lower air sampling flow rates when compared to solvent based methods. In contrast to conventional isothermal GC injection, CIS injection was mild and therefore minimised artefacts of analyte decomposition/conversion during injection.

Silicone degradation products appeared in the chromatogram due to thermal degradation of the silicone rubber during heating (desorption stage) which can cause potential chromatographic peak interferences. Higher temperatures are required to desorb less volatile compounds from silicone rubber and therefore the work reported in this thesis was confined to more volatile compounds. Future work will focus on modes of obtaining stable silicone rubber to reduce thermal breakdown during desorption. Gas chromatographic fraction collection and desorption efficiencies of less volatile compounds will be addressed.